

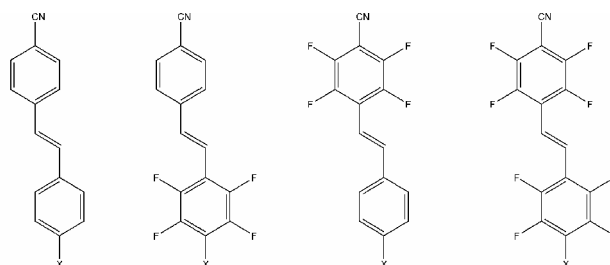
# Preparation of donor-acceptor substituted fluorostilbenes and crystal chemistry of fluorinated (*E*)-4-(4-halogeno-styryl) benzonitriles

Raúl Mariaca<sup>a</sup>, Gaël Labat<sup>a</sup>, Norwid-Rasmus Behrnd<sup>a</sup>, Michel Bonin<sup>a</sup>, Fabien Helbling<sup>a</sup>, Patrick Eggli<sup>a</sup>, Gaëtan Couderc<sup>a</sup>, Antonia Neels<sup>b</sup>, Helen Stoeckli-Evans<sup>b</sup> and Jürg Hulliger<sup>a\*</sup>

a) Department of Chemistry and Biochemistry, University of Berne, Freiestrasse 3, CH-3012 Berne, Switzerland.

b) Institut de Microtechnique, Jaquet Droz 1, CP 526, CH-2002 Neuchâtel, Switzerland.

## Graphical Abstract



X= F, Cl, I

# Preparation of donor-acceptor substituted fluorostilbenes and crystal chemistry of fluorinated (*E*)-4-(4-halogeno-styryl)-benzonitriles

Raúl Mariaca<sup>a</sup>, Gaël Labat<sup>a</sup>, Norwid-Rasmus Behrnd<sup>a</sup>, Michel Bonin<sup>a</sup>, Fabien Helbling<sup>a</sup>, Patrick Egli<sup>a</sup>, Gaëtan Couderc<sup>a</sup>, Antonia Neels<sup>b</sup>, Helen Stoeckli-Evans<sup>b</sup> and Jürg Hulliger<sup>a\*</sup>

a) Department of Chemistry and Biochemistry, University of Berne, Freiestrasse 3, CH-3012 Berne, Switzerland.

b) Institute of Microtechnique, Jaquet Droz 1, CP 526, CH-2002 Neuchâtel, Switzerland.

## Abstract

The syntheses and crystal structures of a series of fluoro-substituted halogeno (Cl, Br, I)-cyano-stilbenes containing donor and acceptor groups (D- $\pi$ -A) are reported. These molecules show a tendency to form anti-parallel chain-like structures and herringbone packing, crystallising predominantly in a centric space group. However, second harmonic generation measurements bear evidence for orientational disorder leading to partial polar order below the ordinary X-ray structure determination limit. Some co-crystals are isostructural with their components. The non-fluoro as well as the halogeno-fluoro substituted components of co-crystals seems to impose their crystal structure on the complementary fluoro or cyano-fluoro substituted components. Co-crystallization enhanced the deviation from centrosymmetry.

*Keywords:* Donor acceptor halogenostyryl-benzonitriles, HWE approach, Heck coupling, Halogen bonding, Co-crystals, SHG, Crystal structure.

## Introduction

Compared to interactions observed in crystal structures between arenes, relative strong

intermolecular interactions between arene and perfluoroarenes have been reported in many areas of chemistry and biochemistry. Binary

co-crystals, i.e., crystals containing complementary pairs of molecules, provide an interesting class of materials for understanding intermolecular non-covalent interactions [1]. Some examples such as the co-crystallisation of octafluoronaphthalene with *trans*-stilbene from solutions have been reported recently [2]. We have extended this topic by exploring the formation and structural properties of new co-crystals based on fluorinated (*E*)-4-(4-halogenostyryl)-benzonitriles and their corresponding H-analogues [3]. However, many of the synthetic procedures leading to fluorine containing materials are not as preponderant as for the hydrogen containing analogues. They require readily accessible fluorinated materials and detailed reports on versatile synthetic procedures. In this contribution we focus on the synthesis of a series of fluorinated molecules pertaining to fundamental studies of fluoro-organic compounds.

Some molecules we present here show crystal structures having CN $\cdots$ I interactions that have been described as important motifs for making co-crystals [4]. Halogen bonding (XB) is a strong, specific and directional interaction that gives rise to well defined supramolecular synthons. XB relevance in fields as various as superconductors has been found [5]. Indeed supramolecular organic conductors based on halogen-bonded iodotetrathiafulvalenes (TTF's) have been reported [6]. Recently, XB has also proven to be able to form liquid crystals from nonmesomorphic components.

This is the case of the complexes between 4-alkoxystibazoles and iodopentafluorobenzene [7]. Substrat-receptor bindings allowing the resolution of racemic compounds i.e., resolution of (rac)-1,2-dibromo-hexafluoropropane through halogen-bonded supramolecular helices have been highlighted [8]. Particularly important reviews on XB issues have been published by P. Metrangolo *et al.* [9].

In addition, it has been shown that fluorination of an iodo/bromo substituted phenyl ring, greatly enhances the electron-acceptor ability of such substituents [10]. The attractive nature of the halogen (XB) bonding causes CN $\cdots$ X distances shorter than the sum of van der Waals radii of involved atoms. The stronger the interaction, the shorter the CN $\cdots$ X distance is [11].

Although some tetra- and penta-fluorostilbenes are known and examples containing fluorinated push-pull stilbenes have been described in the literature [12], the use of perfluorinated aromatic stilbenes A- $\pi$ -D bearing substituents such as CN (A) and halogens X (D) represents a new concept. For this reason we report on the synthesis and crystal structures of an octafluoro compound featuring acceptor and donor properties, including particularly hydrogen analogues and tetrafluorinated derivatives (see Scheme 1)

**Scheme 1** Basic building blocks used to form co-crystals.

## 2. Results and discussion

### 2.1 Horner-Wadsworth-Emmons approach

Horner and coworkers were the first to modify the Wittig reaction: They reacted phosphoryl-stabilized carbanions with ketones and aldehydes to make alkenes [13]. Derivatives of diphenyl-phosphineoxide and diethylbenzyl phosphonate were used to obtain these particular carbanions. Wadsworth and Emmons, on the other hand, focused primarily on phosphonate carbanions to produce olefins [14]. Both phosphonate-mediated modifications of the Wittig reaction were combined and referred to, as the Horner-Wadsworth-Emmons (HWE) olefination reaction.

The HWE reaction provides many advantages over the traditional Wittig reaction. Phosphonate carbanions are recognized to be more nucleophilic than phosphonium ylides, providing a higher diversity of aldehydes and ketones to react with these particular carbanions [15]. A problem associated with the Wittig reaction is the phosphineoxide formed, which is often difficult to separate from the desired product. The phosphate ion formed from the HWE reaction is water-soluble, thus providing easier separation from the final product. Finally, smooth alkylation is possible on the  $\alpha$ -carbon of the phosphonatecarbanion, whereas phosphonium ylides generally do not alkylate well [16].

The preparation of phosphonates takes place through the Michaelis-Arbuzov reaction [17],

i.e. the reaction of trialkyl phosphate with a benzyl halide to produce an alkyl phosphonate. We have prepared fluorinated stilbenes by using sodium hydride in tetrahydrofuran or sodium ethanolate in ethanol. The **HWE-precursors** have been prepared by using the methods described below.

### 2.2 Preparation of HWE precursors

Precursors like 4-fluoro- and 4-chloro-benzaldehyde were commercially available. 4-iodobenzaldehyde **3** was prepared as described in the literature [18], by reduction ( $\text{NaBH}_4$ ) followed by an oxidation step with  $\text{CrO}_3$ /pyridine/ $\text{MeCl}_2$  (PCC) (Scheme 2).

**Scheme 2** Preparation of 4-iodobenzaldehyde **3**: (a)  $\text{NaBH}_4$ , THF; (b)  $\text{CrO}_3$ /pyridine/ $\text{MeCl}_2$ .

An efficient synthesis of 2,3,5,6-tetrafluoro-4-halogenatedbenzaldehyde **5** was developed to obtain chloro or bromo derivatives as described in the literature [19]. In this procedure, a mixture of commercial available pentafluoro-benzaldehyde **4** and lithium salt was heated to 150 °C in absolute *N*-methylpyrrolidone for 3 h (Scheme 3).

**Scheme 3** Preparation of 4-chloro-2,3,5,6-tetrafluorobenzaldehyde: **5**: (c)  $\text{LiCl}$ /*NMP*, 150 °C.

For the preparation of 2,3,5,6-tetrafluoro-4-iodo-benzaldehyde **9**, we followed the method published in a recent paper [20] (Scheme 4).

**Scheme 4** Synthetic route for 4-iodo-2,3,5,6-tetrafluorobenzaldehyde **9**: (d) *n*-BuLi; EtO-CHO; HO-CH<sub>2</sub>-CH<sub>2</sub>-OH/*p*-TsOH; (e) *n*-BuLi, I<sub>2</sub>; (f) TFA/HCl/H<sub>2</sub>O.

The commercially available starting material **6** was lithiated. After formylation with an excess of ethyl formate, the obtained tetrafluorinated benzaldehyde was subsequently protected by forming the acetal **7**, lithiation of compound **7** and subsequent iodination of the lithio derivative led to the 4-iodoacetal **8**. After acetal hydrolysis, the desired iodinated aldehyde **9** was isolated.

The preparation of the fluorinated phosphonate **13** as precursor for the HWE-coupling was already reported [3] by the route described in Scheme 5.

**Scheme 5** Synthetic route for the preparation of 4-(bromomethyl)-2,3,5,6-tetrafluorobenzonitrile **13**: (g) SOCl<sub>2</sub>/NH<sub>4</sub>OH; (h) pyridine/POCl<sub>3</sub>; (i) NBS/CCl<sub>4</sub>.

### 2.3 Synthesis of H- and F-stilbenes

HWE reactions were carried out at room temperature using a base (*Method A*) and/or (*Method B*) and stirring overnight. *Trans*-stilbenes **16**, **17** and **18** were obtained by coupling of **15** with the corresponding aldehydes described before (Scheme 6). The progress of the reaction was followed by GC-MS analysis. Products were obtained (42-70 %) and no trace of the *cis*-isomer was detected. *E*-stilbenes **19**, **20** and **21** were prepared similarly by coupling the aldehydes **4**, **5** and **9**, with the phosphonate derivative **15**

(16-50 %). Compound **13** undergoes the Michaelis-Arbuzov reaction to obtain a fluorophosphonate as intermediate, which reacts with the corresponding aldehydes to afford **22**, **23** and **24**. In the same way, the synthesis of the octafluorinated stilbenes **25**, **26** and **27** was performed by HWE coupling of **4**, **5** and **9** with **13** (30-50 %). Solid products were isolated by crystallization in dichloromethane or methanol and characterized by their melting points (Table 1).

Comparing both series: X-C<sub>6</sub>F<sub>4</sub>-CH=CH-C<sub>6</sub>F<sub>4</sub>-CN and X-C<sub>6</sub>H<sub>4</sub>-CH=CH-C<sub>6</sub>H<sub>4</sub>-CN, the former showed lower melting temperatures probably due to weak molecular F...F interactions and the lack of N...I interactions in **25** and **26**. Compound **27** makes an exception and has a higher melting point. The interesting fact is that all iodine compounds showed higher melting temperatures than the fluoro and chloro analogues. This might be related to a stronger N...I interaction; indeed the highest values (211 °C and 240 °C) correspond to the compounds where the I-atom is attached to the fluorinated phenyl ring [10].

**Scheme 6** (j) P(OEt)<sub>3</sub>, 110 °C; (k) NaH/THF; (l) NaOEt/EtOH.

### 2.4 Heck approach

Nowadays, the Heck reaction [21] is one of the most valuable C-C bond-forming process promoted by transition metals offering an

alternative access towards stilbenes, which we used for the preparation of H-cyanostilbenes **17**, **18**, as well as F-cyanostilbenes **19** and **25**.

Cross-coupling reactions were carried out using a catalyst composed of Pd(OAc)<sub>2</sub>, P(*o*-tolyl)<sub>3</sub> each in 1 % molar ratio compared to the aryl halide. A slight excess (1.5 equivalents) of the appropriate styrene was employed. The reaction took place during refluxing over 12 h, in dry deoxygenated amine solvents. The progress of the reactions was monitored by GC-MS, which could also detect the formation of side products. Using the Heck coupling, previously tested on the preparation of H-stilbenes, good results and full conversion of the substrates (Scheme 10), were obtained. By applying this method on the fluorinated compounds, however, we observed only partial conversion of the olefinic substrate, when the entire brominated compound was consumed. In most of cases, traces of the reduced bromide were found.

These observations indicate that the olefin and the bromide are competing in the coordination sphere of Pd(0): coordination-insertion against oxidative addition. Albeniz *et al.* [22] observed that the reaction increases with higher concentration of styrene, favouring the oxidative addition process. However, a large excess can stop the reaction. Indeed, for tetrafluoroaryl and pentafluoroaryl bromides, these authors could prove that the coordination-insertion is rate determining, and can be switched to oxidative addition if a large excess of olefin is used. Thus, the best

reaction conditions can be reached by adjusting the actual ratio of halo-aryl to olefin for each combination of substrates. Working with a small olefin excess (1:1.5) led to **12** and **22** (Scheme 7). Despite these limitations, the authors reported about new catalytic systems for the Heck reaction using an efficient catalyst including fluorinated precursors [Pd(C<sub>6</sub>F<sub>5</sub>)Br(NCMe)<sub>2</sub>] and (NBu<sub>4</sub>)<sub>2</sub>[Pd<sub>2</sub>-μ-Br)<sub>2</sub>(C<sub>6</sub>F<sub>5</sub>)Br<sub>2</sub>].

**Scheme 7** Heck-coupling for the preparation of **17**, **19**, **25** and **28**: (m) Pd(OAc)<sub>2</sub>, NEt<sub>3</sub>/P(*o*-tolyl)<sub>3</sub>, dioxane, reflux; (n) Pd(OAc)<sub>2</sub>, NEt<sub>3</sub>/P(*o*-tolyl)<sub>3</sub>, CH<sub>3</sub>CN reflux.

The competition between the HWE and the Heck approach depends on the ease of the corresponding precursors preparation, and the robustness of the reaction protocols for these substrates, often altered in their reactivity if compared to their H-analogues.

For the Heck coupling, the precursors are most of all 4-halogenated-tetrafluoro-styrenes, which may be obtained over several reaction steps [23] (Scheme 8). While, for the HWE-approach, the different 4-bromo- and chloro-tetrafluoro-benzaldehydes are often easily accessible by nucleophilic substitution of the commercially available pentafluoro-benzaldehyde (Schemes 3 and 4).

**Scheme 8** Synthesis of 4-halo-2,3,5,6-tetrafluoro-styrene **32**: (o) Mg, THF; (p) CH<sub>3</sub>-CHO/THF; (q) distilled over P<sub>2</sub>O<sub>5</sub>.

All the obtained stilbenes were identified by  $^1\text{H-NMR}$ ,  $^{13}\text{C-NMR}$  and  $^{19}\text{F-NMR}$  spectroscopy. The chemical displacements of olefinic protons  $\text{H}_a$  and  $\text{H}_b$  and their doublet multiplicities ( $\delta = 6.57\text{-}7.46$  and  $6.97\text{-}7.60$  with large coupling constants of about  $J = 16$  Hz), were found by  $^1\text{H NMR}$ , which are specific for *trans*-stilbenes.

The UV spectra of the perfluorinated  $\text{X-C}_6\text{F}_4\text{-CH=CH-C}_6\text{F}_4\text{-CN}$  series (**25**, **26**, **27**) as well as the partial fluorinated  $\text{X-C}_6\text{F}_4\text{-CH=CH-C}_6\text{H}_4\text{-CN}$  (**19**, **20**, **21**) analogues showed a hypsochromic shift (blue shift) compared to the H-homologues  $\text{X-C}_6\text{H}_4\text{-CH=CH-C}_6\text{H}_4\text{-CN}$  (**16**, **17**, **18**). In contrast, the series  $\text{X-C}_6\text{H}_4\text{-CH=CH-C}_6\text{F}_4\text{-CN}$  (**22**, **23**, **24**) showed a bathochromic shift (red shift) compared to the H-homologues (**16**, **17**, **18**). This is due to the inversion of the charge distribution, which has been described in our previous work on the subject, calculated for the bromo derivatives [3]. Indeed, when the acceptors (CN or F) are placed on one side of the benzene ring (**22**, **23**, **24**), making up the largest dipole moment, a red shift took place. Whereas in all cases where the acceptors are placed on both aromatic rings (**19**, **20**, **21** and **25**, **26**, **27**; dipole moment being smaller) a blue shift was observed.

## 2.5 Crystal structures (see Table 2, 3)

### (*E*)-4-(4-fluorostyryl)-benzonitrile **16**

Compound **16** crystallized in the non-centrosymmetric space group  $P2_1$  (Figs. 1-3). It forms crystals showing a typical

herringbone pattern with nearly orthogonal oriented planes ( $79.26^\circ$ ). The packing of this molecule undergoes some orientational disorder over two positions for F and CN. For clarity on the graph-set drawing, the F atom is omitted, as it does not create any special interaction with other atoms. At a first look (first level graph-set), the crystal structure is characterized by H-bonding between  $\text{C}_{\text{Ph}}\text{-H}$  and the cyano group or the F atom of adjacent molecules, forming endless molecular chains, which are described as C1,1(12) and C1,1(23) creating parallel chains and C1,1(12) creating a herringbone pattern ( $\text{C-H}\cdots\text{N}$  2.685 Å). At the second level graph-set, molecules generate ring patterns R2,2(10) or R2,2(9) created through the same two  $\text{C-H}\cdots\text{N}$  hydrogen bonds (2.431 Å and 2.465 Å) and  $\text{C-H}\cdots\text{F}$  motives (3.016 Å and 3.069 Å) between two adjacent molecules as for the parallel chains. The stacks along the *a*-axis are held together through  $\text{CN}\cdots\text{Ph}$ ,  $\text{F}\cdots\text{Ph}$  and  $\text{C=C}\cdots\text{Ph}$  interactions ( $d_{\text{min}} = 3.49$  Å) and hydrogen bonds, with an interlayer distance of 3.451 Å.

**Figure 1.** View of **16** along the *c*-axis, through the *ab*-plane.

**Figure 2.** View of **16** crystal packing related to its graph-set drawing (Figure 3).

**Figure 3a.** View of **16** crystal structure graph-set, showing the herringbone pattern through  $\text{CN}\cdots\text{H}$  bonds.

**Figure 3b.** View of **16** crystal structure graph-set, showing endless chains formed by  $\text{CN}\cdots\text{H}$  and  $\text{F}\cdots\text{H}$  contacts.

#### **(E)-4-(4-chlorostyryl)-benzonitrile 17**

Compound **17** crystallized in a centric space group  $P2_1/c$  (Fig. 4). The structure is similar to that of **16**, *i.e.* molecules are arranged in parallel chains aligned by short  $\text{CN}\cdots\text{H}$  and  $\text{Cl}\cdots\text{H}$  bonds (2.470 Å and 2.908 Å).  $\text{CH}_8\text{Cl}$  **17** shows a typical herringbone structure with nearly orthogonally oriented planes (76.15°). Stacking along the *c*-axis is held through  $\text{CN}\cdots\text{H}$  bonds (2.736 Å). Similarly to molecule **16**, the crystal structure of **17** reveals orientational disorder over two positions of Cl and CN. However, contrary to F, Cl produces intermolecular contacts in the packing. Therefore, 3 different graph-set drawings (Figs 4) are presented below to resume these interactions. These representations reveal similar infinite chains C1,1(12), C1,1(23) and rings R2,2(10), R2,2(9). However, some extra features appear in the first and second level graph set such as C1,1(5), C1,1(11), C1,1(7) and R2,2(8), mainly due to the Cl atom replacing the F atom in **16**.

**Figure 4a.** View of **17** crystal structure graph-set, showing a 3D network built by  $\text{Cl}\cdots\text{H}$  bonds.

**Figure 4b.** View of **17** crystal structure graph-set, showing the herringbone pattern through  $\text{CN}\cdots\text{H}$  bonds.

**Figure 4c.** View of **17** crystal structure graph-set, showing endless chains formed by  $\text{CN}\cdots\text{H}$  and  $\text{F}\cdots\text{H}$  contacts.

#### **(E)-4-(4-iodostyryl)-benzonitrile 18**

Compound **18** crystallized in the centric space group  $P2_1/n$  (Figs. 5, 6). The molecules form antiparallel helicoidal endless chains through  $\text{CN}\cdots\text{I}$  contacts (3.261 Å, 172.06°) described at the first level graph-set as C1,1(13). The individual molecules also exhibit a dihedral angle between the phenyl rings of 16.48°. The chains are connected by very short interplanar  $\text{H}\cdots\text{I}$  bonds (3.162 Å), creating another infinite chain C1,1(10), resulting in an interlayer distance of 3.440 Å.

**Figure 5.** View of **18** along the *a*-axis, through the *bc*-plane.

**Figure 6.** View of **18** crystal structure graph-set, showing a 3D network built by  $\text{CN}\cdots\text{I}$  and  $\text{I}\cdots\text{H}$  contacts.

#### **(E)-4-(4-fluoro-2,3,5,6-tetrafluorostyryl)-benzonitrile 19**

Compound **19** crystallized in the centric space group  $P2_1/c$  with 2 independent molecules in the unit cell (Figs. 7, 8). Again, this compound forms crystals showing a typical herringbone structure with nearly orthogonally oriented planes (77.48° and 77.95°) created by infinite chains C1,1(10), C2,2(15), C2,2(16), C2,2(18), C2,2(19) and rings R1,2(7), R2,2(9). Molecules are stacked in endless head to head chains through strong  $\text{CN}\cdots\text{H}$

(2.645 Å and 2.649 Å) and F $\cdots$ F (2.708 Å and 2.836 Å) contacts as described at the second level graph-set by 2 rings R2,2(8), R2,2(10). Additional F $\cdots$ H (2.598 Å, 2.609 Å, 2.620 Å and 2.633 Å) and F $\cdots$ F (2.832 Å, 2.881 Å, 2.933 Å and 2.937 Å) interactions with neighboring molecules form a 3D network. Parallel chains are stacked and held together through CN $\cdots$ Ph, F $\cdots$ Ph and C=C $\cdots$ Ph interactions with interlayer distances as short as 3.4-3.6 Å. Molecules are also packed in parallel and antiparallel pairs through similar interactions.

**Figure 7.** View of **19** along the *a*-axis, through the *bc*-plane.

**Figure 8a.** View of **19** crystal structure graph-set, showing a 3D network built by F $\cdots$ H, F $\cdots$ F, CN $\cdots$ H interactions.

**Figure 8b.** View of **19** crystal structure graph-set, showing the herringbone pattern through CN $\cdots$ H and F $\cdots$ H contacts.

#### **(*E*)-4-(4-chloro-2,3,5,6-tetrafluorostyryl)-benzonitrile 20**

Compound **20** crystallized in the centrosymmetric space group  $P2_1/c$  (Figs. 9, 10). Molecules are packed in a similar manner as for compound **16** and **17**, *i.e.* crystals show a typical herringbone structure created by R2,2(13) rings. However, in the case of compound **20**, the planes dihedral angle is far from orthogonal (165.42°). Adjacent molecules are stacked in 2D antiparallel layers

through short CN $\cdots$ H (2.548 Å), F $\cdots$ H (2.467 Å and 2.546 Å) bonds and by head to edge Cl $\cdots$ F (2.977 Å) contacts that form infinite chains such as C1,1(6), C1,1(9), C2,2(12), C2,2(15), C2,2(17) and C2,2(18). These layers are connected by short F $\cdots$ F (2.840 Å) and C $\cdots$ F (3.109 Å) interactions to form a 3D network described in the graph-set by endless chains C1,1(5), C1,1(6) and rings R4,4(18).

**Figure 9.** View of **20** along the *c*-axis, through the *ab*-plane.

**Figure 10a.** View of **20** crystal structure graph-set, showing the herringbone pattern through CN $\cdots$ H and F $\cdots$ H contacts.

**Figure 10b.** View of **20** crystal structure graph-set, showing a tetramer built by Cl $\cdots$ F and F $\cdots$ F interactions.

#### **(*E*)-4-(4-iodo-2,3,5,6-tetrafluorostyryl)-benzonitrile 21**

Compound **21** crystallized in the centric space group  $P\bar{1}$  (Figs. 11, 12). The CH<sub>4</sub>F<sub>4</sub>I molecules form endless C1,1(13) chains through short CN $\cdots$ I contacts (2.997 Å, 174.85°). These chains are arranged in a 2D networks through F $\cdots$ H bonds (2.568 Å and 2.633 Å), creating in the first level of the graph-set endless chains C1,1(9), C1,1(10), C2,2(11) and C2,2(19), which are related by an inversion center. These planes are stacked by C $\cdots$ F (3.051 Å and 3.127 Å) interactions and feature an interlayer distance of 3.121 Å.

**Figure 11.** View of **21** along the *b*-axis, through the *ac*-plane.

**Figure 12.** View of **21** crystal structure graph-set, showing a 2D network built by F $\cdots$ H, and CN $\cdots$ I contacts.

**(E)-4-(4-fluorostyryl)-2,3,5,6-tetrafluorobenzonitrile 22**

Compound **22** crystallized in the centric space group  $P\bar{1}$  (Figs. 13, 14). Molecules form parallel chains aligned by short CN $\cdots$ H bonds (2.499 Å), building antiparallel 2D networks through F $\cdots$ H bonds (2.559 Å, 2.628 Å and 2.633 Å). All these D-H $\cdots$ A hydrogen bonds create (see graph set) several rings and infinite chains like R2,2(8), R2,2(20), R4,2(12), R4,4(20), C1,1(12), C2,1(14), C2,2(10), C2,2(12), C2,2(14), C2,2(16) and C2,2(20). The molecular planes are stacked by short F $\cdots$ F (2.857 Å) and C $\cdots$ F (3.090 Å) and show an interplanar distance of 3.340 Å.

**Figure 13.** View of **22** along the *a*-axis, through the *bc*-plane.

**Figure 14a.** View of **22** crystal structure graph-set, showing di and trimers built by F $\cdots$ H bonds.

**Figure 14b.** View of **22** crystal structure graph-set, showing bi, tri, tetra and hexamers built by F $\cdots$ H bonds.

**(E)-4-(4-chlorostyryl)-2,3,5,6-tetrafluorobenzonitrile 23**

Similarly to compounds **17** and **20**, **23** crystallized in the centrosymmetric space group  $P2_1/c$ . Molecules are (like for **17** and **20** Fig. 15), arranged in a typical herringbone packing and form antiparallel chains, aligned by short CN $\cdots$ H (C1,1(12)) and Cl $\cdots$ F bonds (2.604 Å and 3.073 Å). The herringbone structure, described on the graph set by endless chains C2,2(12) and C2,2(18), has nearly orthogonal oriented planes (70.28°). The packing displays flattened tetramers held together through F $\cdots$ F short contacts (2.757 Å and 2.773 Å), and other tetramers connected by F $\cdots$ F short contacts (2.773 Å), F $\cdots$ H bonds (2.616 Å) and Ph $\cdots$ Ph interactions. The antiparallel chains are stacked by CN $\cdots$ Ph, Cl $\cdots$ Ph and C=C $\cdots$ Ph interactions and short F $\cdots$ F short contacts (3.092 Å), giving an interplanar distance of 3.471 Å. A 3D network appears through short F $\cdots$ H bonds (2.616 Å and 2.631 Å).

**Figure 15.** View of **23** crystal structure graph-set, showing the herringbone pattern through F $\cdots$ H bonds.

**(E)-4-(4-iodostyryl)-2,3,5,6-tetrafluorobenzonitrile 24**

This compound crystallized in the non-centrosymmetric space group  $Cc$  (Figs. 16, 17) with three molecules per asymmetric unit. Among these series of compounds, this is the only polar space group, also confirmed by a

second harmonic generation (SHG) powder test. The architecture of **24** is dominated by short CN $\cdots$ I bonds (3.260 Å, 171.75°; 3.188 Å, 163.71°; 3.170 Å, 163.62°) forming antiparallel endless chains (C1,1(13) along the *b*-axis. The packing displays a 2D network perpendicular to the *ac*-plane, held together by short CN $\cdots$ I, F $\cdots$ H bonds (2.446 Å, 2.615 Å, 2.701 Å and 2.745 Å) and F $\cdots$ F contacts (2.821 Å). The 3D structure displays a parallel arrangement of planes in an offset stacked geometry with interplanar distances as short as 3.20 Å and short F $\cdots$ F contacts (2.881 Å and 2.933 Å). The polarity of this sample is explained by the molecular arrangement in the crystal structure and specially the molecular dipoles determined physically (see Fig. 16b). Consequently, one can observe a resulting polarity vector along the *c*-axis.

**Figure 16a.** View of **24** along the *b*-axis, through the *ac*-plane.

**Figure 16b.** View of **24** along the *a*-axis, onto the *bc*-plane showing net polarity along the *c*-axis. The arrows represent polar vectors, which remain under application of point symmetry.

**Figure 17a.** View of **24** crystal structure graph-set, showing a 3D network built by F $\cdots$ H and CN $\cdots$ I interactions.

**Figure 17b.** View of **24** crystal structure graph-set, showing endless chains formed by F $\cdots$ H contacts.

### **(*E*)-4-(4-fluoro-2,3,5,6-tetrafluorostyryl)-2,3,5,6-tetrafluorobenzonitrile 25**

This compound **25** crystallizes in the centrosymmetric space group *C2/c* (Figs. 18, 19). The molecules are packed in a flattened herringbone structure, which shows molecules arranged as head to head pairs, through F $\cdots$ F interactions (2.894 Å) creating rings R2,2(8) in the graph set. These pairs of molecules are connected side by side to their neighboring pairs by other F $\cdots$ F contacts (2.849 Å, 2.864 Å, 2.880 Å and 2.903 Å), forming parallel offset 2D layers described by many infinite chains and rings, orthogonal to the *bc*-plane at an interlayer distance of 3.143 Å. The herringbone structure has again nearly orthogonally oriented planes (79.26°) that are stacked along the *b*-axis by a CN $\cdots$ Ph head to edge interaction (3.086 Å).

**Figure 18.** View of **25** along the *a*-axis, through the *bc*-plane.

**Figure 19.** View of **25** crystal structure graph-set, showing a 2D network built by F $\cdots$ F interactions.

### **(*E*)-4-(4-chloro-2,3,5,6-tetrafluorostyryl)-2,3,5,6-tetrafluorobenzonitrile 26**

Compound **26** crystallized in the centrosymmetric space group *C2/c* (Fig. 20). The structure and graph set are similar to compound **25**, *i.e.* molecules are packed in a flattened herringbone structure. Indeed, molecules are piled as head to head pairs in a similar manner to **25**, by Cl $\cdots$ F interactions

(3.178 Å and 3.203 Å). These pairs of molecules are connected side by side to their neighboring pairs by other F $\cdots$ F contacts (2.886 Å, 2.888 Å, 2.919 Å and 2.922 Å), forming parallel offset 2D layers, orthogonal to the *bc*-plane at an interlayer distance of 3.112 Å. The herringbone structure has again nearly orthogonally oriented planes (78.62°) that are stacked along the *b*-axis by a CN $\cdots$ Ph head to edge interaction (3.110 Å).

**Figure 20.** View of **26** crystal structure graph-set, showing a 2D network built by F $\cdots$ F and Cl $\cdots$ F interactions.

**(*E*)-4-(4-iodo-2,3,5,6-tetrafluorostyryl)-2,3,5,6-tetrafluoro benzonitrile 27**

In contrary to **25** and **26**, compound **27** crystallized in the centric space group  $P\bar{1}$  (Fig. 21). The packing is dominated by CN $\cdots$ I bonds (3.042 Å, 172.47°), defining a 1D molecular chain C1,1(13). The additional short F $\cdots$ F contacts (2.745 Å, 2.906 Å, 2.925 Å and 2.930 Å) form 2D layers parallel to the *bc*-plane, described at the first level in the graph-set by endless chains like C1,1(8), C1,1(10), C2,2(17) and C2,2(18). Each plane is antiparallel to its neighbor with an interlayer distance of about 3.20 Å. Layers are held together by I $\cdots$ Ph (3.732 Å), F $\cdots$ Ph (3.656 Å) and F $\cdots$ F (2.927 Å) contacts. A 3D-network is built-up by several infinite chains and rings as shown in the graph-set.

**Figure 21a.** View of **27** crystal structure graph-set, showing a 2D network built by F $\cdots$ F and CN $\cdots$ I contacts.

**Figure 21b.** View of **27** crystal structure graph-set, showing a 2D network built by F $\cdots$ F contacts.

**Co-crystallization of stilbenes**

**[16•25]**

The molecular formula of this co-crystal **[16•25]** should be read as {[C<sub>15</sub>H<sub>10</sub>NF][C<sub>15</sub>H<sub>2</sub>NF<sub>9</sub>]}. Similarly to compounds **17** and **23**, **[16•25]** crystallized in the centrosymmetric space group  $P2_1/c$  (Fig. 22). Molecules are arranged in similar fashion as for compound **16**, *i.e.* molecules form a typical herringbone structure with nearly orthogonally oriented planes (77.01°). The molecular packing revealed some orientational disorder over two group positions for F and CN. The molecules are arranged in parallel chains aligned by short CN $\cdots$ H (2.625 Å) and CN $\cdots$ F (2.247 Å) bonds, at an interlayer distance of 3.468 Å. The stacks along the *a*-axis are held together through CN $\cdots$ Ph, F $\cdots$ Ph and C=C $\cdots$ Ph interactions with  $d_{\min} = 3.48$  Å, supported by F $\cdots$ F (2.468 Å, 2.706 Å and 2.843 Å) and CN $\cdots$ F (2.638 Å and 2.781 Å) contacts. One should note that molecule **16** seems to have imposed its structural symmetry to compound **25** in the co-crystal **[16•25]**.

**Figure 22.** View of compound **[16•25]** and its orientational disorder, PLUTON and Ortep [24] drawing at 50 % probability.

**[17•26]**

The molecular formula of co-crystal **[17•26]** should be read as  $\{[C_{15}H_{10}NCl][C_{15}H_2NF_8Cl]\}$ . Compound **[17•26]** also crystallized in the space group  $P2_1/c$ . Molecules are arranged in the same fashion as for compound **[16•25]**. Therefore, one can observe comparable interactions, interplanar angles and distances. A similar observation to compound **[16•25]** can be drawn on the imposed symmetry of **17** to compound **26** in the co-crystal. An additional observation confirms this hypothesis as the co-crystal melted at 181 °C, compared to the melting point of the pure components  $C_{15}H_2NClF_8$  **26** (136-137 °C) and  $C_{15}H_{10}NCl$  **17** (182-183 °C).

**[18•27]**

Similarly to compound **27**, co-crystal of  $\{[C_{15}H_{10}NI][C_{15}H_2NF_8I]\}$  **[18•27]** crystallized in the centric triclinic space group  $P\bar{1}$  (Fig. 23). Molecules are packed in the same fashion as for **27**, meaning that the latter forced molecule **18** to set into its structural architecture. Indeed, the melting point was lowered (188 °C) compared to the pure components **18** (197-198 °C) and **27** (200-201 °C), respectively. However, in contrary to the crystal structure of **27** and co-crystals **[16•25]** and **[17•26]**, here there are two independent molecules in the unit cell. One molecular site is occupied by compound **27** and the other one by **18**. Crystal packing is dominated by strong  $CN\cdots I$  contacts (3.142 Å,

176.53°; 3.214 Å, 177.53°) that arrange molecules in chains alternating **18** and **27** species and by edge to edge  $F\cdots H$  bonds (2.481 Å, 2.487 Å, 2.540 Å and 2.567 Å), forming antiparallel offset 2D layers with interplanar distance of 3.232 Å. Planes are stacked together by  $F\cdots CN$  (3.126 Å),  $F\cdots C=C$  (3.546 Å),  $F\cdots F$  (2.816 Å) and  $F\cdots Ph$  (3.345 Å) interactions.

**Figure 23.** View of **[18•27]** along the *b*-axis, through the *ac*-plane.

**[21•24]**

Co-crystal of  $\{[C_{15}H_4NF_4I][C_{15}F_4NH_4I]\}$  **[21•24]** crystallized in the triclinic polar space group  $P1$  (Fig. 24). One should notice that **24** also crystallized in a polar space group. There are two independent molecules in the unit cell. One of these molecular sites is fully occupied by compound **21** and the other position is shared in a 0.8:0.2 ratio by **21** and **24**. Crystal packing is dominated, by strong  $CN\cdots I$  contacts (3.014 Å, 172.66°; 3.031 Å, 168.93°; 3.152 Å, 171.28°) that arrange molecules in antiparallel chains, and by edge to edge  $F\cdots H$  bonds (2.421 Å, 2.479 Å, 2.576 Å, 2.618 Å and 2.653 Å),  $F\cdots F$  (3.161 Å, 3.204 Å, 3.424 Å and 2.973 Å) and  $F\cdots I$  (3.370 Å and 3.542 Å) interactions forming antiparallel offset 2D layers with interplanar distance of 3.232 Å. Planes are stacked together by  $F\cdots CN$  (3.340 Å, 3.388 Å and 3.479 Å),  $F\cdots I$  (3.405 Å, 3.650 Å and 3.705 Å),  $F\cdots F$

(2.948 Å and 3.001 Å) and F $\cdots$ Ph (Table 3) interactions. Effects of polarity are well established by second harmonic generation (SHG) experiments, showing a strong SHG effect for the co-crystal. The melting point of [21•24] is 193-195 °C, which is lower compared to those of the pure components NC-C<sub>6</sub>H<sub>4</sub>-C<sub>2</sub>H<sub>2</sub>-C<sub>6</sub>F<sub>4</sub>-I **21** (256 °C), NC-C<sub>6</sub>F<sub>4</sub>-C<sub>2</sub>H<sub>2</sub>-C<sub>6</sub>H<sub>4</sub>-I **24** (206 °C), respectively.

**Figure 24.** View of [21•24] along the *b*-axis, through the *ac*-plane.

The structures [16•25], [17•26] and [18•27] are showing almost no SHG effects, which may come up from preferential orientational defects. Here, the antiparallel alignment of the dipole moments may favour a non-polar structure. In the case of [21•24], there are complementary stacks without 180 °C orientational disorder. Adjacent chains take advantage of the complementary charge distribution in H- and F-aromatic compounds, thus inducing the formation of polar planes.

## 2.6 Melting behaviour of single compounds and co-crystals

We have recently published the crystal structure of new polyfluorinated (*E*)-4-(4-bromostyryl)-benzonitriles [3]. Here, we compare the motifs formed by interactions of at least two molecules of the single compounds of the halogenated stilbenes from F-, Cl-, Br- and I-derivatives.

The melting point of a solid depends mainly on the strength of the intermolecular interactions and this dependence cannot be easily quantified due to the numerous parameters affecting the crystal packing. Nevertheless, this thermal behaviour may be taken as an indication of developing specific and relatively strong intermolecular interactions. For instance, the fluoro-compound **16** containing CN $\cdots$ H interactions and forming a 10-member ring may explain a higher melting point (183-185 °C). The chloro derivative of **17** contains similar 10-member rings with N $\cdots$ H and Cl $\cdots$ H motifs and shows a relative high melting point (174-177 °C). In addition, the structures of **17** and **16** are isomorphic.

Br-C<sub>6</sub>H<sub>4</sub>-CH=CH-C<sub>6</sub>H<sub>4</sub>-CN [3] contains linear Br $\cdots$ Br chains with complementary Br $\cdots$ H and N $\cdots$ H motifs. In contrast, the iodo-analogue **18** forms linear chains with CN $\cdots$ I and interchain H $\cdots$ I motifs, but adjacent chains are oriented in an antiparallel mode. The high melting point of this compound (189-195 °C) seems to reflect the strength of these interactions.

**Scheme 9** graph-set of molecules **16**, **17** and **18**. 10-member rings being drawn by intermolecular interactions on compounds **16** and **17**.

The fluoro-compound **19** contains CN $\cdots$ H motifs forming 10-member rings. The chloro-analogue **20** forms 12-member rings interactions of F $\cdots$ Cl and F $\cdots$ H at the one side

and 12-member rings interactions of  $\text{CN}\cdots\text{H}$  and  $\text{H}\cdots\text{F}$  at the other side of the molecule.  $\text{Br-C}_6\text{F}_4\text{-CH=CH-C}_6\text{H}_4\text{-CN}$  and **21** are characterized by  $\text{CN}\cdots\text{Br}$  and  $\text{CN}\cdots\text{I}$  motifs. Both are isomorphous. The melting points of all these compounds are very high: 150-153 °C for **19**, 212-214 °C for **20** and 240 °C for **21**, respectively.

**Scheme 10** graph-set of molecules **19**, **20** and **21**. 10 and 12-member rings being drawn by intermolecular interactions on compounds **19** and **20**.

Fluoro- and chloro-derivatives **22**, **23**, and  $\text{Br-C}_6\text{H}_4\text{-CH=CH-C}_6\text{F}_4\text{-CN}$  contain the same  $\text{CN}\cdots\text{H}$  motif but different interhalogen motifs:  $\text{Cl}\cdots\text{F}$ ,  $\text{Br}\cdots\text{F}$  and  $\text{F}\cdots\text{F}$  interactions. Additionally  $\text{H}\cdots\text{F}$  interactions are observed. Compound **23** is isomorphous with  $\text{Br-C}_6\text{H}_4\text{-CH=CH-C}_6\text{F}_4\text{-CN}$ . Only **24** contains  $\text{CN}\cdots\text{I}$  motifs. Here also, the melting points are reflecting the strength of the cyclic interactions (9-member ring) of **23** (212-213 °C) and the strong linear  $\text{CN}\cdots\text{I}$  interactions of **24** (211-213 °C).

**Scheme 11** graph-set of molecules **22**, **23** and **24**. 9-member rings being drawn by intermolecular interactions on compound **23**.

The fluoro compound **25** contains only weak  $\text{F}\cdots\text{F}$  interactions forming a typical herringbone structure with lower melting point (84-87 °C). The chloro-compound **26** contains only  $\text{F}\cdots\text{Cl}$  motifs, arranged in an 8-member ring, (melting point is 136-138 °C).

Besides,  $\text{Br-C}_6\text{F}_4\text{-CH=CH-C}_6\text{F}_4\text{-CN}$  is isomorphous with the iodo analogue **27**, showing strong  $\text{CN}\cdots\text{Br}$  and  $\text{CN}\cdots\text{I}$  interactions. Lateral  $\text{F}\cdots\text{F}$  interactions are also present.

**Scheme 12** graph-set of molecules **25**, **26** and **27**. 8-member rings being drawn by intermolecular interactions on compounds **25** and **26**.

### Co-crystals

[**16•25**] represents an ordered centric structure with 1:1 stoichiometry based on 9-member ring  $\text{CN}\cdots\text{F}$  motifs (2.25 Å) and  $\text{N}\cdots\text{H}$  and  $\text{F}\cdots\text{F}$  interactions. The structure of [**17•26**] is very similar to this, featuring also 9-member ring  $\text{CN}\cdots\text{F}$ ,  $\text{CN}\cdots\text{H}$ ,  $\text{F}\cdots\text{F}$  and  $\text{Cl}\cdots\text{F}$  motifs. In contrast, the co crystals [**18•27**] (1:1) showed only linear  $\text{CN}\cdots\text{I}$  chains.

**Scheme 13** graph-set of co-crystals [**16•25**], [**17•26**] and [**18•27**]. 9-member rings being drawn by intermolecular interactions on compounds [**16•25**] and [**17•26**].

In [**21•24**] with a stoichiometry 9:1, we find strong interactions  $\text{CN}\cdots\text{I}$  (3.10 Å) complemented by the  $\text{H}\cdots\text{F}$  and  $\text{F}\cdots\text{F}$  contacts.

**Scheme 14** graph-set of co-crystal [**21•24**].

### 3. Experimental

#### 3.1 Analytical methods

$^1\text{H}$ -NMR,  $^{13}\text{C}$ -NMR and  $^{19}\text{F}$ -NMR were recorded on a Bruker AVANCE 300 or Bruker DRX400 spectrometer at a resonance frequency of 300 MHz ( $^1\text{H}$ ), 100 MHz or 75 MHz ( $^{13}\text{C}$ , decoupled) and 375 MHz ( $^{19}\text{F}$ ), respectively. Chemical shifts are reported in ppm, with the residual or with  $\text{CFCl}_3$  as external standard ( $^{19}\text{F}$ -NMR). IR spectra were recorded on a JASCO FT-IR 460 Plus in ATR modus. GC-MS analyses were performed on a Finnigan Trace GC-MS spectrometer with EI source (70 eV) and equipped with a siloxane-coated column.

#### 3.2 Materials

4-iodo-benzoylchloride, 4-fluoro-benzaldehyde, 4-chloro-benzaldehyde, 4-iodo-benzaldehyde, 4-bromo-benzonitrile, 1,2,4,5-tetrafluoro-benzene, 2,3,4,5,6-pentafluoro-benzaldehyde, 1,3,5,6 tetrafluoro-4-toluolic acid were purchased from Aldrich Chemical Company in *purum* quality and used without further purification.

All reactions were carried out under argon atmosphere. Triethylamine was distilled over  $\text{CaH}_2$  and degassed with argon. Dioxane was distilled over Na/benzophenone.

#### 3.3 General procedures

##### 3.3.1 Horner-Wadsworth-Emmons approach

###### Method A

A mixture of **13** or **14** (5 mmol), trimethylphosphite (2 ml, 17 mmol) and THF (10 ml) was heated to 150 °C for 2 h. After cooling with dry ice and acetone, a suspension in kerosene of NaH (60 wt %, 375 mg, 7.5 mmol) was added and after another 30 min, a solution of the aldehyde (5 mmol) in THF (5 ml) followed dropwise. The mixture was stirred overnight warming slowly to room temperature. After addition of water the mixture was extracted with methylene chloride (50 ml). The organic phase was subsequently washed with 1M NaOH (10 ml), brine and dried over  $\text{Na}_2\text{SO}_4$  and concentrated by evaporation to yield the product, which was purified by recrystallisation.

###### Method B

**13** or **14** (4.6 mmol) and trimethylphosphite (0.7 ml, 5.9 mmol) were heated for 4 h to 90 °C. After cooling, the reaction mixture containing the phosphonic acid dimethylester was diluted with absolute EtOH (4.20 ml) and mixed with a solution of the corresponding aldehyde (5.2 mmol) in EtOH (3.5 ml). A sodium ethanolate solution (sodium: 5.1 mmol, EtOH: 3.5 ml) was added dropwise during 10 min. After 20 h stirring at room temperature, the precipitate was filtered off at room temperature and rinsed with EtOH. The product was purified by recrystallisation.

##### 3.3.2 Heck approach

###### Method C

*E-4-(4-styryl)benzonitrile 25*

4-bromobenzonitrile (182 mg 1.0 mmol) with 20 mg Pd(OAc)<sub>2</sub>, 60 mg of P(o-tolyl)<sub>3</sub> were placed in a flask under argon atmosphere. 0.5 ml of NEt<sub>3</sub> and 0.2 ml styrene in 5.0 ml dioxane (distilled over Na) was added and stirred under reflux over 12 h. The reaction was quenched with 50 ml sat. NH<sub>4</sub>Cl solution, filtered over Cellite and the residue extracted with 50 ml ether, washed with saturated NaCl solution, dried over MgSO<sub>4</sub> and the solvent distilled. The dark brown residue was purified by sublimation in vacuum to yield 1.4 g (80 %) of the desired product. Mp.: 120-121 °C; <sup>1</sup>H NMR (300 MHz, CDCl<sub>3</sub>): δ 7.09 (1H, d, *J* = 17 Hz), 7.22 (1H, d, *J* = 17 Hz), 7.3-7.5 (5H, m), 7.57-7.64 (4H, dd), *J* = 8.6 Hz); <sup>13</sup>C NMR (100 MHz, CDCl<sub>3</sub>): δ 111.2, 117.9, 127.9, 132.5, 133.3.

*4-chloro-2,3,5,6-tetrafluorobenzaldehyde 5*

Pentafluorobenzaldehyde (3.92 g, 20 mmol) and LiCl (0.93 g, 22 mmol) were dissolved in absolute *N*-methylpyrrolidone (30 ml) and heated under vigorous stirring for 3 h to 150 °C. The hot brown reaction mixture was poured under stirring into crushed ice (150 g). Methylene chloride (200 ml) was added. The organic phase was washed with brine, dried (MgSO<sub>4</sub>) and distilled under high vacuum. The crude product was sublimated to give 2.13 g, (50 %) of an orange solid. Mp.: 101-103 °C; <sup>1</sup>H NMR (300 MHz, CDCl<sub>3</sub>): δ 10.22 (1H, s), *J* = 1.3 Hz; <sup>13</sup>C NMR (75 MHz, CDCl<sub>3</sub>): δ 182, 149.9, 148.3, 117.2, 112.2; <sup>19</sup>F

NMR (375 MHz, CDCl<sub>3</sub>): δ -139.52 (m, 2F), -144.67 (m, 2F); GC-MS (EI) *m/z* (rel. int.), 211(M<sup>+</sup>, 79), 183 (24), 149 (22), 133 (37), 99 (100), 79 (42), 42 (67).

*4-(bromomethyl)-2,3,5,6-tetrafluorobenzonitrile 13*

2,3,5,6-tetrafluoro-4-methyl-benzonitrile (4.5 g, 23.8 mmol) and dibenzoyl-peroxyde (0.1 g, 0.4 mmol) were dissolved in dry CCl<sub>4</sub> (50 ml). NBS (6.35 g, 35.7 mmol) was added. The yellow suspension was then heated to reflux for 65 h under irradiation with a 300 W photo lamp. After cooling to room temperature, methylene chloride (30 ml) was added and the organic phase was washed with aqueous sodiumthiosulfate solution, dried (MgSO<sub>4</sub>) and concentrated under high vacuum. The crude product, orange oil, (5.90 g, 92 %) was distilled under high vacuum (70-85 °C) with a Büchi Kugelrohr apparatus to give a white liquid, which solidified at room temperature (5.70 g, 89 %). Mp.: 35 °C; <sup>1</sup>H NMR (300 MHz, CDCl<sub>3</sub>): δ 4.51 (2H, t, *J* = 1.3 Hz); <sup>13</sup>C NMR (100 MHz, CDCl<sub>3</sub>): δ 150.9, 146.9, 121.4, 106.9, 89.1; <sup>19</sup>F NMR (375 MHz, CDCl<sub>3</sub>): δ -132.17 (2F, m), -139.59 (2F, m); GC-MS (EI) *m/z* (rel. int.) 268 (M<sup>+</sup>, 100), 187 (29), 168 (20), 137 (18), 81 (19), 79 (25).

*(E)-4-(4-fluorostyryl)benzonitrile 16*

*Method A*: 930 mg (42 %), *method C*: 350 mg (85 %). Mp.: 183-185 °C, λ<sub>max</sub> (CH<sub>2</sub>Cl<sub>2</sub>)/nm 322 (25000); IR (KBr) cm<sup>-1</sup>: ν 2228 (nitrile), 1600 (C=C), 1482, 1464 (aromatic), 1405,

1070 (C-F), 960 (trans C=C), 870, 854, 825, 651, 619;  $^1\text{H}$  NMR (300 MHz,  $\text{CDCl}_3$ ):  $\delta$  7.00 (1H, d,  $J = 16.1$  Hz), 7.07 (1H, m,  $J = 8.8$  Hz), 7.09 (1H, m,  $J = 8.5$  Hz), 7.17 (1H, d,  $J = 16.8$  Hz), 7.49 (1H, m,  $J = 4.2$  Hz), 7.51 (1H, m,  $J = 3.9$  Hz), 7.56 (2H, m,  $J = 8.2$  Hz), 7.63 (2H, m,  $J = 8.5$  Hz);  $^{13}\text{C}$  NMR (100 MHz,  $\text{CDCl}_3$ ):  $\delta$  110.64, 115.76, 115.98, 118.95, 126.77, 128.46, 128.54, 131.12, 132.49, 141.65, 164.10;  $^{19}\text{F}$  NMR (375 MHz,  $\text{CDCl}_3$ ):  $\delta$  -112.83 (1F, s.); GC-MS:  $m/z$  (EI) (rel. int) 223 ( $\text{M}^+$ , 100), 208 (28), 183 (14), 120 (16), 98 (17), 75 (32), 50 (24), 39 (13); HRMS (EI) for  $\text{C}_{15}\text{H}_{10}\text{NF}$  calculated: 223.07, found: 223.08.

*(E)-4-(4-chlorostyryl)benzotrile 17*

Method B: 1.25 g (56 %), Method C: 500 mg (70 %); Mp.: 174-177 °C,  $\lambda_{\text{max}}$  ( $\text{CH}_2\text{Cl}_2$ ) nm 329(48000); IR (KBr)  $\text{cm}^{-1}$   $\nu$  3050 (aromatic) 2220 (nitrile), 1600 (C=C), 1485, 1413 (aromatic), 1169, 1088, 1009 (C-F), 959 (trans C=C), 824, 670;  $^1\text{H}$ -NMR (300 MHz,  $\text{CDCl}_3$ ):  $\delta$  7.05 (1H, d,  $J = 16.4$  Hz.), 7.16 (1H, d,  $J = 16.4$  Hz.), 7.37 (2H, m,  $J = 8.5$  Hz), 7.47 (1H, m,  $J = 8.5$  Hz), 7.57 (1H, m,  $J = 8.3$  Hz.), 7.64 (1H, m,  $J = 8.7$  Hz.);  $^{13}\text{C}$  NMR (100 MHz,  $\text{CDCl}_3$ ):  $\delta$  110.81, 118.89, 126.87, 127.28, 128.02, 129.02, 131.00, 132.49, 134.28, 134.76, 141.43; GC-MS (EI)  $m/z$  (rel. int.) 239 ( $\text{M}^+$ , 74), 204 (100), 177 (22), 151 (18), 102 (21), 88 (51), 75 (29), 63 (15), 51 (18), 39 (10); HRMS (EI) for  $\text{C}_{15}\text{H}_{10}\text{NCl}$  calculated: 239.05, found: 239.05.

*(E)-4-(4-iodostyryl)benzotrile 18*

Method A: 1.09 g (70 %). Mp.: 189-195 °C,  $\lambda_{\text{max}}$  ( $\text{CH}_2\text{Cl}_2$ )/nm: 329 (67500); IR (KBr)  $\text{cm}^{-1}$ :  $\nu$  2800-3050 (aromatic), 2221 (nitrile), 1598 (C=C), 1500, 1482 (aromatic), 1397, 1326, 1172, 1058, 1004 (C-F), 972, 943 (trans C=C), 875, 824, 698;  $^1\text{H}$  NMR (300 MHz,  $\text{CDCl}_3$ ):  $\delta$  7.07 (1H, d,  $J = 16.4$  Hz), 7.13 (1H, d,  $J = 16.4$  Hz), 7.26 (2H, d,  $J = 8.3$  Hz), 7.56 (2H, d,  $J = 8.5$  Hz), 7.64 (2H, d,  $J = 8.5$  Hz), 7.71 (2H, d,  $J = 8.5$  Hz);  $^{13}\text{C}$  NMR (100 MHz,  $\text{CDCl}_3$ ):  $\delta$  94.13, 110.91, 118.89, 126.92, 128.48, 131.19, 132.51, 135.78, 137.95, 141.38; GC-MS  $m/z$  (EI) 331 ( $\text{M}^+$ , 100), 203 (82), 176 (37), 151 (15), 127 (16), 102 (19), 88 (31), 75 (25), 63 (19), 50 (26), 39 (11); HRMS (EI) for  $\text{C}_{15}\text{NH}_{10}\text{Na}$  calculated: 353.98, found: 353.97.

*(E)-4-(4-fluoro-2,3,5,6-tetrafluorostyryl)-benzotrile 19*

Method A: 470 mg (16 %), Method C in acetonitrile: 174 mg (30 %). Mp.: 150-153 °C,  $\lambda_{\text{max}}$  ( $\text{CH}_2\text{Cl}_2$ ) 312 nm: (52400); IR (KBr)  $\text{cm}^{-1}$ :  $\nu$  2800-3100 (aromatic), 2225 (nitrile), 1604 (C=C), 1494, 1413 (aromatic), 1228, 1009 (C-F), 960 (trans C=C), 877, 845, 734, 653. $\text{cm}^{-1}$ ;  $^1\text{H}$  NMR (300 MHz,  $\text{CDCl}_3$ ):  $\delta$  7.07 (1H, d,  $J = 17$  Hz), 7.41 (1H, d,  $J = 17$  Hz), 7.59 (1H, m,  $J = 8$  Hz), 7.66 (2H, m,  $J = 8$  Hz), 7.76 (1H, m,  $J = 8$  Hz);  $^{13}\text{C}$  NMR (100 MHz,  $\text{CDCl}_3$ ):  $\delta$  112.17, 116.36, 118.57, 127.32, 127.9, 132.6, 135.05, 136.18, 140.78, 143.38, 146.62;  $^{19}\text{F}$  NMR (375 MHz,  $\text{CDCl}_3$ ):  $\delta$  -142.3(m, 2F), -154.7(m) 1F, -162.6 (m) 2F; MS (EI)  $m/z$  (rel. int) 295 ( $\text{M}^+$ ,100), 275 (84),

244 (38), 226 (44), 192 (18), 122 (18), 75 (20), 50 (20); HRMS (EI) for  $C_{15}H_6NF_5$  calculated: 295.00, found: 295.04.

*(E)-4-(4-chloro-2,3,5,6-tetrafluorostyryl)-benzonitrile 20*

Method B: 0.41 g (57 %). Mp.: 185-187 °C,  $\lambda_{max}$  ( $CH_2Cl_2$ ) nm: 318 (62000); IR (KBr)  $cm^{-1}$ :  $\nu$  3000-3100 (aromatic), 2222 (nitrile), 1594, 1507 (C=C), 1417 (aromatic), 1230, 1175, 1158, 1096 (C-F), 969 (trans C=C), 835, 781;  $^1H$  NMR (300 MHz,  $CDCl_3$ ):  $\delta$  6.57 (1H, d,  $J = 16.8$  Hz), 6.67 (2H, m,  $J = 8.1$  Hz), 6.96 (2H, m,  $J = 8.5$  Hz), 6.97 (1H, d,  $J = 16.6$  Hz);  $^{13}C$  NMR (100 MHz,  $CDCl_3$ ):  $\delta$  143.8, 140.4, 136.1, 132.8, 127.6, 118.9, 118.4, 116.4, 113.1, 112.6;  $^{19}F$  NMR (375 MHz,  $CDCl_3$ ):  $\delta$  -141.2 (2F, m), -142.4 (2F, m); GC-MS (EI) m/z (rel. int.), 311( $M^+$ , 100), 291 (90), 275 (44), 257 (52), 226 (45), 138 (28), 123 (22), 99 (21), 75 (47), 50 (47); HRMS (EI) for  $C_{15}H_6NF_4Cl$  calculated: 311.01, found: 311.01.

*(E)-4-(4-iodo-2,3,5,6-tetrafluorostyryl)-benzonitrile 21*

Method B: 1.0 g (50 %). Mp.: 256°C;  $\lambda_{max}$  ( $CH_2Cl_2$ )/nm 324 (35000); IR (KBr)  $cm^{-1}$ :  $\nu$  3100-2800 (aromatic), 2229 (nitrile), 1600 (C=C), 1469 (aromatic), 1331, 1052 (C-F), 950 (trans C=C), 869, 817, 607;  $^1H$  NMR (300 MHz, acetone  $d_6$ ):  $\delta$  7.23 (1H, d,  $J = 16.8$  Hz), 7.50 (1H, d,  $J = 17.0$  Hz), 7.71 (2H, m,  $J = 8.7$  Hz), 7.80 (2H, m,  $J = 8.3$  Hz),  $^{13}C$  NMR (100 MHz,  $CDCl_3$ ):  $\delta$  79.18, 128.98,

130.09, 133.90, 207.28;  $^{19}F$  NMR (375 MHz,  $CDCl_3$ ):  $\delta$  -140.87 (2F), -123.04 (2F), MS: m/z (EI) 405.2 (1.3), 404.2 (18), 403.2 ( $M^+$ , 100), 402.0 (0.8) 226.2 (58). HRMS (EI) for  $C_{15}H_6NF_4I$  calculated: 402.95, found: 402.95.

*(E)-4-(4-fluorostyryl)-2,3,5,6-tetrafluorobenzonitrile 22*

Method A: 0.80 g (54 %). Mp.: 145-147 °C,  $\lambda_{max}$  ( $CH_2Cl_2$ ) nm: 328 (26100); IR (KBr)  $cm^{-1}$ :  $\nu$  2800-3100 (aromatic), 2240 (nitrile), 1626 (C=C), 1595, 1509, 1484 (aromatic), 1333, 1303, 1227, 1164, 1027, 1100 (C-F), 974, 945, 927 (trans C=C), 829, 643;  $^1H$  NMR (300 Mhz,  $CDCl_3$ ):  $\delta$  6.99 (1H, d,  $J = 16.8$  Hz), 7.09 (1H, m,  $J = 8.7$  Hz), 7.13 (1H, m,  $J = 8.5$  Hz), 7.54 (1H, m,  $J = 8.3$  Hz), 7.55 (1H, m,  $J = 8.9$  Hz), 7.61 (1H, d,  $J = 17.0$  Hz);  $^{13}C$  NMR (100 MHz,  $CDCl_3$ ):  $\delta$  29.69, 107.70, 112.27, 116.17, 129.23, 139.83, 162.48, 164.98;  $^{19}F$  NMR ( $CDCl_3$ ):  $\delta$  -140.64 (2F, m), -134.04 (2F, m), -110.29 (m, 1F), MS (EI) m/z (rel. int.) 295( $M^+$ , 64), 275 (100), 244 (25), 226 (20), 199 (8), 137 (8), 124 (11), 96 (38), 75 (32), 57 (24), 50 (22); HRMS (EI) for  $C_{15}H_6NF_5$  calculated: 295.04, found: 295.04.

*(E)-4-(4-chlorostyryl)-2,3,5,6-tetrafluorobenzonitrile 23*

Method A: 1.02 g (66 %). Mp.: 212-214 °C,  $\lambda_{max}$  ( $CH_2Cl_2$ )  $cm^{-1}$ : 332 (33100); IR (KBr)  $cm^{-1}$ :  $\nu$  2800-3100 (aromatic), 2244 (nitrile), 1619, 1590 (C=C), 1485 (aromatic), 1330, 1299, 1086, 1009 (C-F), 974 (trans C=C),

925, 817, 698, 642;  $^1\text{H}$  NMR (300 MHz,  $\text{CDCl}_3$ ):  $\delta$  7.05 (1H, d,  $J = 16.8$  Hz), 7.40 (2H, m,  $J = 8.5$  Hz), 7.51 (2H, m,  $J = 8.5$  Hz), 7.60 (1H, d,  $J = 16.8$  Hz);  $^{13}\text{C}$  NMR (100 MHz,  $\text{CDCl}_3$ ):  $\delta$  139.7, 136.0, 135.9, 134.1, 131.9, 129.2, 128.6, 126.1, 122.4, 118.1, 113.0, 107.6;  $^{19}\text{F}$  NMR (375 MHz,  $\text{CDCl}_3$ ):  $\delta$  -140.45 (m, 2F), -133.91 (m, 2F), GC-MS (EI) m/z (rel. int.) 311 ( $\text{M}^+$ , 97), 291 (46), 276 (82), 257 (48), 226 (100), 137 (26), 112 (37), 75 (40), 50 (33); HRMS (EI) for  $\text{C}_{15}\text{H}_6\text{NF}_4\text{Cl}$  calculated: 311.01, found: 311.01.

*(E)-4-(4-iodostyryl)-2,3,5,6-tetrafluorobenzonitrile 24*

Method A: 1.0 g (42 %). Mp.: 211-213 °C;  $\lambda_{\text{max}}$  ( $\text{CH}_2\text{Cl}_2$ )/nm: 339 (66300); IR (KBr)  $\text{cm}^{-1}$ :  $\nu$  2220 (nitrile), 1615 (C=C), 1582, 1485 (aromatic), 1329, 1300, 1059, 1005 (C-F), 980, 960 (trans C=C), 930, 808, 681, 640;  $^1\text{H}$  NMR (300 MHz,  $\text{CDCl}_3$ ):  $\delta$  7.06 (1H, d,  $J = 16.8$  Hz), 7.27 (1H, m,  $J = 8.2$  Hz), 7.53 (1H, d,  $J = 16.8$  Hz), 7.60 (1H, d,  $J = 8.5$  Hz), 7.74 (1H, dm,  $J = 8.5$  Hz);  $^{13}\text{C}$  NMR (100 MHz,  $\text{CDCl}_3$ ):  $\delta$  18.41, 30.89, 96.14, 107.61, 113.21, 128.89, 135.14, 138.21, 139.91;  $^{19}\text{F}$  NMR (375 MHz,  $\text{CDCl}_3$ ):  $\delta$  -140.37 (2F), -133.94 (2F); GC-MS: m/z (EI): 405.2 (1), 404.2 (13), 403.1 (100), 226.3 (100), 226.2 (58); HRMS (EI) for  $\text{C}_{15}\text{H}_6\text{NF}_4$  calculated: 402.95, found: 402.95.

*(E)-4-(4-fluoro-2,3,5,6-tetrafluorostyryl)-2,3,5,6-tetrafluorobenzonitrile 25*

Method B: 860 mg (51 %), Method C: 110 mg in dioxane (30 %). Mp.: 84-87 °C,  $\lambda_{\text{max}}$  ( $\text{CH}_2\text{Cl}_2$ )/nm: 312 (54000); IR (KBr)  $\text{cm}^{-1}$ :  $\nu$  2250 (nitrile), 1650, 1520 (C=C), 1491, 1422 (aromatic), 1339, 1302, 1153, 1137, 1110, 1020 (C-F), 961 (trans C=C), 721, 660, 613;  $^1\text{H}$  NMR (300 MHz,  $\text{CDCl}_3$ ):  $\delta$  7.39 (1H, d,  $J = 17.3$  Hz), 7.52 (1H, d,  $J = 17.1$  Hz);  $^{13}\text{C}$  NMR (100 MHz,  $\text{CDCl}_3$ ):  $\delta$  93.01, 107.24, 110.9, 120.8, 122.1, 125.03, 136.2, 139.55, 143.15, 145.62, 149.09;  $^{19}\text{F}$  NMR (375 MHz,  $\text{CDCl}_3$ ):  $\delta$  -161.8 (2F, m), -151.9 (1F, m), -141.3 (2F, m), -139.7 (2F, m), -133.2 (2F, m); GC-MS (EI) m/z: 367 (100), 298 (62), 192 (14), 168 (14), 123 (14), 99 (14), 75 (20), 50 (20); HRMS (EI) for  $\text{C}_{15}\text{H}_2\text{NF}_9\text{Na}$  calculated: 389.99, found: 389.99.

*(E)-4-(4-chloro-2,3,5,6-tetrafluorostyryl)-2,3,5,6-tetrafluorobenzonitrile 26*

Method B: 0.74 g (42 %). Mp.: 136-138 °C;  $\lambda_{\text{max}}$  ( $\text{CH}_2\text{Cl}_2$ ) nm 318 (65000); IR (KBr)  $\text{cm}^{-1}$ :  $\nu$  2222 (nitrile), 1650, 1630 (C=C), 1487, 1414 (aromatic), 1335, 1304 (C-F), 965 (trans C=C), 877, 654, 610;  $^1\text{H}$  NMR (300 Mhz,  $\text{CDCl}_3$ ):  $\delta$  7.37 (d, 1H,  $J = 17.1$  Hz), 7.49 (d, 1H,  $J = 17.1$  Hz);  $^{13}\text{C}$  NMR (100 MHz,  $\text{CDCl}_3$ ):  $\delta$  71.8, 103.1, 107.9, 113.1, 114.1, 121.3, 125.3, 142.8, 143.3, 146.2, 148.8;  $^{19}\text{F}$  NMR (375 MHz,  $\text{CDCl}_3$ ):  $\delta$  -161.8 (2F,m), -151.9 (2F,m), -141.2(2F,m), 139.7(2F,m), -133.1; MS (EI) m/z (rel. int.) 383( $\text{M}^+$ ,100), 329 (22), 298 (42), HRMS (EI) for  $\text{C}_{15}\text{H}_2\text{NF}_4\text{Cl}$  calculated: 383.01, found: 383.01.

*(E)*-4-(4-iodo-2,3,5,6-tetrafluorostyryl)-  
2,3,5,6-tetrafluorobenzonitrile **27**

Method A: 1.0 g (42 %). Mp.: 211 °C  $\lambda_{\max}$  (CH<sub>2</sub>Cl<sub>2</sub>)/nm: 326 (72000); IR (KBr) cm<sup>-1</sup>:  $\nu$  2252 (nitrile), 1645 (C=C), 1489, 1471 (aromatic), 1342, 1303 (C-F), 978, 959, 923 (trans C=C), 815, 650, 605; <sup>1</sup>H NMR (300 MHz, CDCl<sub>3</sub>):  $\delta$  7.46 (d, 1H, *J* = 17.1 Hz), 7.57 (d, 1H, *J* = 17.1 Hz); <sup>13</sup>C NMR (100 MHz, CDCl<sub>3</sub>):  $\delta$  128.09; <sup>19</sup>F NMR (375 MHz, CDCl<sub>3</sub>):  $\delta$  -140.29 (2F), -139.68 (2F), -133.33 (2F), -120.79 (2F); MS: *m/z* (EI) 477.2 (1), 476.2 (12), 475.1 (100), 298.2 (63); HRMS (EI) for C<sub>15</sub>H<sub>2</sub>NF<sub>8</sub>I calculated: 474.91, found: 474.91.

### 3.3.3. Co-crystals and solid solutions

*Co-crystal of (E)*-4-(4-fluorostyryl)benzonitrile **16** and *(E)*-4-(4-fluoro-2,3,5,6-tetrafluorostyryl)-2,3,5,6-tetrafluorobenzonitrile **25**

**16** (22 mg) and **25** (37 mg) were dissolved in dichloromethane. The solvent was evaporated under isothermal conditions and purged with nitrogen. GC-MS analysis for [**16**•**25**]: [1:1].

*Co-crystal of (E)*-4-(4-chlorostyryl)benzonitrile **17** and *(E)*-4-(4-chloro-2,3,5,6-tetrafluorostyryl)-2,3,5,6-tetrafluorobenzonitrile **26**

**17** (22 mg) and **26** (37 mg) were dissolved in dichloromethane. The solvent was evaporated under isothermal conditions and purged with nitrogen. The obtained crystals melted at 181 °C. GC-MS analysis for [**17**•**26**]: [1:1].

*Co-crystal of (E)*-4-(4-iodostyryl)benzonitrile **18** and *(E)*-4-(4-iodo-2,3,5,6-tetrafluorostyryl)-2,3,5,6-tetrafluorobenzonitrile **27**

**18** (22 mg) and **27** (37 mg) were dissolved in dichloromethane. The solvent was evaporated under isothermal conditions and purged with nitrogen. The obtained crystals melted at 188 °C. GC-MS analysis for [**18**•**27**]: [1:1].

*Co-crystal of (E)*-4-(4-iodo-2,3,5,6-tetrafluorostyryl)-benzonitrile **21** and *(E)*-4-(4-iodostyryl)-2,3,5,6-tetrafluorobenzonitrile **24**

**21** (22 mg) and **24** (37 mg) were dissolved in dichloromethane. The solvent was evaporated under isothermal conditions and purged with nitrogen. The obtained crystals melted at 193-195 °C. GC-MS analysis for [**21**•**24**]: [9:1].

### 3.4 Crystal Structure Determinations

Data were collected on a Stoe Imaging plate diffractometer system [25] equipped with a graphite monochromator. Data collection was performed at -120 °C using Mo K $\alpha$  radiation ( $\lambda$  = 0.71073 Å). The structure were solved by direct methods using SHELXS-97 [26] and refined by full matrix least-squares on *F*<sup>2</sup> with SHELXL-97 [27]. The hydrogen atoms were included in calculated positions and treated as riding atoms using SHELXL-97 default parameters. All non-hydrogen atoms were refined anisotropically. No absorption correction was applied for **16**, **17**, **19**, **20**, **22**, **23**, **25**, **26**, [**16**•**25**] and [**17**•**26**] ( $\mu$  < 1 mm<sup>-1</sup>). For all other structures either a semi-empirical

or an empirical absorption correction was applied using MULABS or DIFABS, respectively, as implemented in PLATON [28] ( $T_{\min}/T_{\max} = 0.523/0.629$  **18**,  $0.441/0.634$  **21**,  $0.383/0.619$  **24**,  $0.383/0.642$  **27**,  $0.452/0.882$  [**18•27**],  $0.408/0.711$  [**21•24**]).

#### 4. Summary and Conclusion

We have been using the HWE approach for the synthesis of *trans*-stilbenes and obtained exclusively *E*-stereoisomers with satisfactory yields. By applying the standard Heck coupling conditions we, however, obtained poor yields and side reactions.

Comparing the H-substituted and F-substituted structures we have observed a considerable difference. On the one side, the structures of the *p*-X-C<sub>6</sub>H<sub>4</sub>-CH=CH-C<sub>6</sub>H<sub>4</sub>-CN series (X = F, Cl, I) are very different from the analogous *p*-X-C<sub>6</sub>F<sub>4</sub>-CH=CH-C<sub>6</sub>F<sub>4</sub>-CN series (X = F, Cl, I), indicating that the fluorine substitution may change the packing structure completely. On the other hand the structures of the *p*-X-C<sub>6</sub>H<sub>4</sub>-CH=CH-C<sub>6</sub>F<sub>4</sub>-CN (X = F, Cl, I) molecules undergo also a different packing compared to *p*-X-C<sub>6</sub>F<sub>4</sub>-CH=CH-C<sub>6</sub>H<sub>4</sub>-CN (X = F, Cl, I) molecules, pointing out that the position of the fluorine substitution has a great influence on the formation of crystal-packing motifs: Fluorine substitution on the halogen side of the benzene ring enhances the acceptor nature of the halogen atoms (X), making the halogen bonding (XB) stronger. N⋯I distances of 3.04 Å were observed in the perfluorinated **27** and 2.99 Å in the partially fluorinated **21**. At

the contrary, fluorine substitution on the benzene ring carrying the CN group has the tendency to diminish the donor nature of the CN-group with longer distances (3.23 Å). However, all these distances are shorter than the sum of the Van der Waals radii (3.69 Å), which coincides with those reported in the literature for similar kinds of structures [8]. The fluorination on the benzene ring carrying the CN group (**24**) increases the strength of the intermolecular interactions (H⋯F bonds), reflected by higher melting point as compared to **18**. Contrary, the effect of fluorine substitution on the iodine side (**21**) strongly shortened the N⋯I interaction by improving the iodine acceptor character due to electron withdrawing, and consequently increases the melting point. Similarly to compounds **18** and **21** fluorination of the iodo side of **24** improves the N⋯I interactions in **27**, which is compensated by weak F⋯F intermolecular interactions instead of F⋯H bonding. Therefore, the melting point of **24** and **27** may not be really affected. In the same way, the higher melting point of **21** is due to the absence of fluorine atoms on the cyano side of the molecule and therefore may be due to the presence of H⋯F bonds, as compared to **27**.

An interesting comparison appearing in the literature [29] is the structure of 4'-bromo-2',3',5',6'-tetrafluorostilbazole, consisting of an infinite unimolecular network involving both interchain  $\pi$ - $\pi$  stacking and N⋯Br halogen bonding. Furthermore, the structure of halogenated tolans of general formula *p*-

$C_6H_4-C\equiv C-C_6F_5$  and  $p-C_6F_4-C\equiv C-C_6H_5$  ( $X = F, Cl, Br, I$ ) are characterized by arene-perfluoroarene, halogen-halogen interactions and herringbone packing [11].

The co-crystal [18•27] is formed with two species, which are connected through  $CN\cdots I$  chains having different distances 3.14 Å and 3.21 Å. The lower melting point (188 °C) of [18•27] indicates a different structure compared to the pure compounds **18** (195 °C) and **27** (211 °C). In the case of the co-crystal [17•26], interactions  $CN\cdots F$  (forming a 10-member ring) can be compared with those of  $CN\cdots H$  (forming a 9-member ring) of the pure compound **17**, because the melting points are very near (175 and 181 °C). In contrast to the interactions of the pure compound **16** ( $F\cdots F$  interactions) and **25** ( $CN\cdots H$  forming a 10 member ring), the co crystal [16•25] shows strong  $N\cdots F$  interactions (9 member ring), lower as the sum of van der Waals radii (2.89 Å).

The structure of [21•24] has been studied in details. It contains two molecular species (9:1) aligned in 1D polar chains  $CN\cdots I$ , located on two symmetrically independent sites, one site containing molecules of one species and the other site contains two molecules (8:2), related by an inversion center. The polarity of this structure was confirmed by a positive SHG effect and the polar space group  $P1$ . This may be related to the polar properties found also (i) **24** and (ii) in the solid solutions of [E-4-(4-bromostyryl)-2,3,5,6-

tetrafluorobenzonitrile)]<sub>x</sub>•[E-4-(4-bromo-2,3,5,6-tetrafluorostyryl)-benzonitrile]<sub>1-x</sub> that we had reported before [3].

In this context one should mention previous partially published work [30] on the polar structures of  $p-X-C_6F_4-CN$  ( $X = Cl, Br, I$ ) in which lateral fluorination was successful to promote the formation of polar structures. Qualitative measurements of an extended series confirmed that about 90 % of these structures were SHG active. However, this study shows clearly, that 8-/9- or 4-fault fluorination in stilbenes has effected only one polar structure (**24**) out of 12. In view of some design principles we have put forward recently [3], this is quite surprising.

### Acknowledgments

We thank PD Dr. Stefan Schürch for the mass spectrometry and elemental analyses. We thank the Regionale Arbeitsvermittlung Bern (Lukas Kaltenrieder) for technical assistance in syntheses.

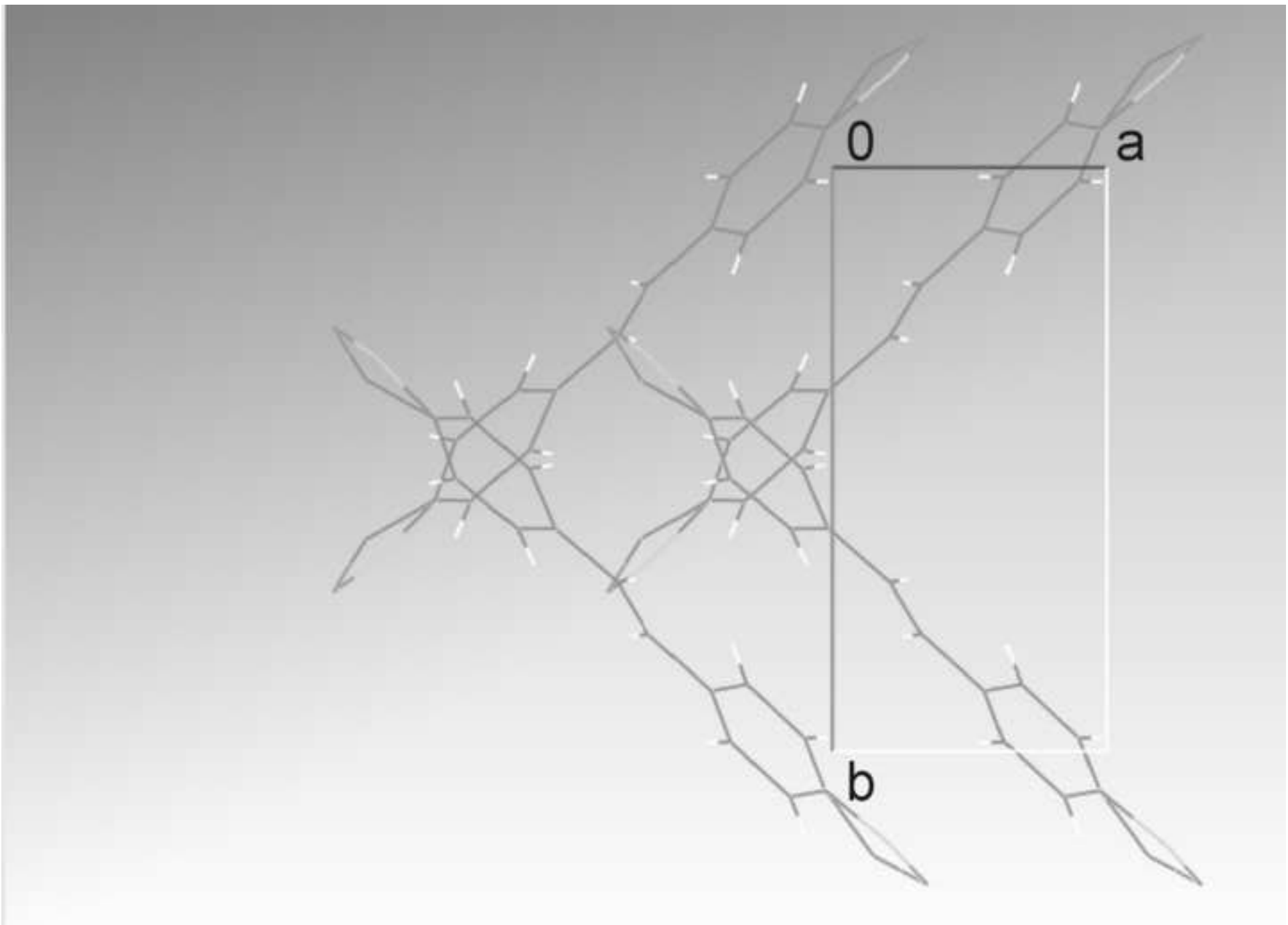
### References

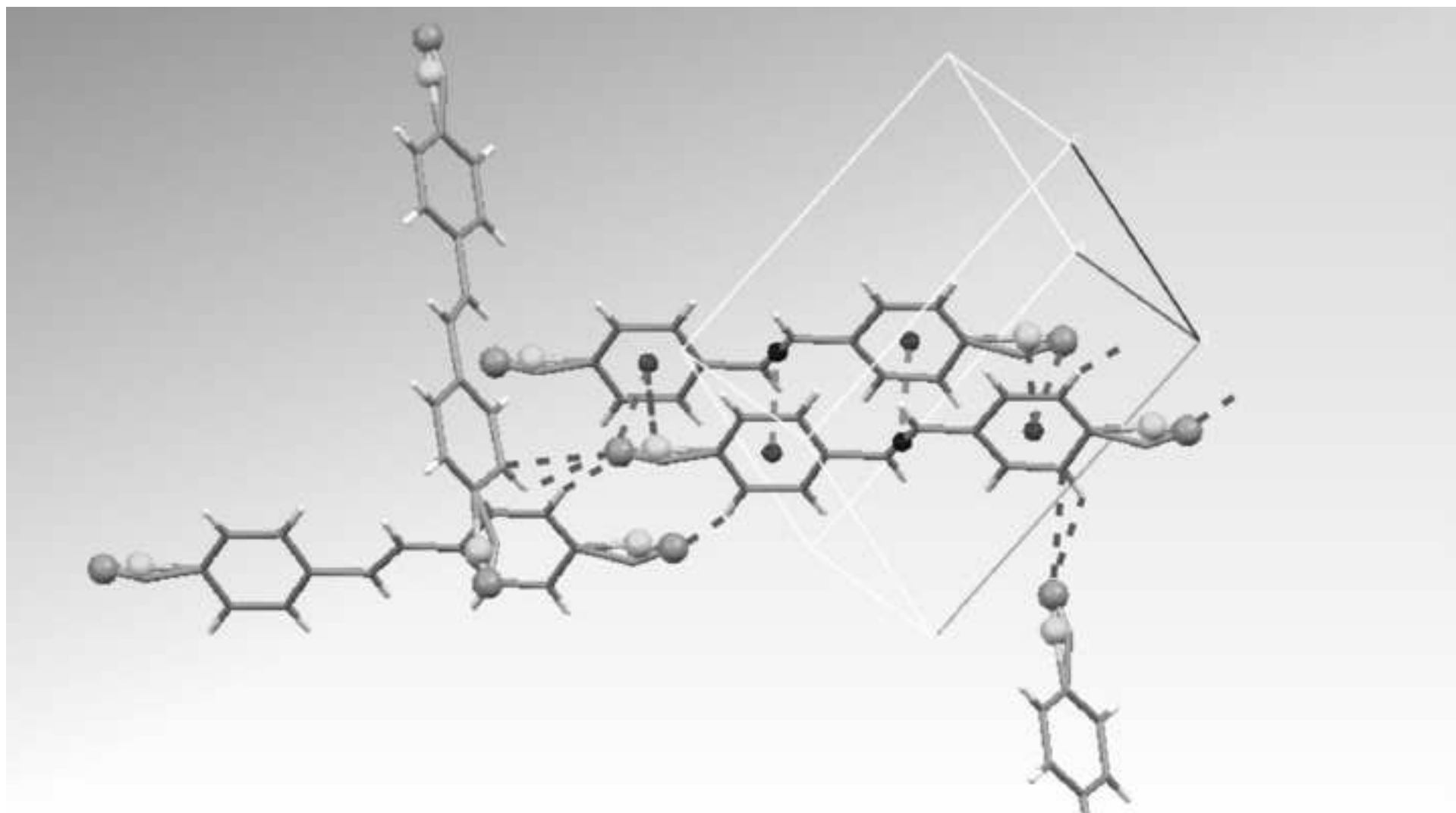
- 
- [1] G.P. Bartholomew, X. Bu, G.C. Bazan, Chem. Mater. 12 (2000) 2311-2318.
  - [2] J.C. Collings, A.S. Batsanov, J.A. K. Howard, D.A. Dickie, J.A.C. Clyburne, H.A. Jenkins, T.B. Marder, J. Fluorine Chem. 126 (2005) 515-519.
  - [3] R. Mariaca, N. Behrnd, P. Egli, H. Stoeckli-Evans, J. Hulliger, Cryst. Eng. Comm. 8 (2006) 222-232.
  - [4] C.B. Aakeröy, J. Desper, B.A. Helfrich, P. Metrangolo, T. Pilati, G. Resnati and A. Stevenazzi, Chem. Commun. (2007) 4236-4238.

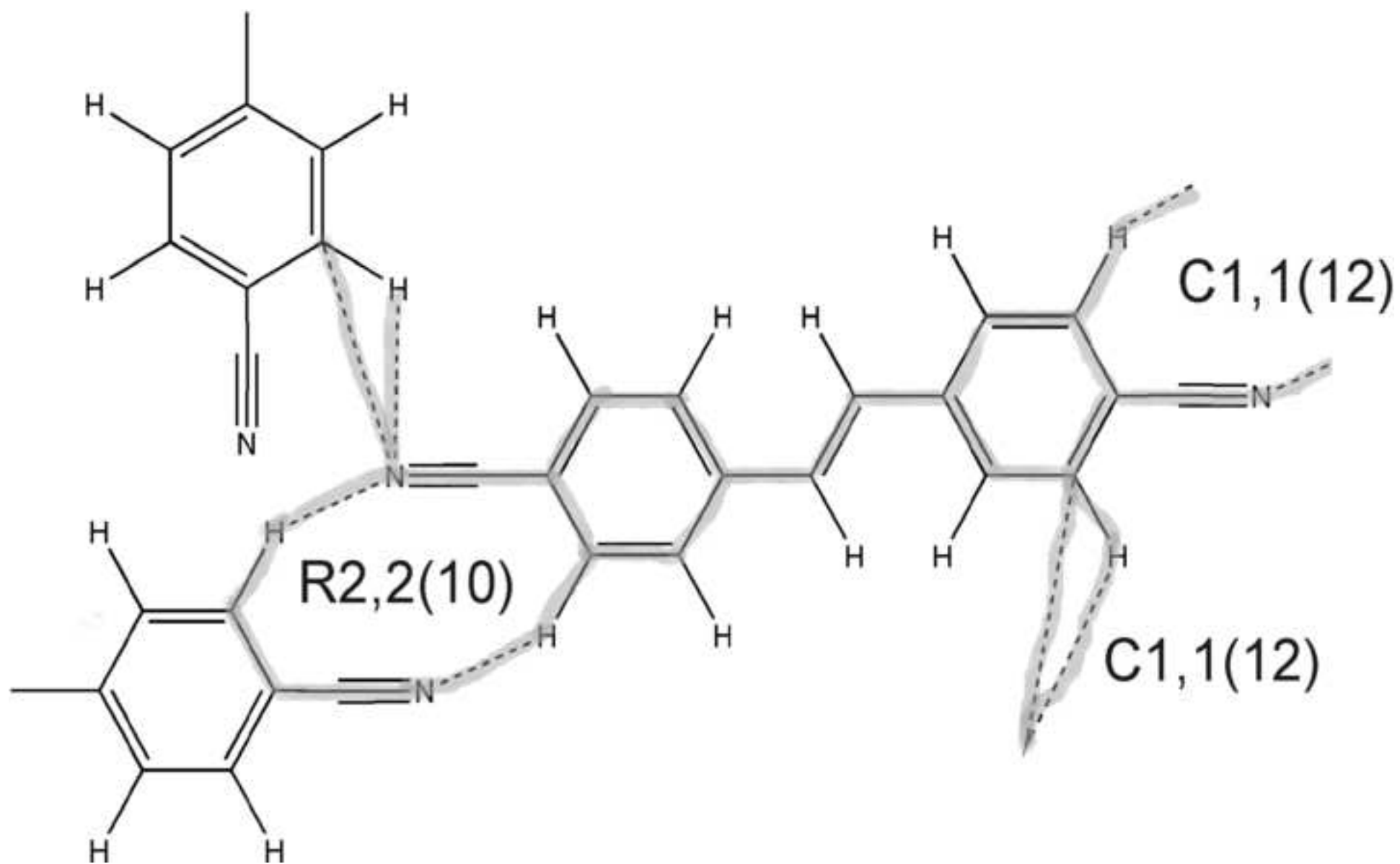
- [5] a) T. Imakuwo, H. Sawa, R. Kato, *Synth. Met.* 73 (1995) 117-122; b) M. Formigué, P. Batail, *Chem. Rev.* 104 (2004) 5379-5418; c) N. Tajima, M. Tamura, R. Kato, Y. Nishio, K. Kajita, *Synth. Met.* 181 (2003) 133-134.
- [6] a) A.S. Batsanov, A.J. Moore, N. Robertson, A. Green, M.R. Bryce, J.A.K. Howard and A.E. Underhill, *J. Mater. Chem.* 7 (3) (1997) 387-389. b) M. Fourmigué, *Struct. Bond.* 126 (2008) 181-207.
- [7] H.L. Nuyen, P.N. Horton, M.B. Hursthouse, A.C. Legon, D.W. Bruce, *J. Am. Chem. Soc.* 126 (2004) 16-17.
- [8] A. Farina, S.V. Meille, M.T. Messina, P. Metrangolo, G. Resnati, G. Vecchio, *Angew. Chem. Int. Ed.* 38 (1999) 2433-2436.
- [9] (a) P. Metrangolo and G. Resnati, *Chem. Eur. J.* 7 (2001) 2511-2520. (b) P. Metrangolo, F. Meyer, T. Pilati, D.M. Proserpio and G. Resnati, *Chem. Eur. J.* 13 (2007) 5765-5772. (c) P. Metrangolo, G. Resnati, T. Pilati, R. Liantonio, F. Meyer, *J. Polym. Sci. Part A: Polymer Chem* 45 (2007) Highlight 1-15. (d) P. Metrangolo, H. Neukirch, T. Pilati and G. Resnati, *Acc. Chem. Res.* 38 (2005) 386-395.
- [10] S.G. Bratsch, *J. Chem. Educ.* 62 (1985) 101-103.
- [11] J.C. Colling, J.M. Burke, P.S. Smith, A.S. Batsanov, J.A.K. Howard and T.B. Marder, *Org. Biomol. Chem.* 2 (2004) 3172-3178.
- 12 A. Papagni, S. Maiorana, P. Del Buttero, D. Perdicchia, F. Cariati, E. Cariati and W. Marcolli, *Eur. J. Org. Chem.* 8 (2002) 1380-1384.
- [13] (a) L. Horner, H. Hoffmann, H.G. Wippel, *Chem. Ber.* 91 (1958) 61-63. (b) L. Horner, H. Hoffmann, H.G. Wippel, G. Klahre, *Chem. Ber.* 92 (1959) 2499-2505.
- [14] W.S. Wadsworth, W.D. Emmons, *J. Am. Chem. Soc.* 83 (1961) 1733-1738.
- [15] L. Horner, H. Hoffmann, W. Klink, *Chem. Ber.* 96 (1963) 3133-3136.
- [16] R. Thomas, J. Boutagy, *Chem. Rev.* 74 (1974) 87-99.
- [17] A.E. Arbuzov and A.F. Razumov, *J. Russ. Phys. Chem. Soc.* 61 (1929) 623-630.
- [18] R.M. Acheson, G.C.M. Lee, *J. Chem. Soc. Perkin Trans. I* (1987), 2321-2332.
- [19] (a) A. Ianni, S.R. Waldvogel, *Synthesis* (2006) 2103-2112. (b) M.J.- Robson, US Patent 5 132 469 (1992). M.J.- Robson, J. Williams, UK patent GB 2 171 994 A (1985).
- [20] J. Leroy, B. Schöllhorn, J.-L. Syssa-Magalé, K. Boubekeur, P. Palvadeau, *J. Fluorine Chem.* 125 (2004) 1379-1382.
- [21] (a) J.M. Campagne, D. Prim. *Les complexes de palladium en synthèse organique, Initiation et guide pratique.* CNRS editions, 2001. (b) E. Negishi (Ed) *Handbook of Organopalladium Chemistry for Organic Synthesis* vol I and II, Wiley, New York, 2002. (c) J.J. Li, G.W. Gribble. *Palladium in Heterocyclic Chemistry. A guide for synthetic Chemist.* Elsevier, Oxford, 2000.
- [22] A.C. Albéniz, P. Espinet, B. Martin-Ruiz and D. Milstein, *Organometallics* 24 (2005) 3679-3684.
- [23] (a) C. Roscher, PhD thesis. University of Würzburg, 1998. (b) C. Roscher, M. Popall in *Better Ceramics Through Chemistry VII: Organic/Inorganic Hybrid Materials* (eds.: B.K. Coltrain, C. Sanchez, D.W. Schaefer, G.L. Wilkes). *Mat. Res. Soc. Symp. Proc.* 435 (1996) 547-552.
- [24] a) A.L. Spek, PLUTON and ORTEP, PLATON for Windows Taskbar v 1.10; University of Utrecht: The Netherlands, 2006. b) A.L. Spek, *Acta Cryst. A* 46 (1990) C34.
- [25] X-Area V1.17 & X-RED32 V1.04 Software; Stoe & Cie GmbH: Darmstadt, Germany (2002).
- [26] (a) G.M. Sheldrick, SHELXS-97, Program for crystal structure determination; University of Göttingen: Germany (1997). (b) G.M. Sheldrick, *Acta Cryst. A* 46 (1990) 267-273.
- [27] G.M. Sheldrick, SHELXL-97, Program for crystal structure refinement; University of Göttingen: Germany (1997).
- [28] A.L. Spek, *J. Appl. Cryst.* 36 (2003) 7-13.
- [29] A.C.B. Lucassen, M. Vartanian, G. Leitius, M.E. Van der Boom, *Cryst. Growth Des.* 5 (2005) 1671-1673.

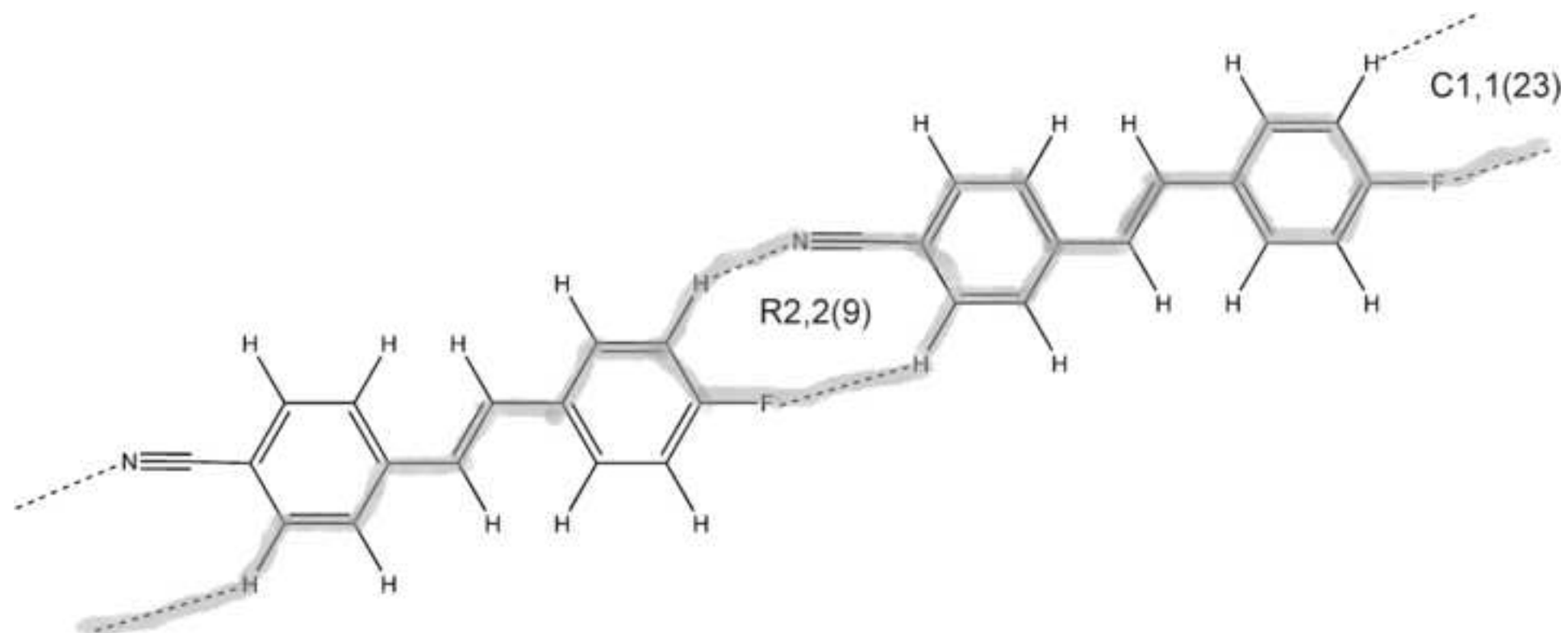
---

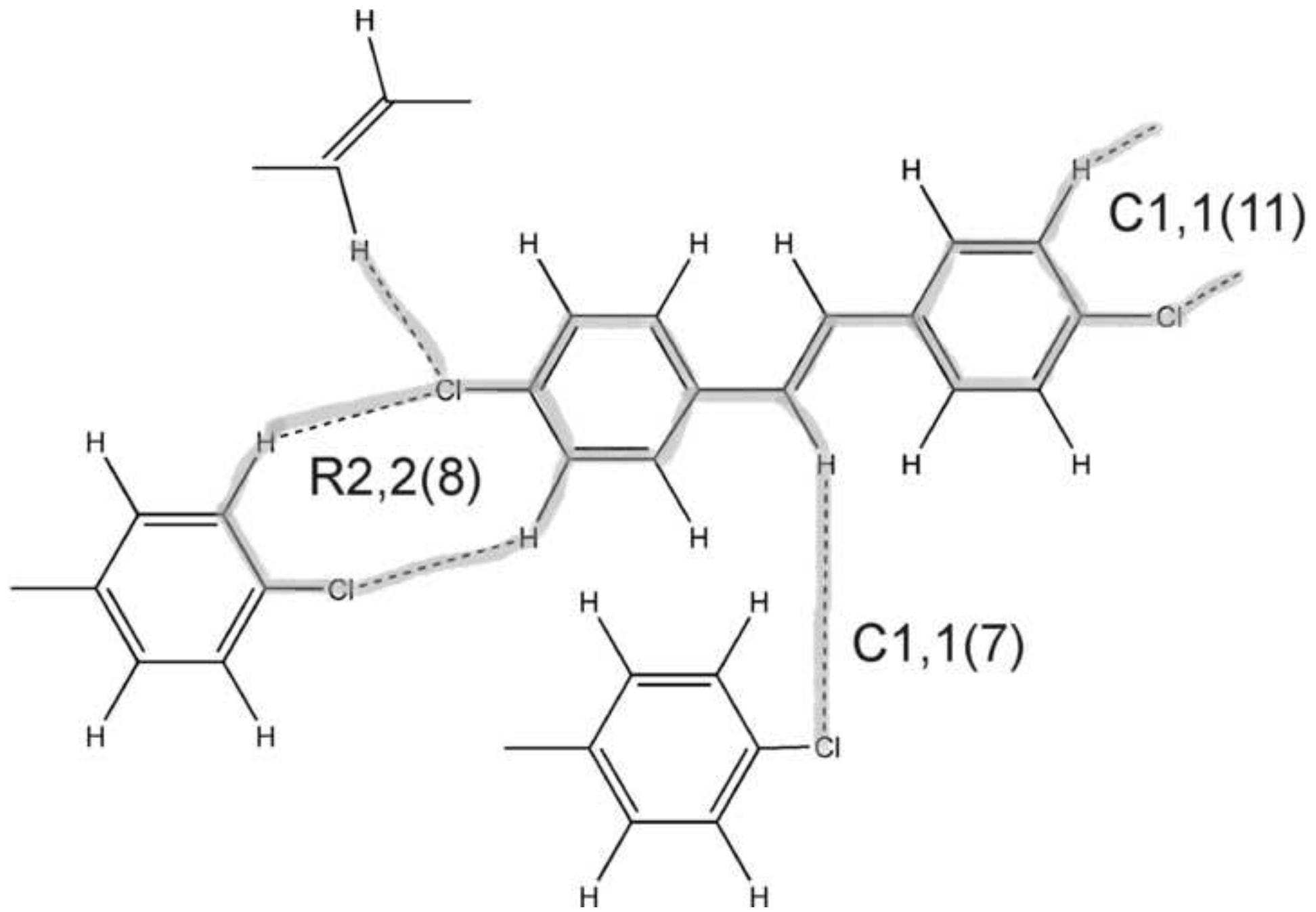
[30] a) A.D. Bond, J. Griffiths, J.M. Rawson, J. Hulliger, J. Chem. Soc. Chem. Commun. (2001) 2488-2489 b) A.D. Bond, J. Griffiths, J.M. Rawson, J. Hulliger, H. Süss, unpublished work.

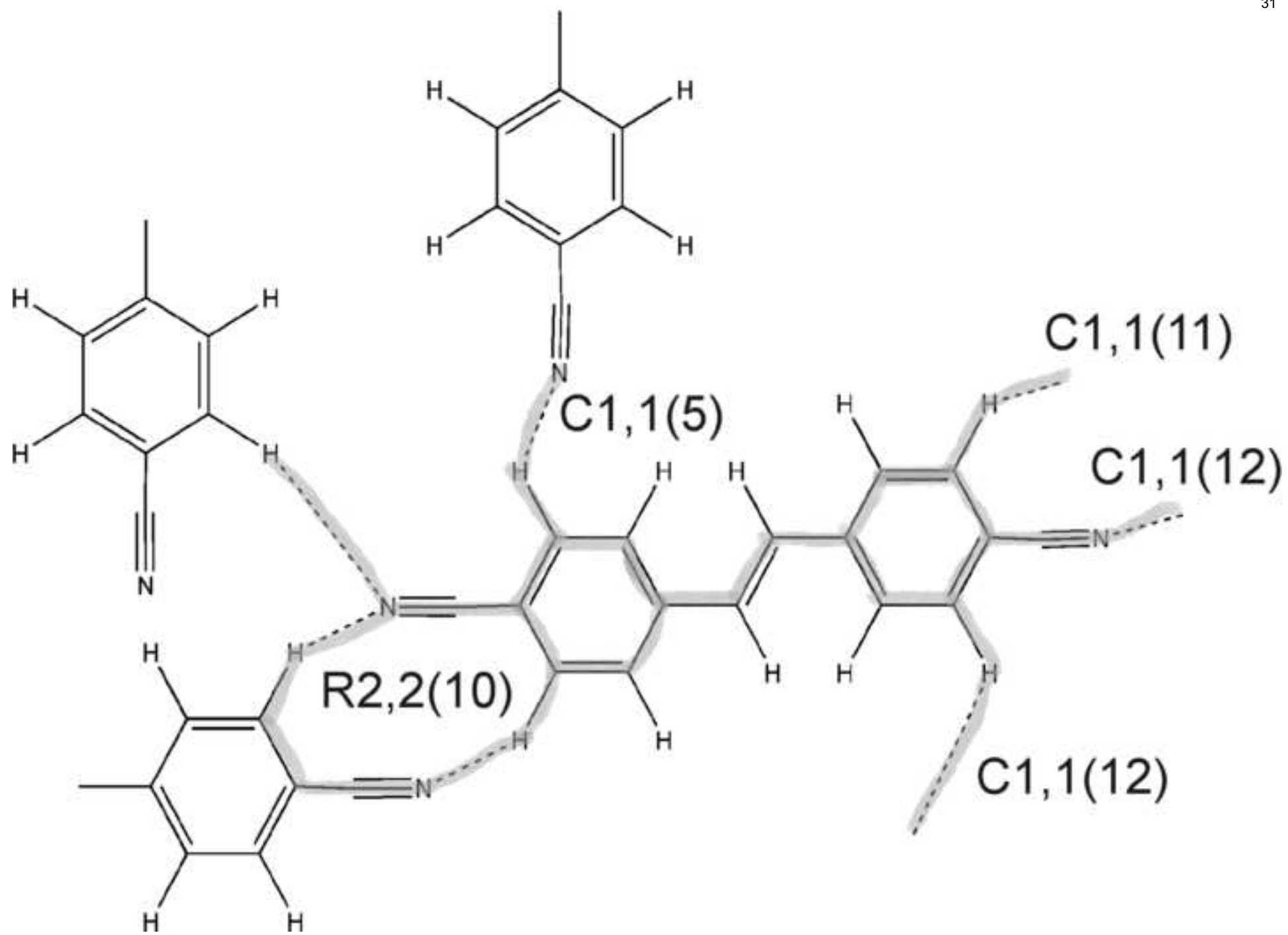


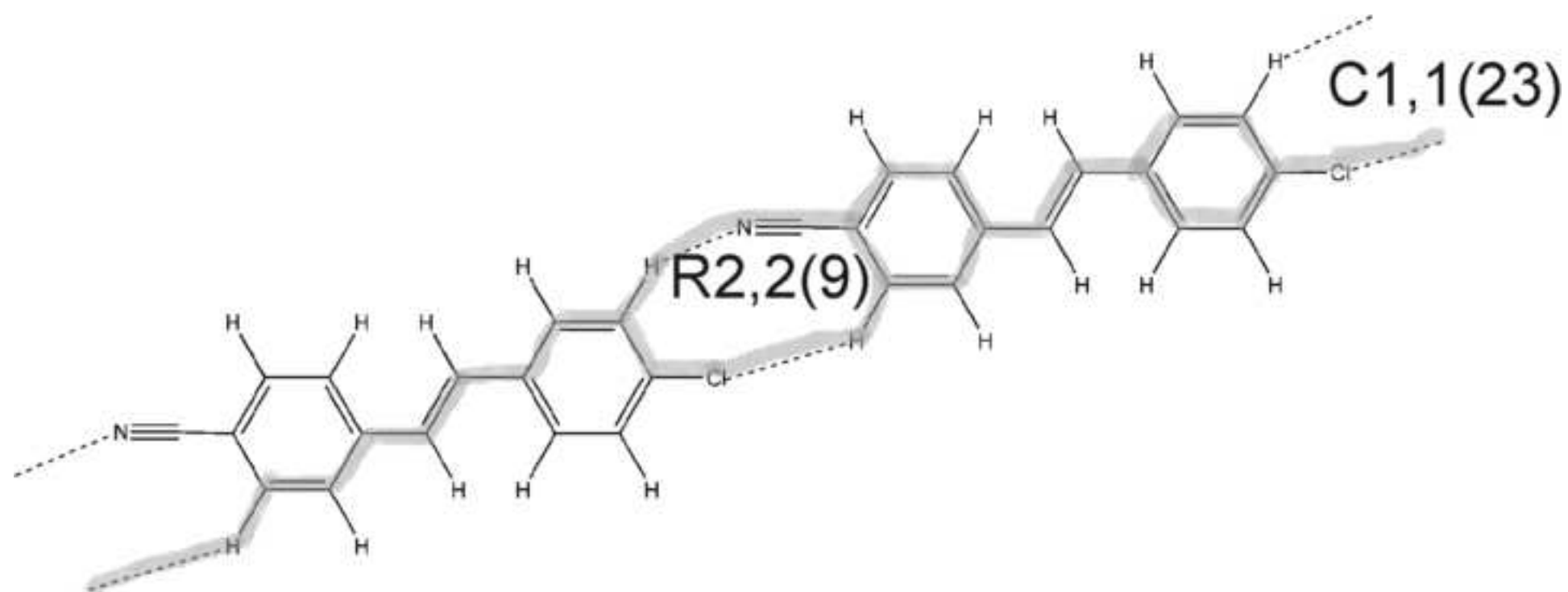


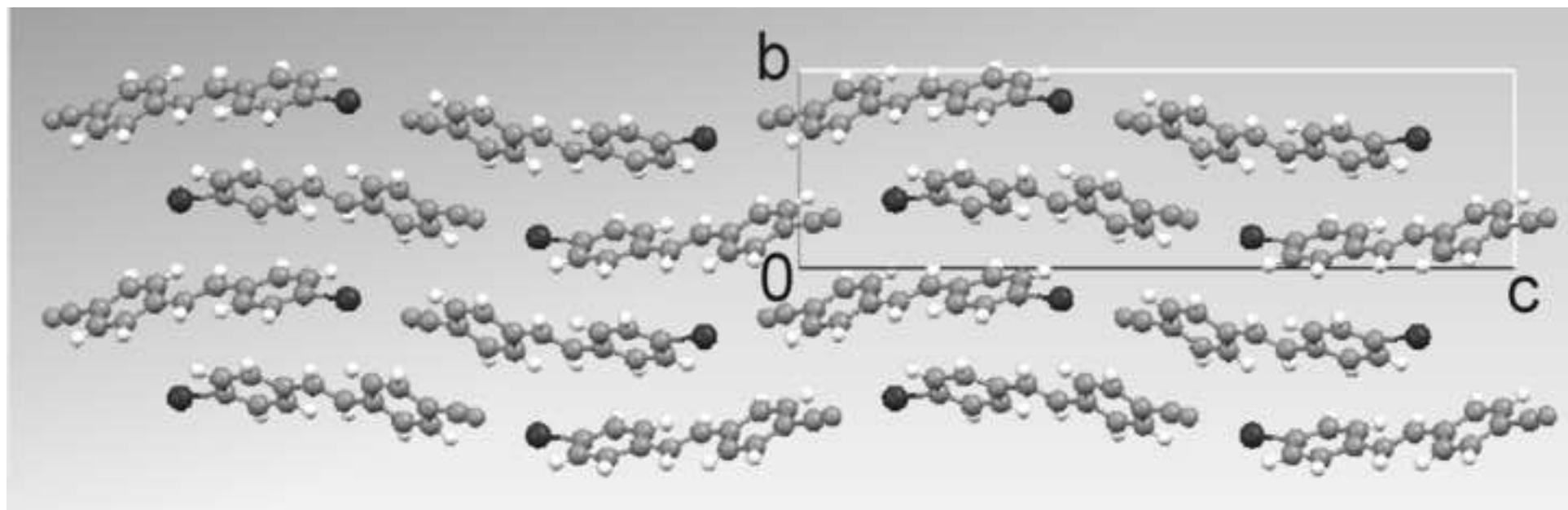


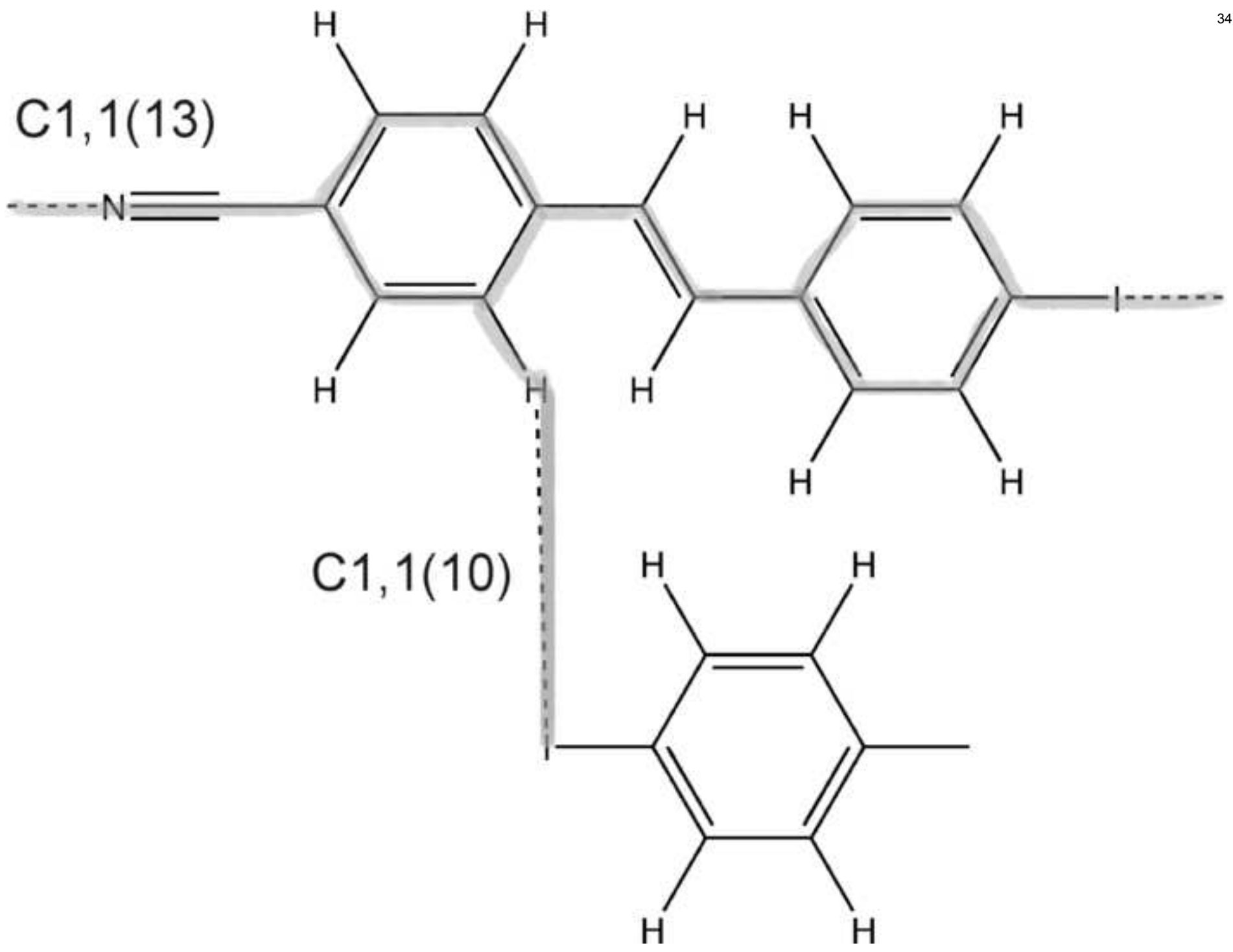


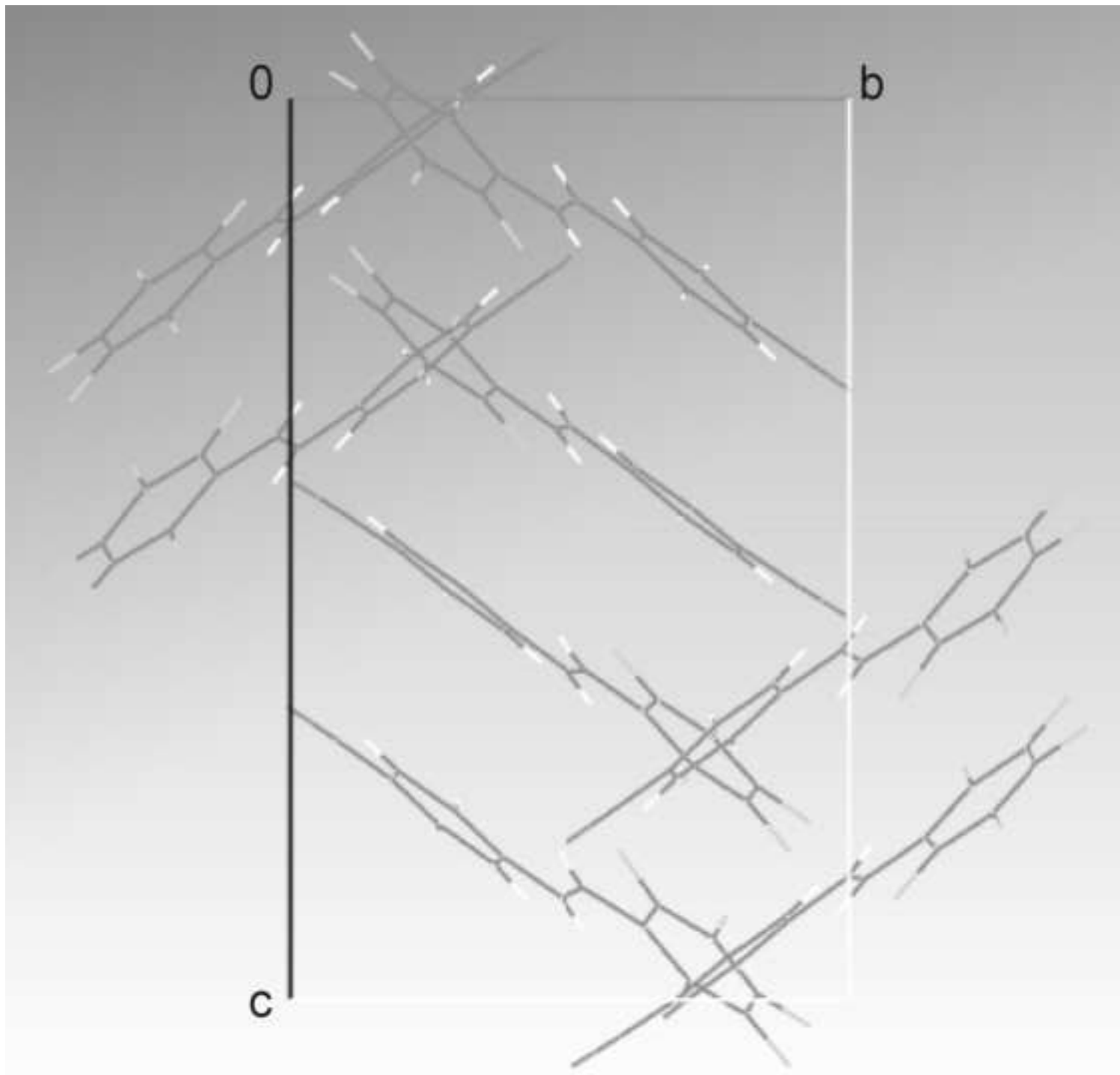


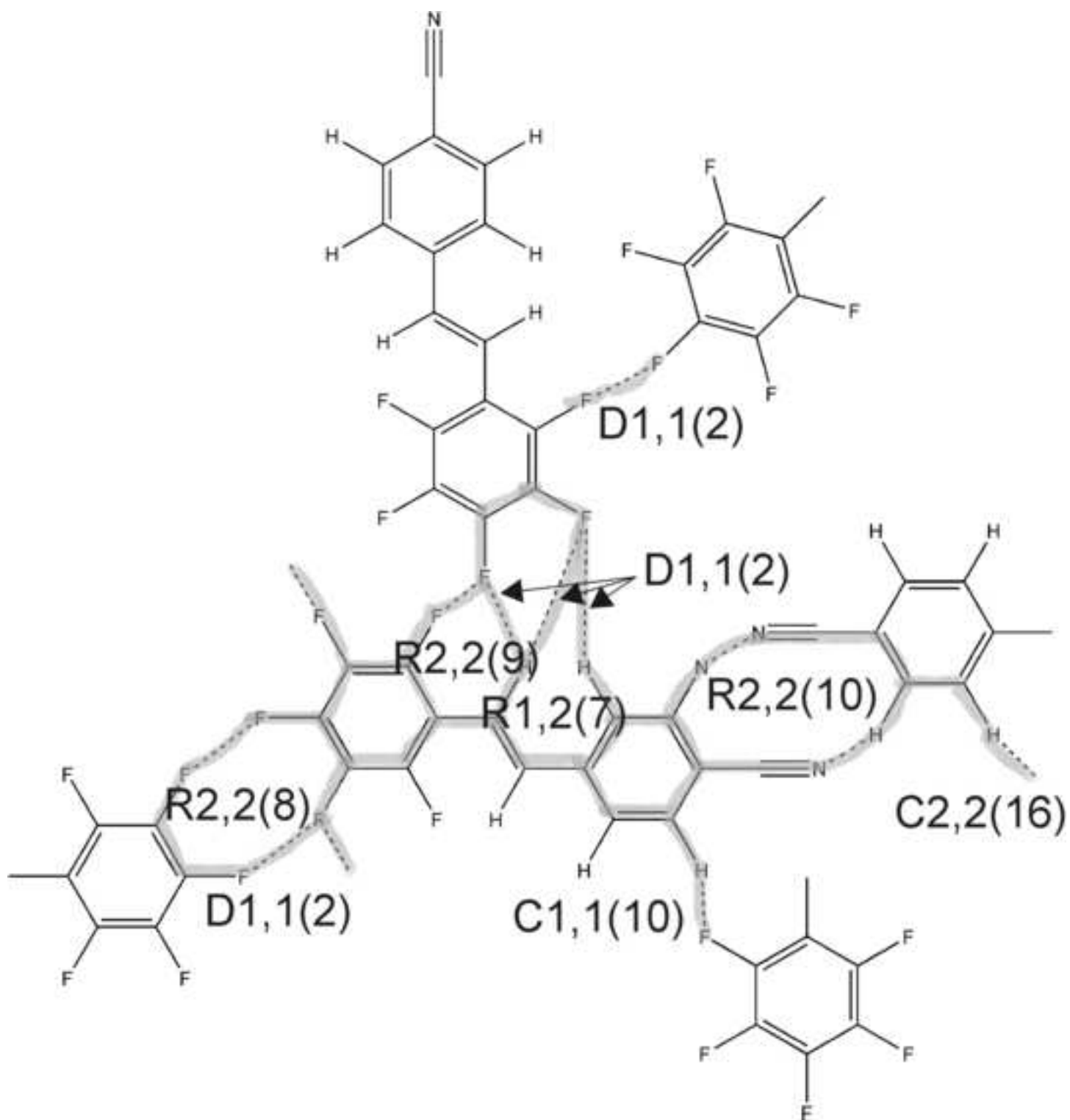


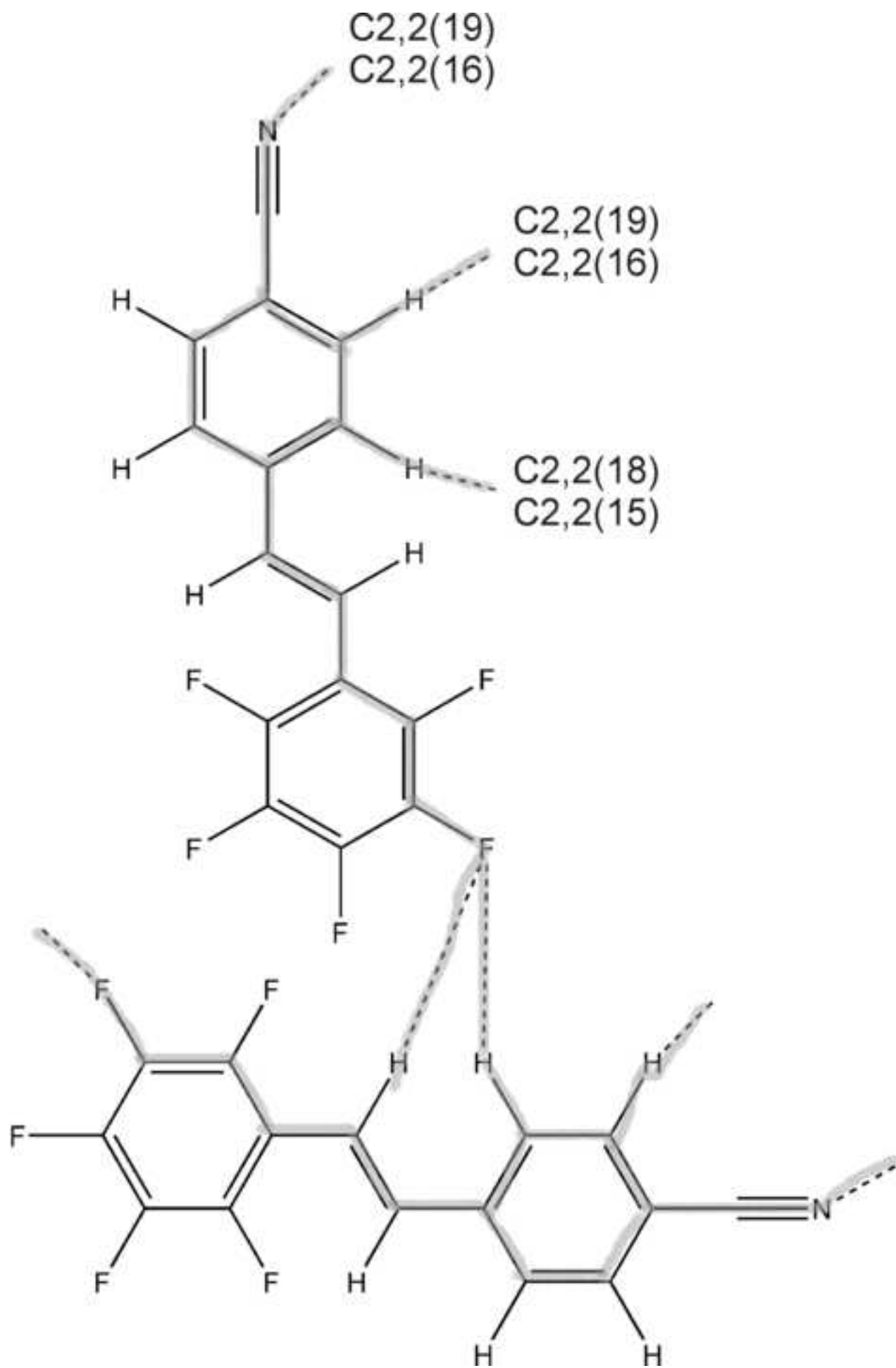


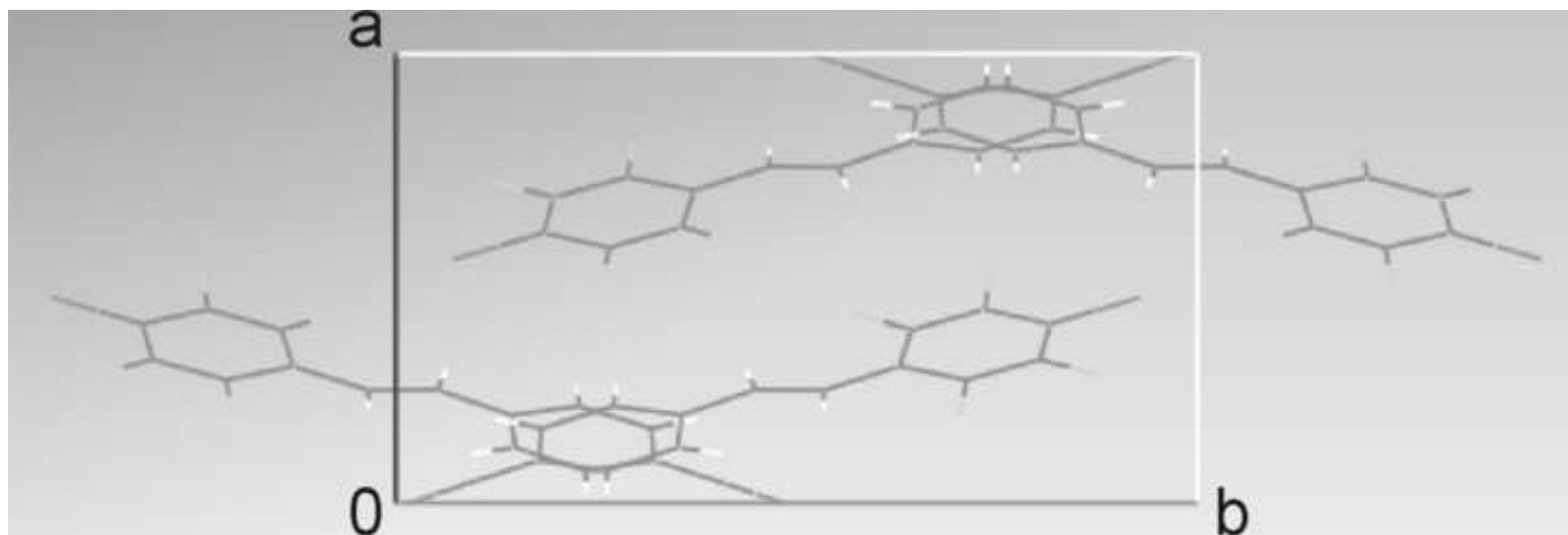


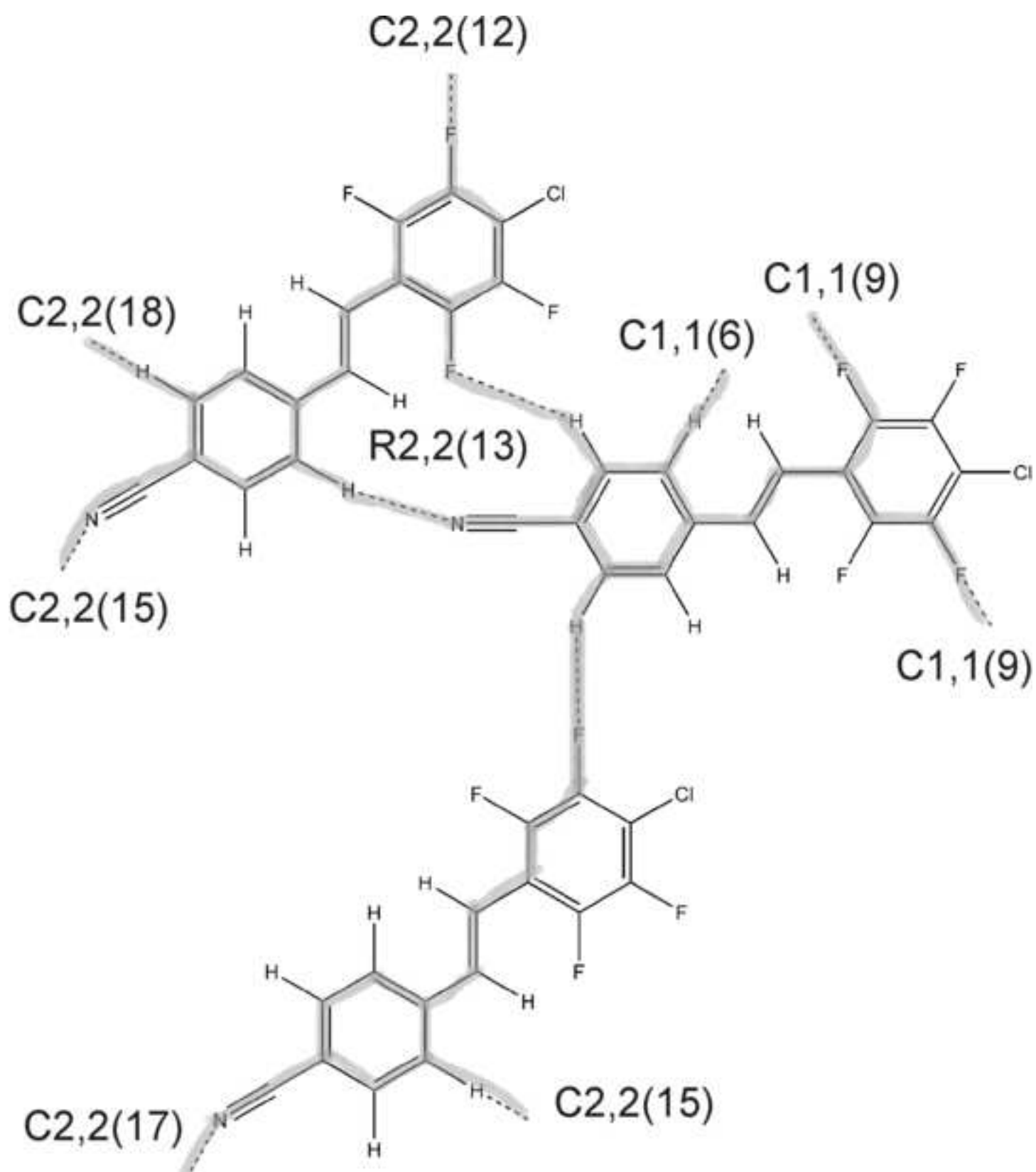


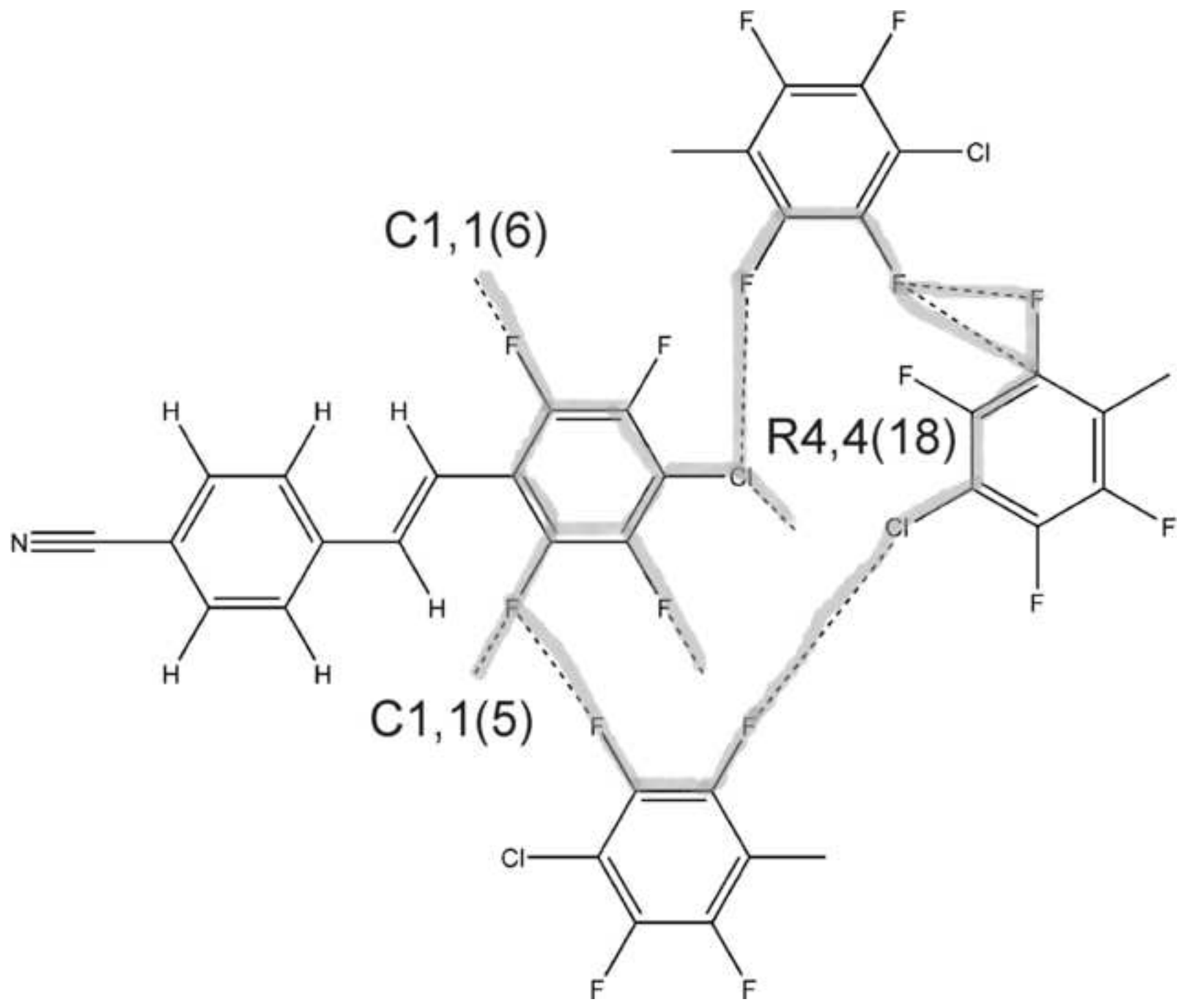


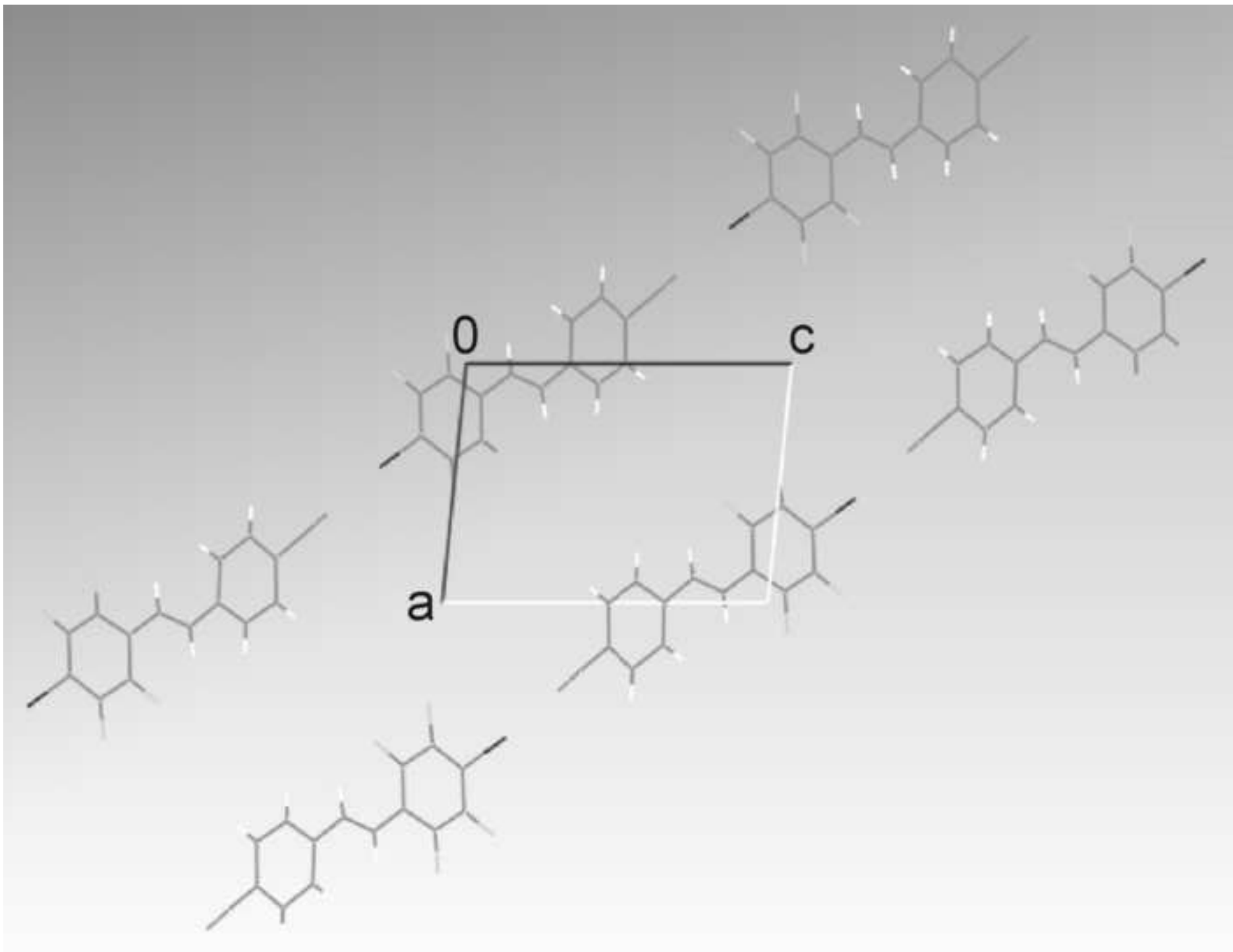


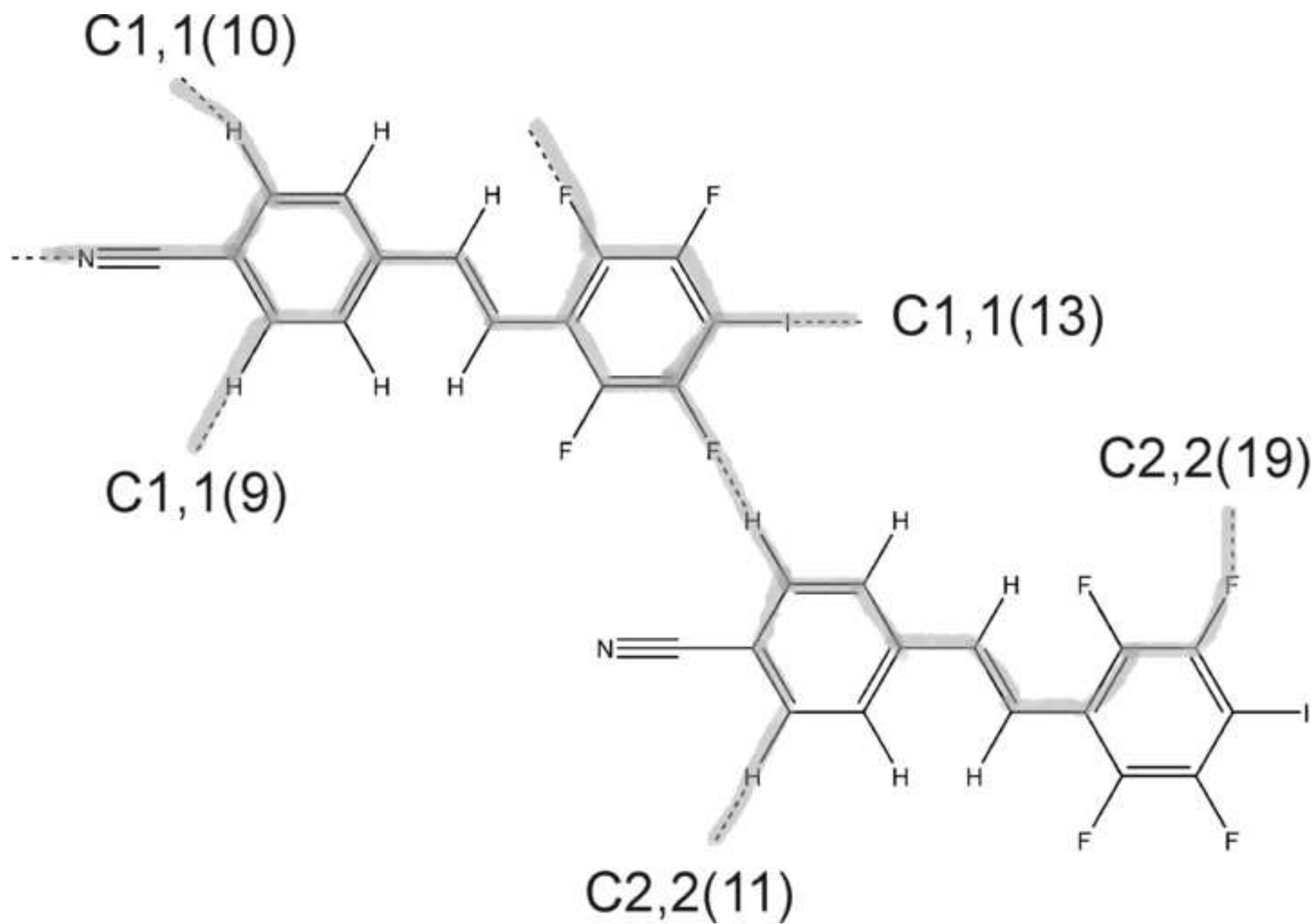


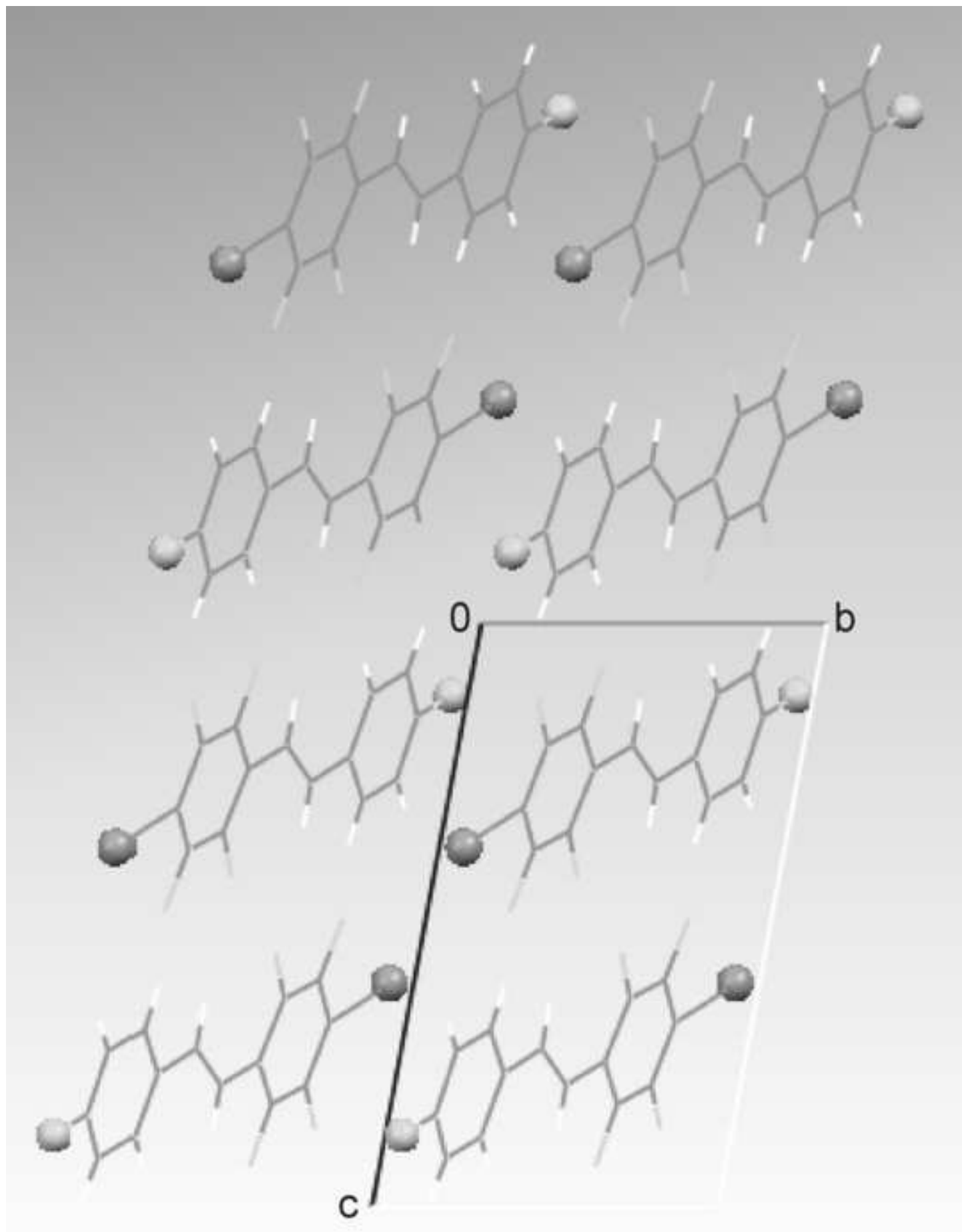


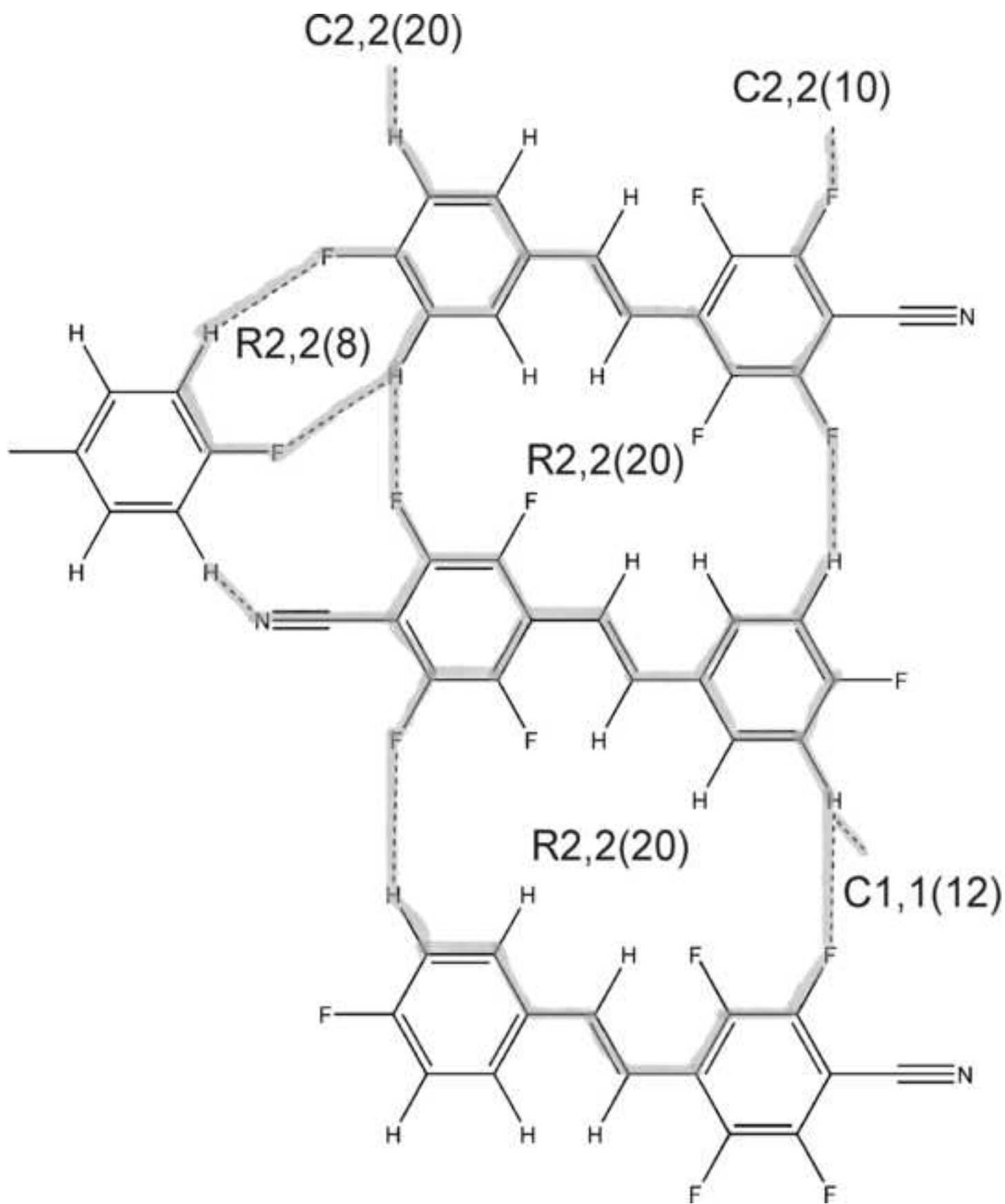


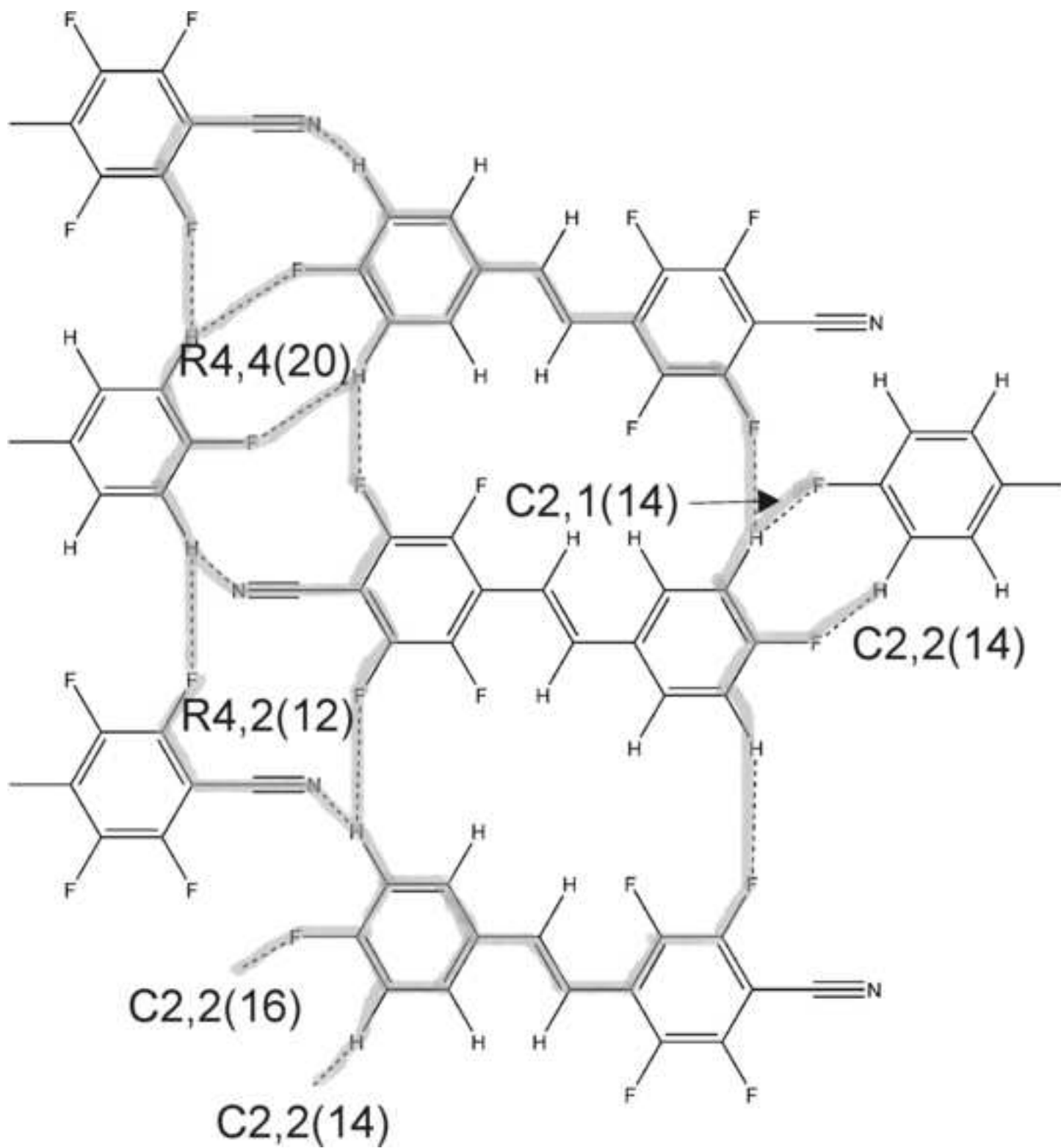


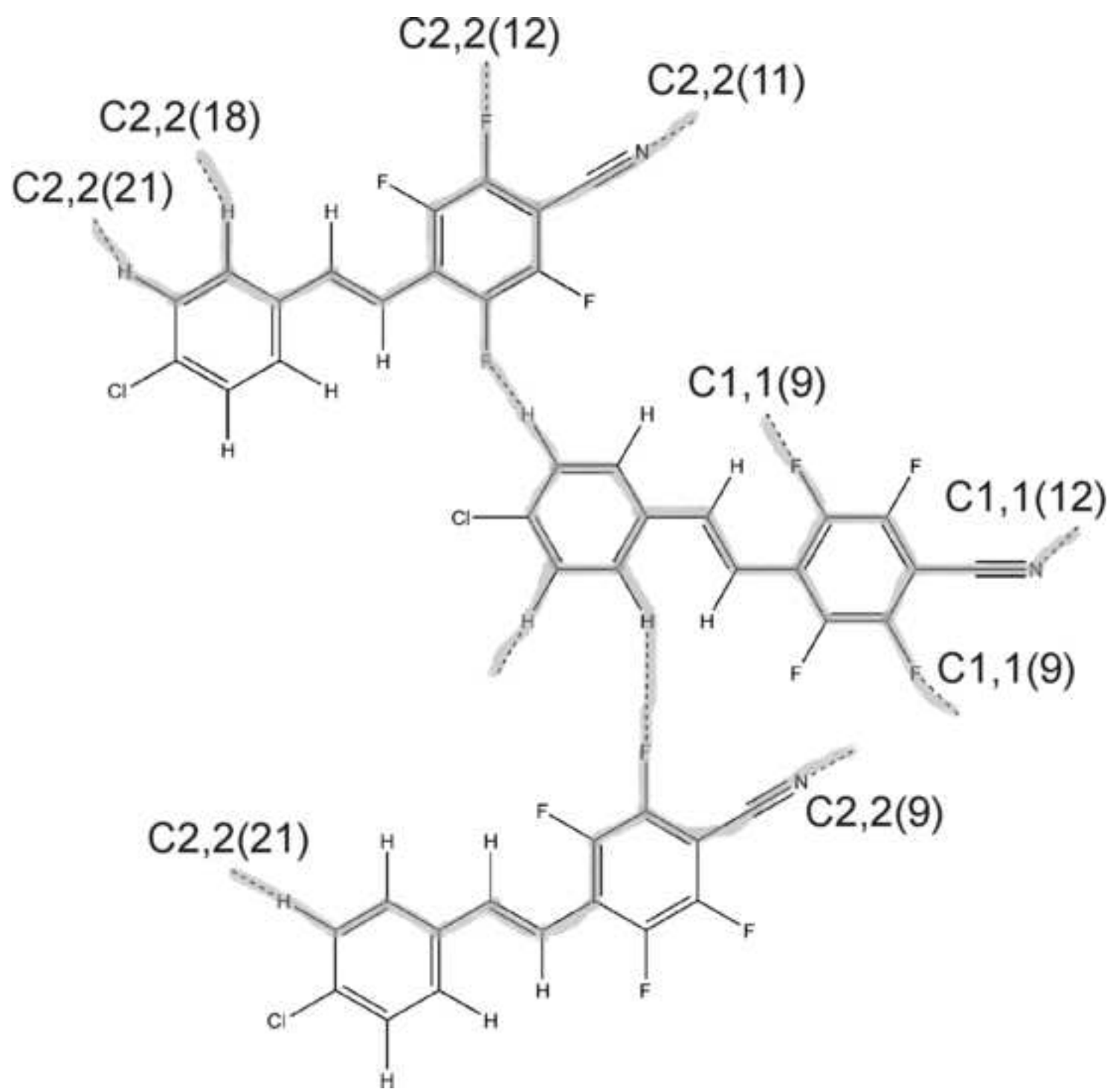


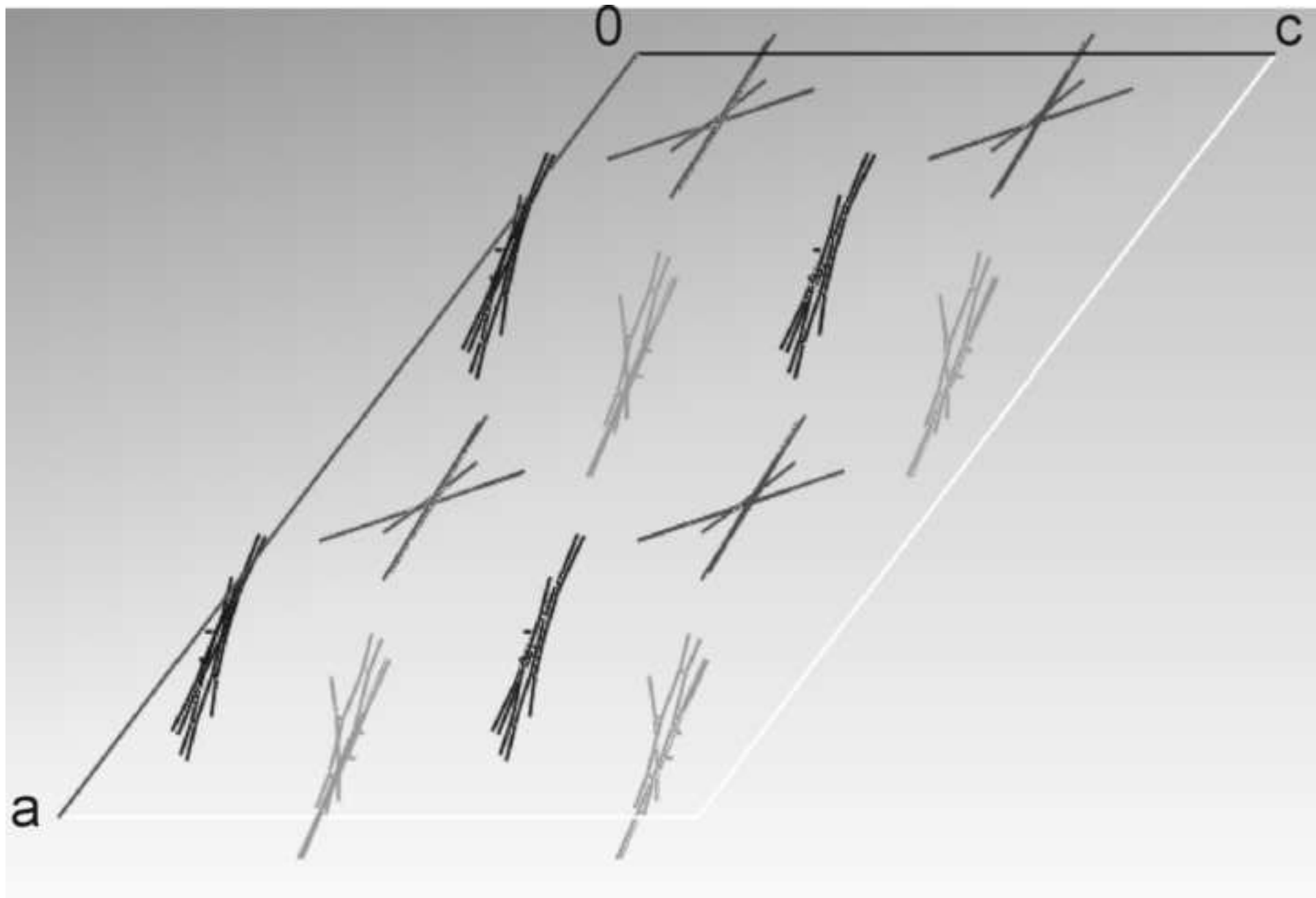


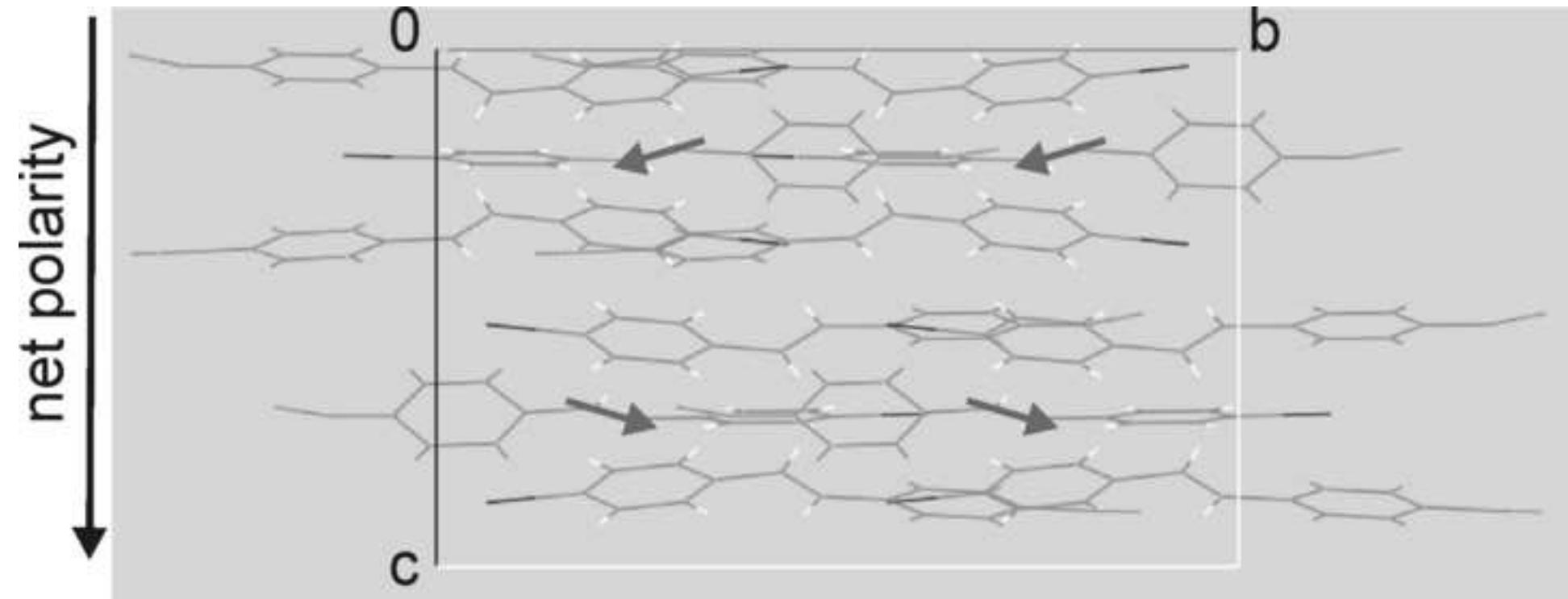


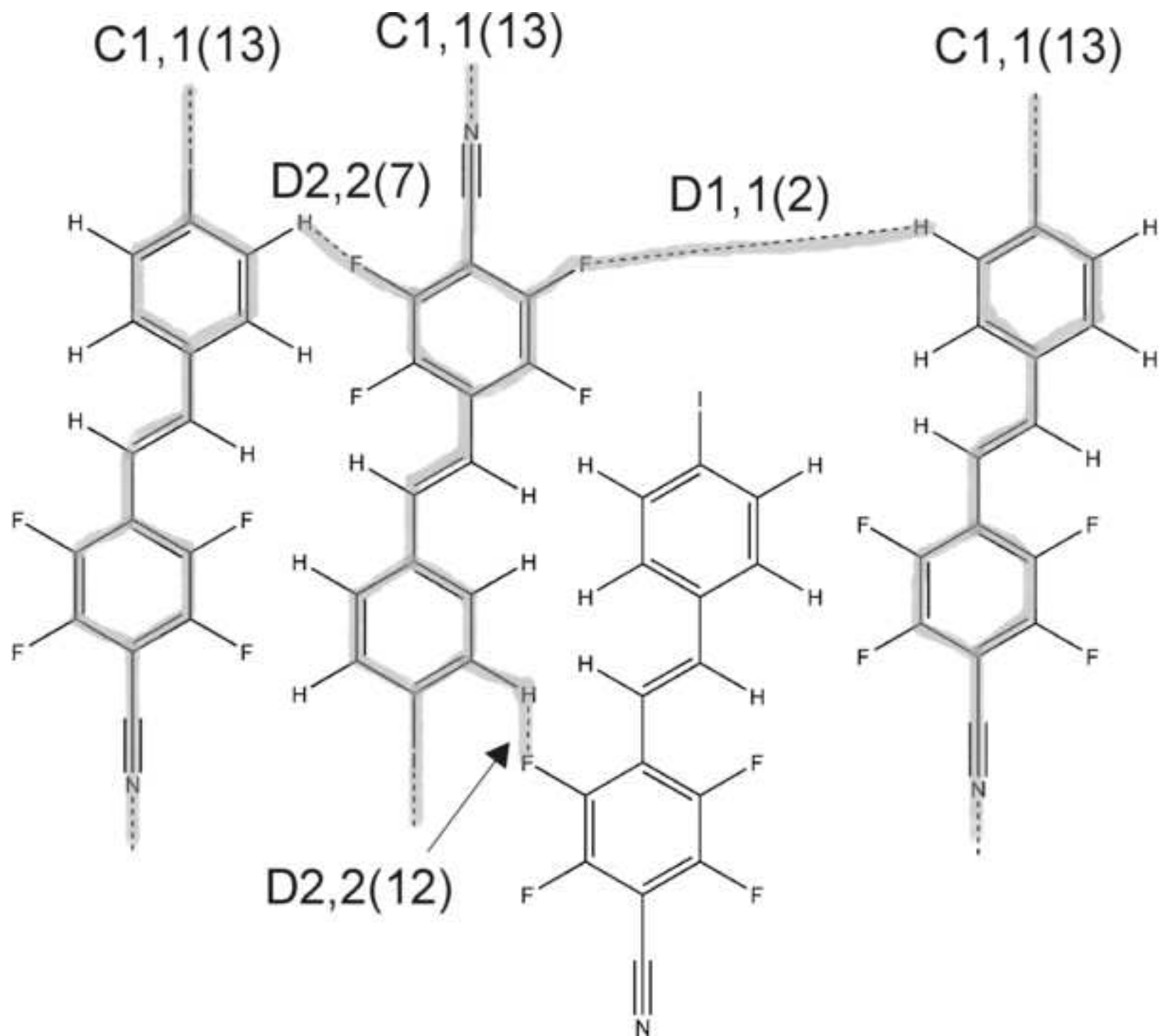


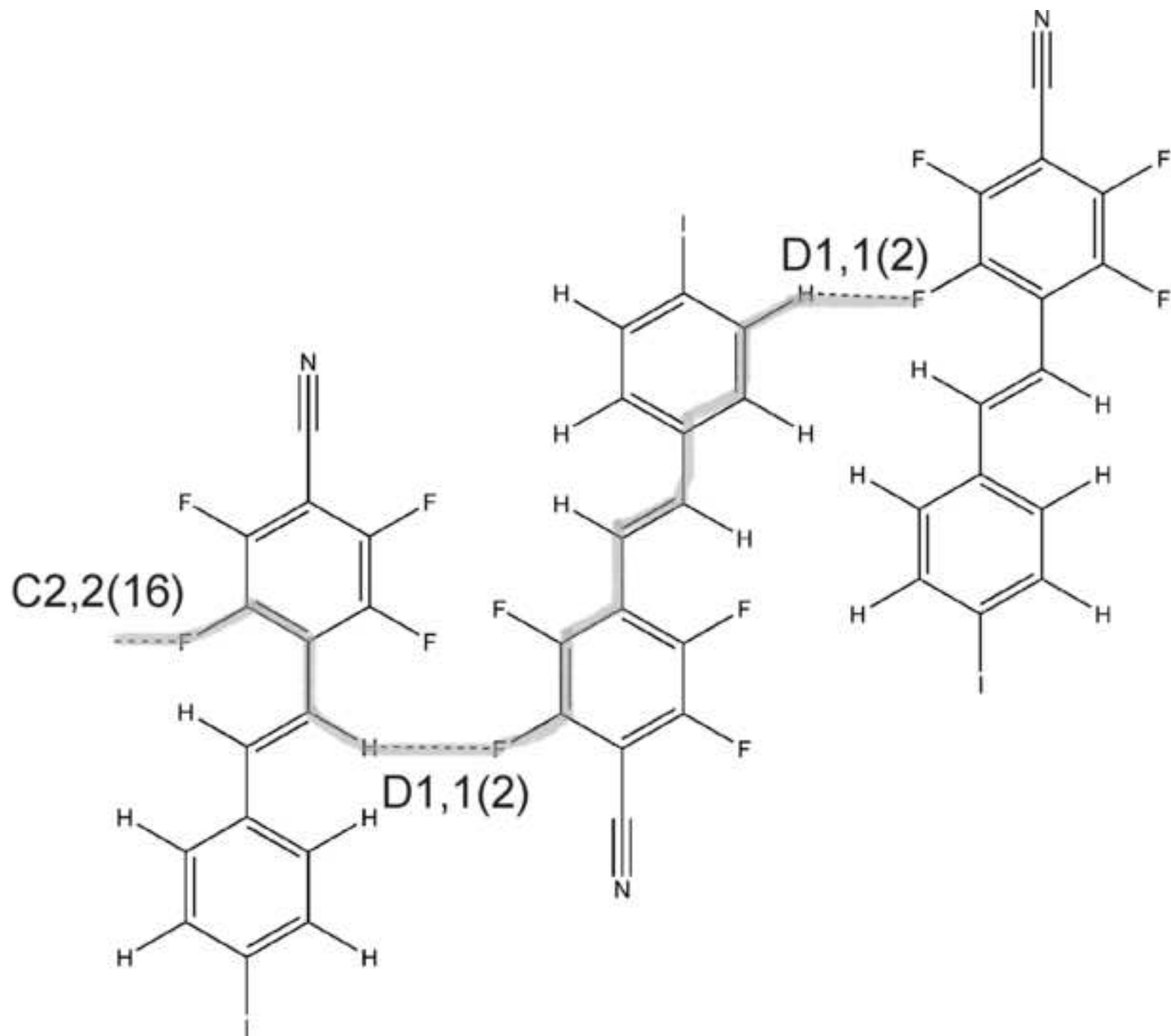


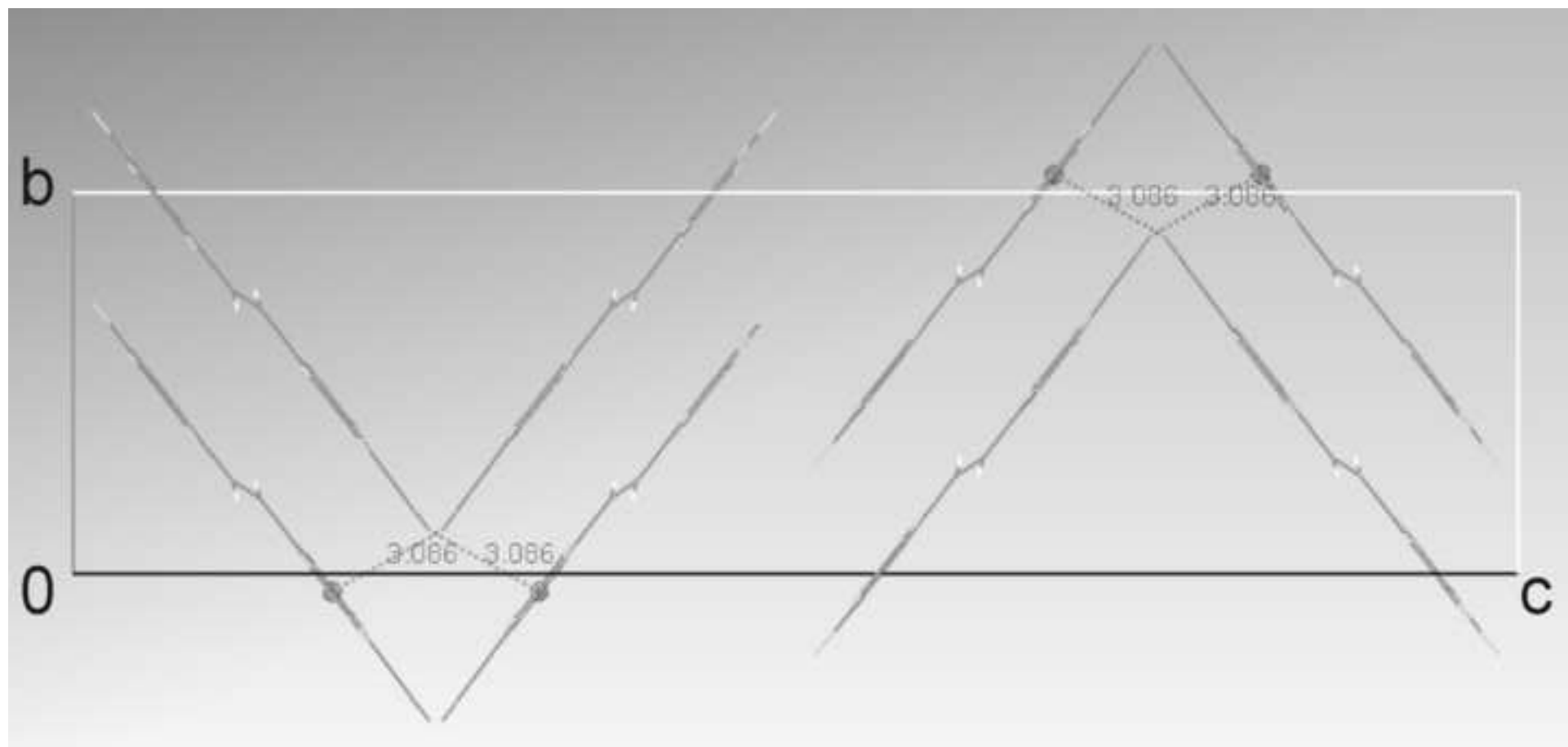


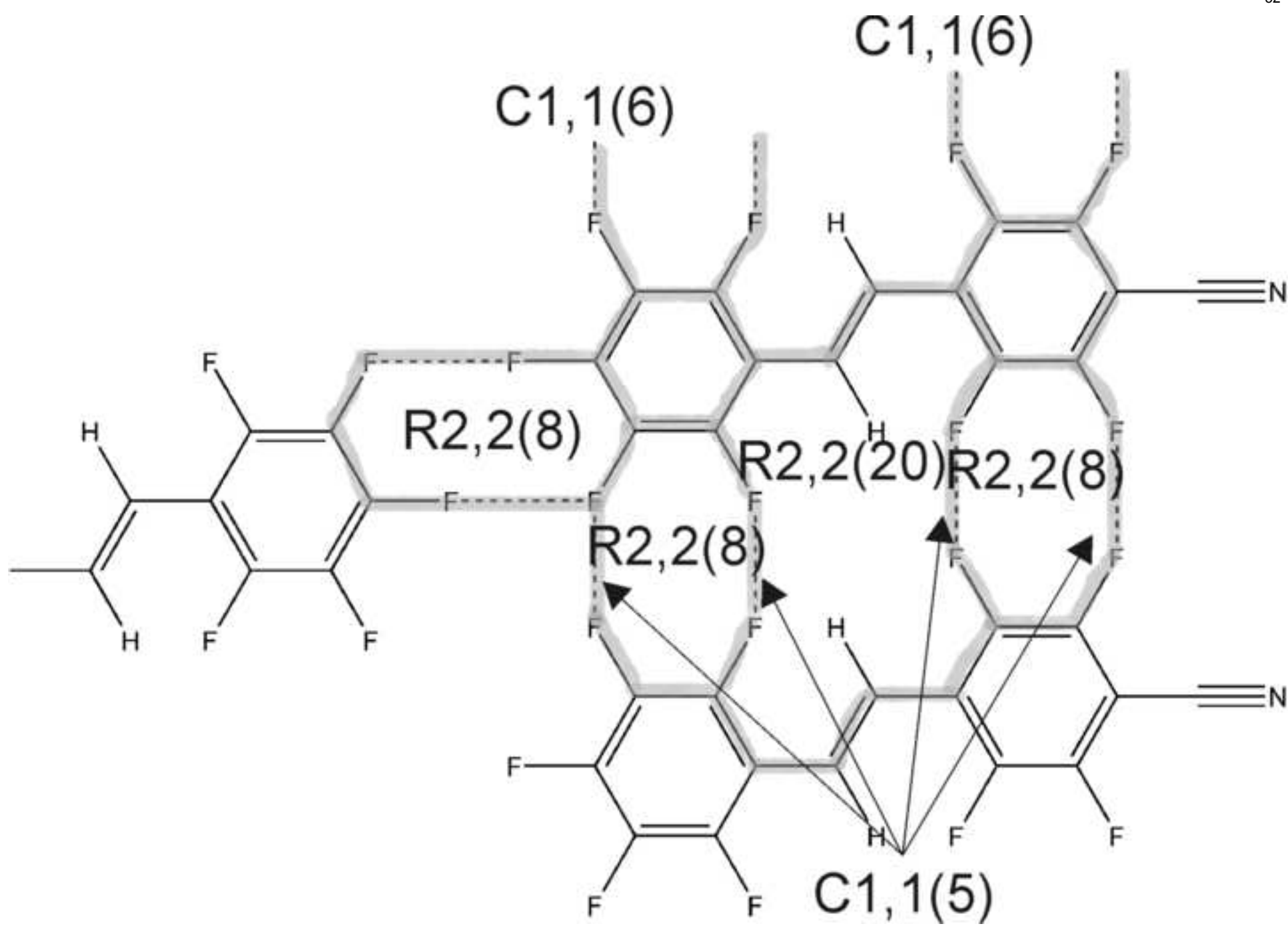


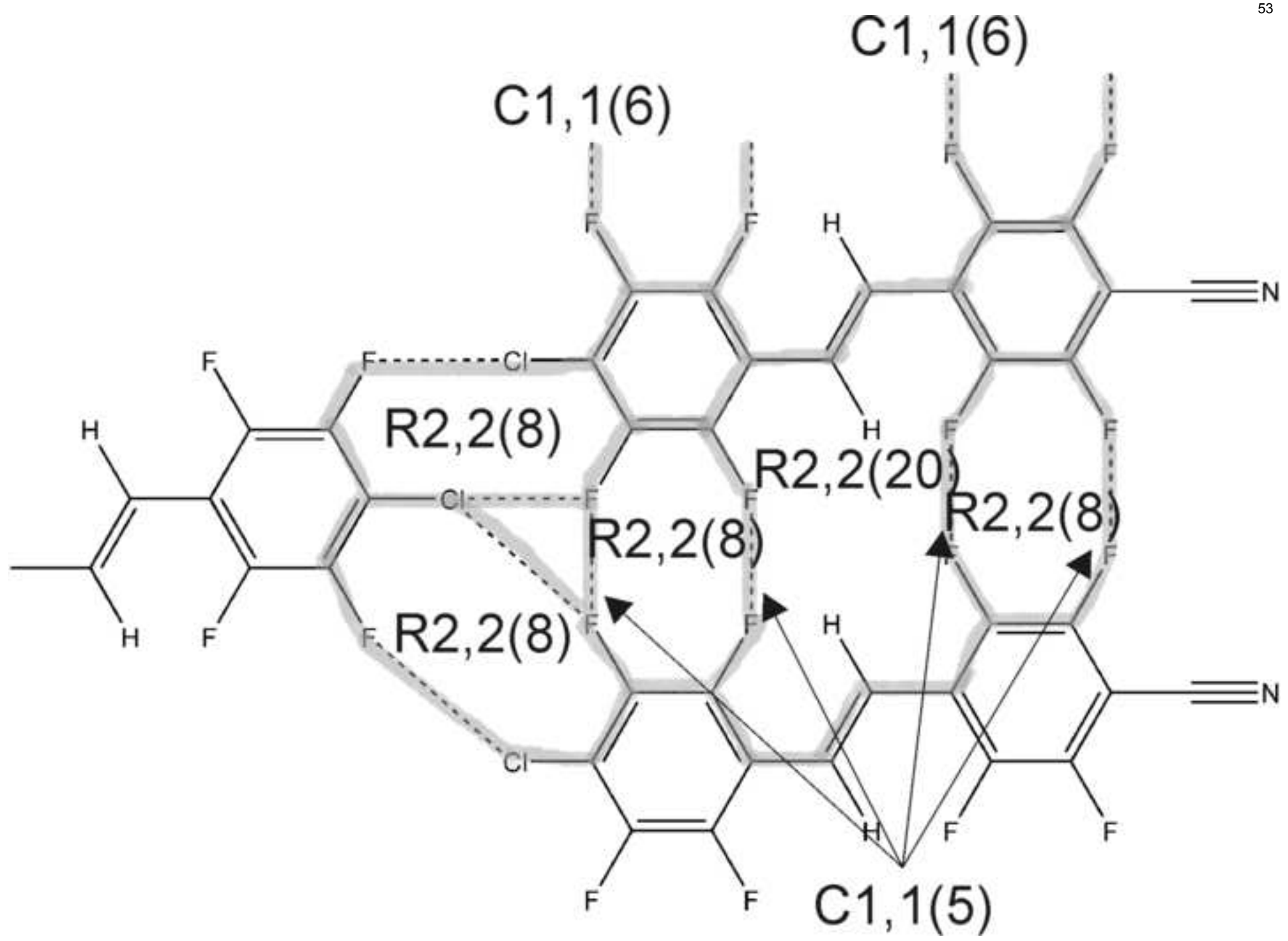


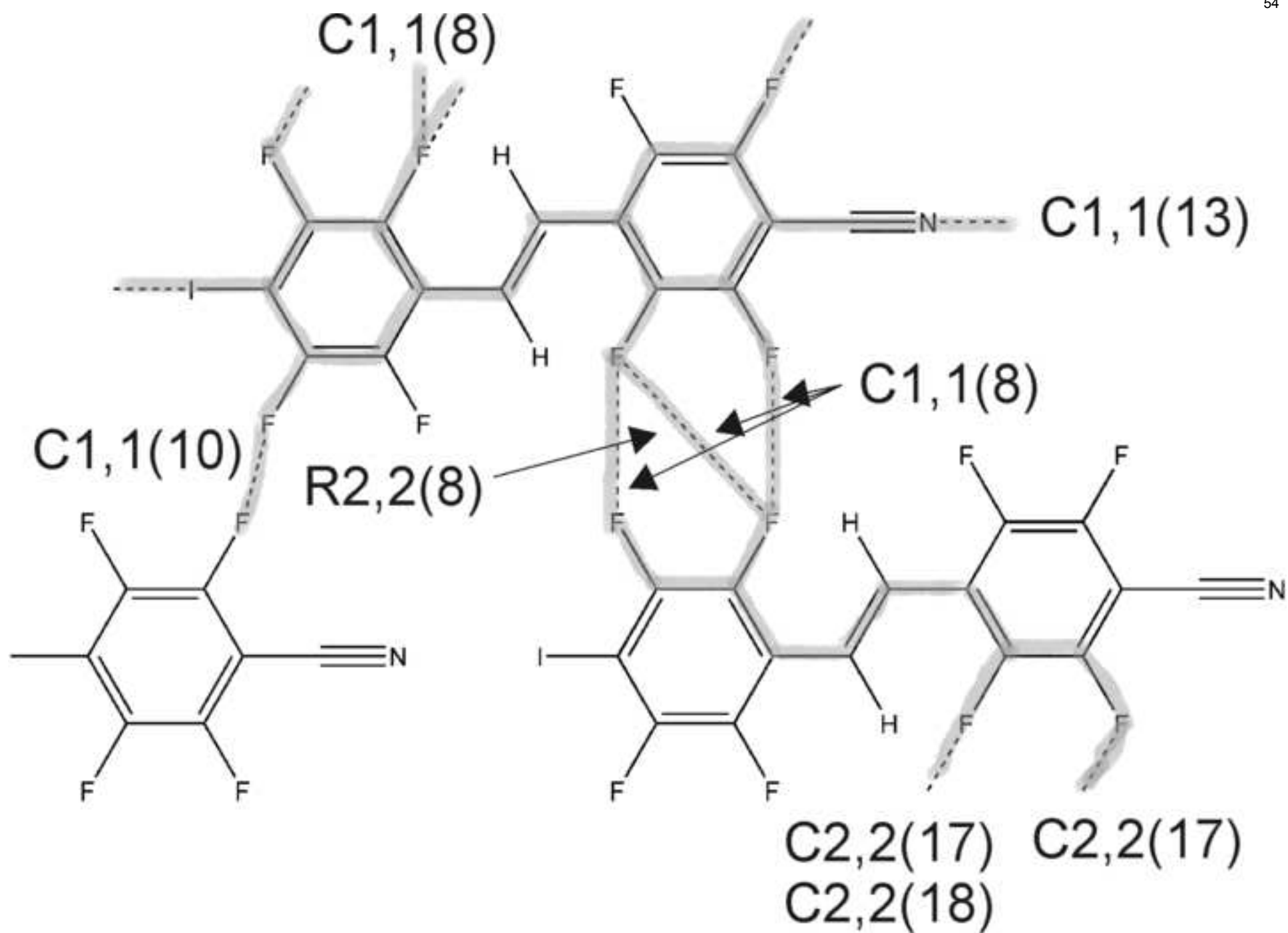


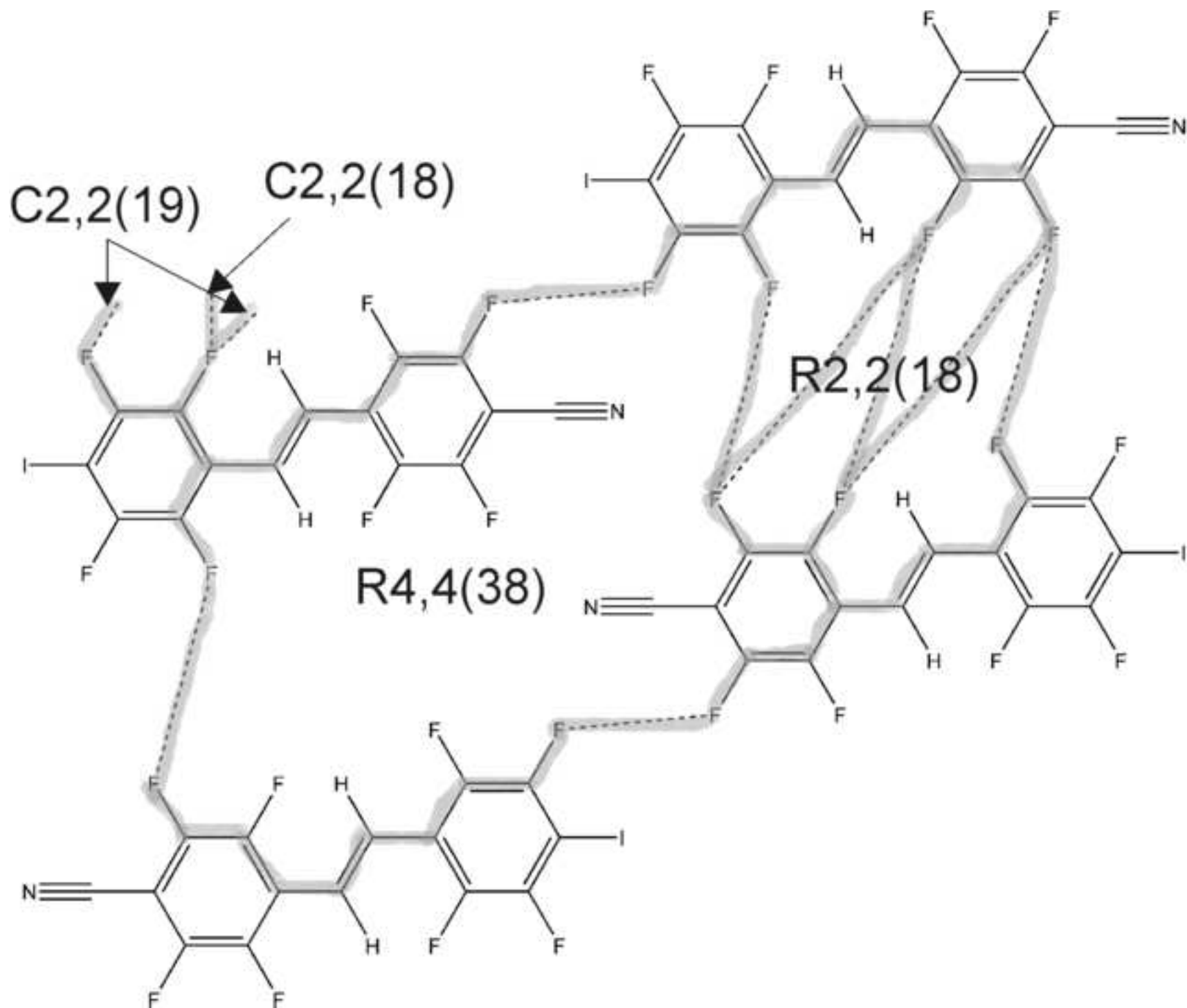


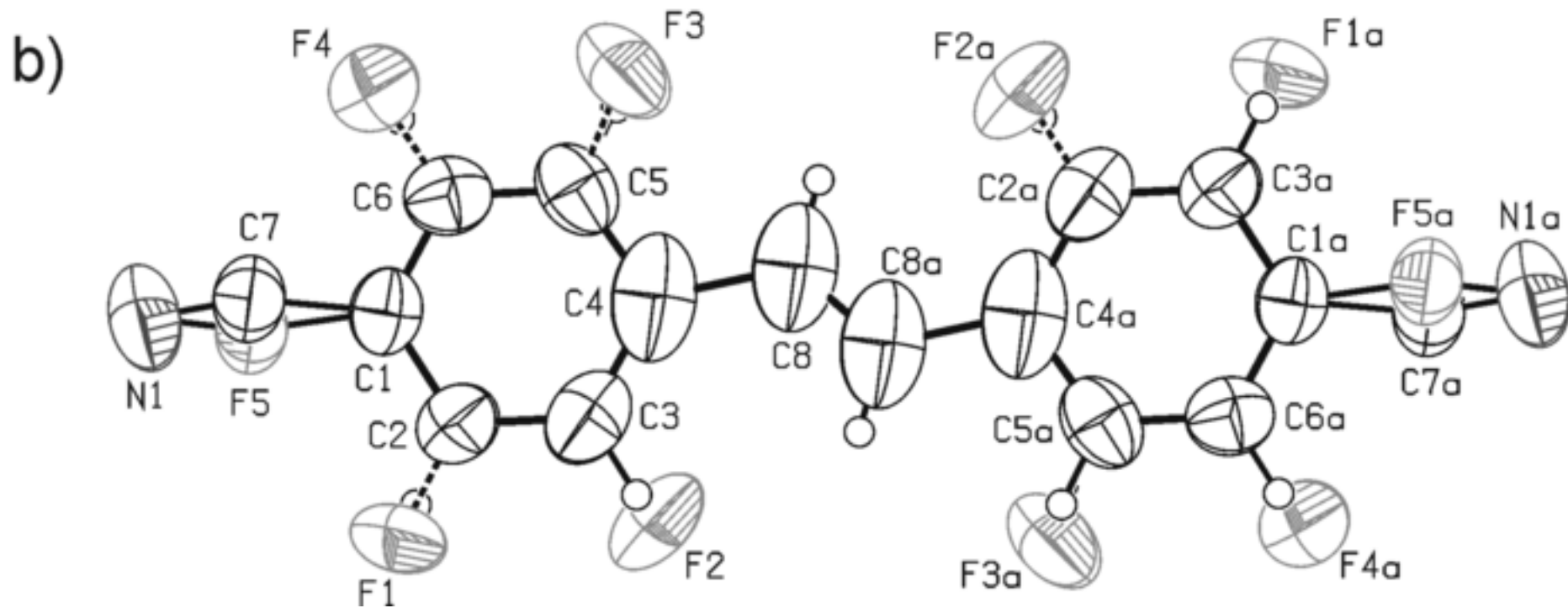
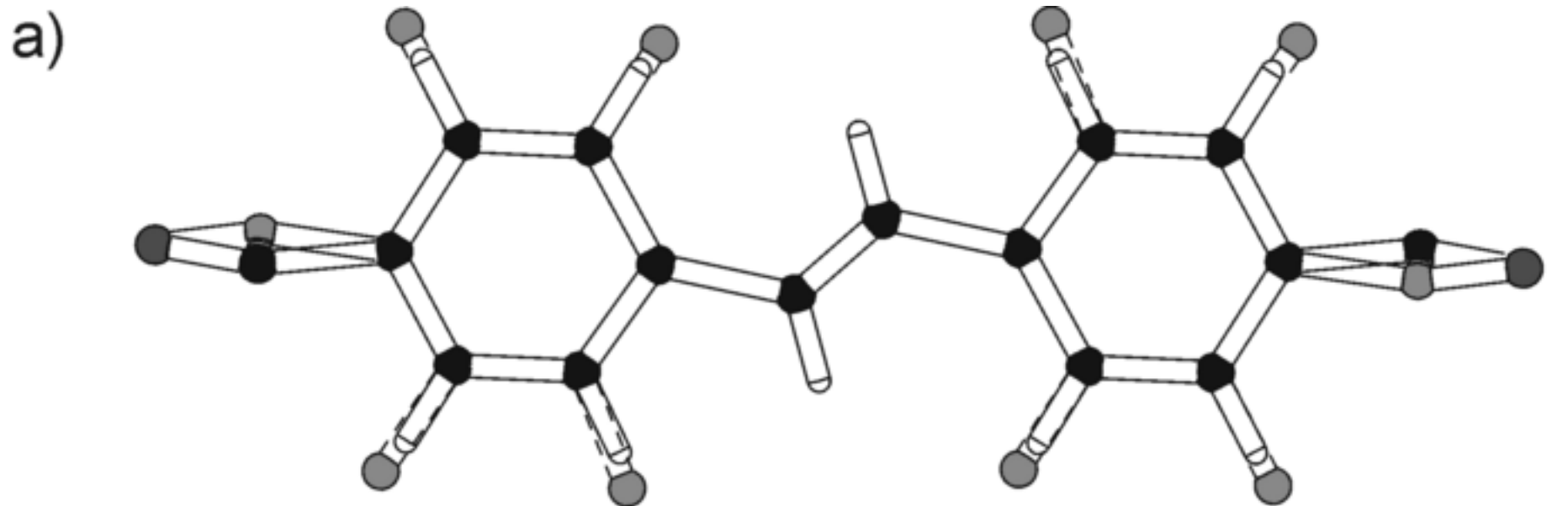


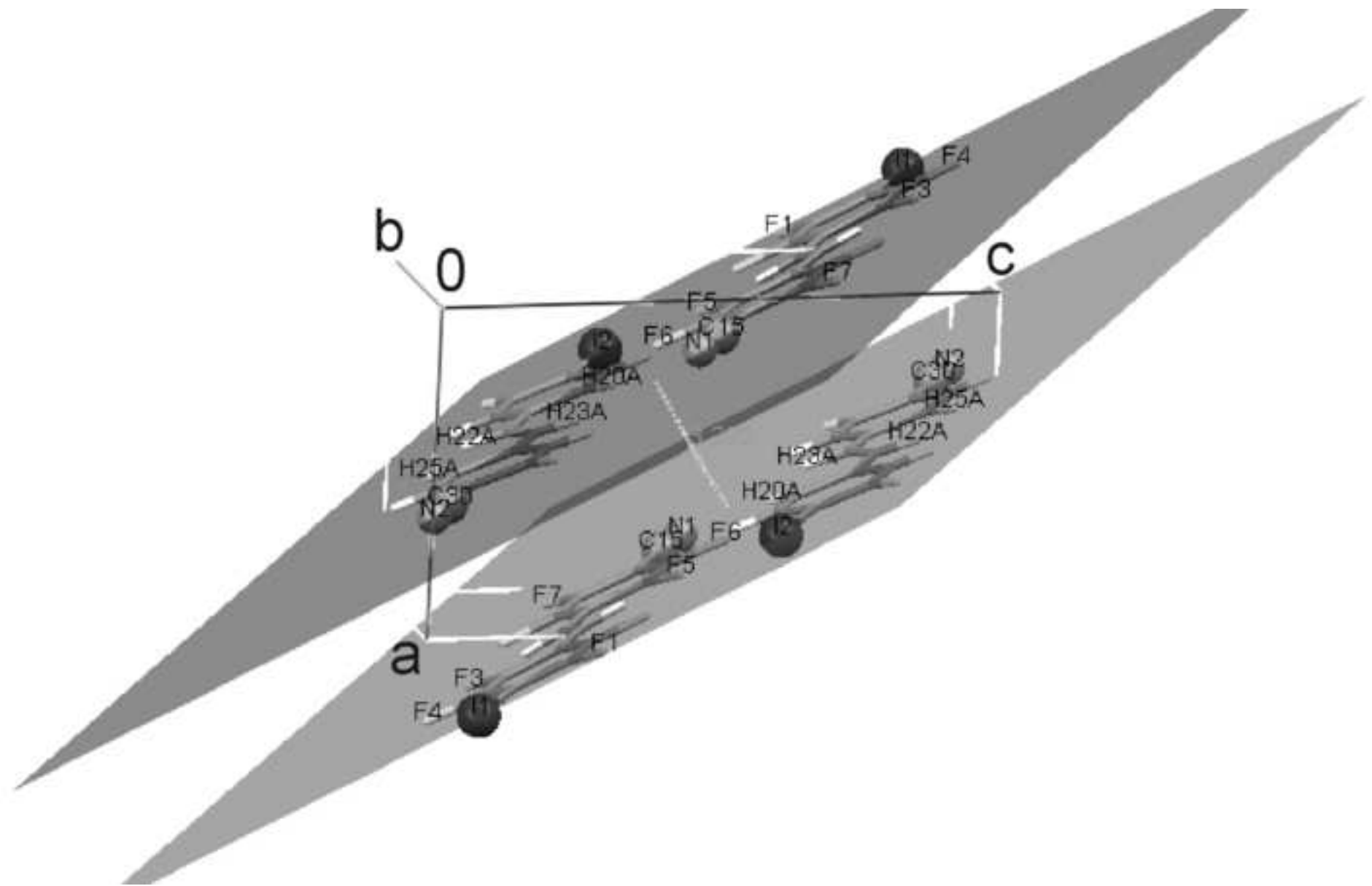


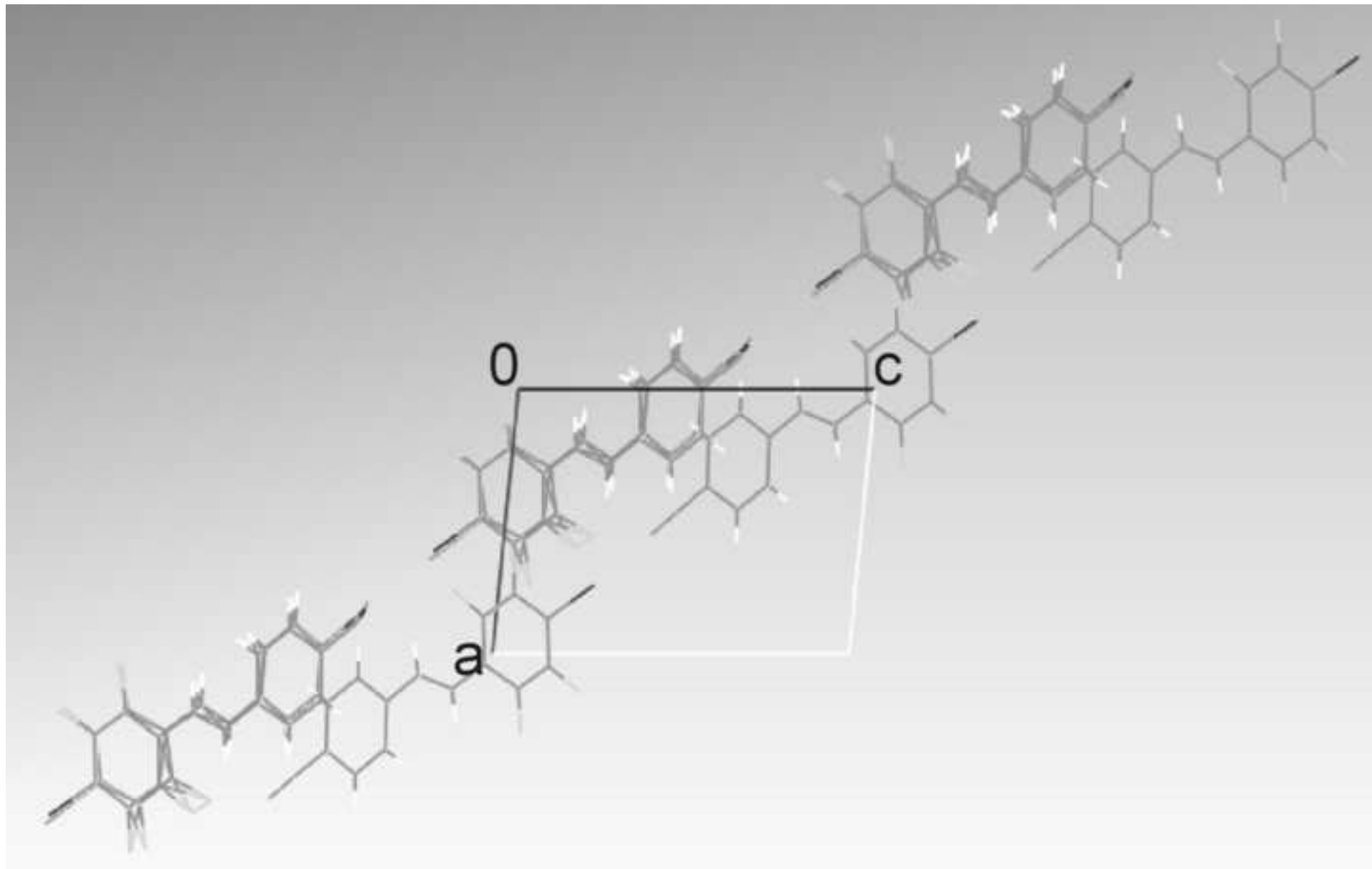


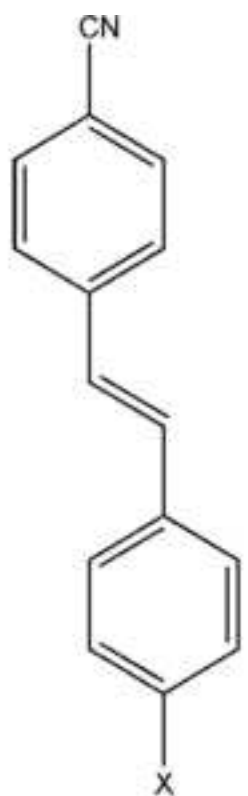




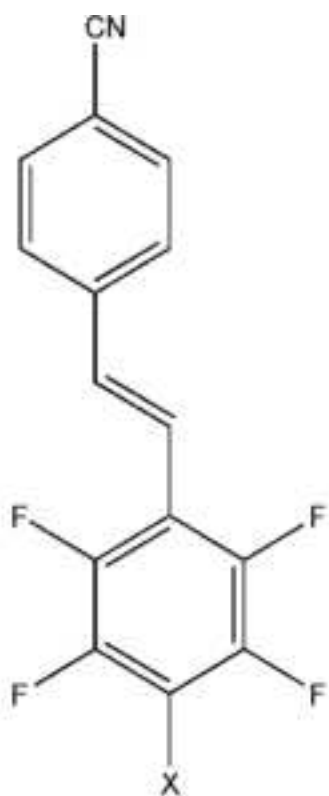




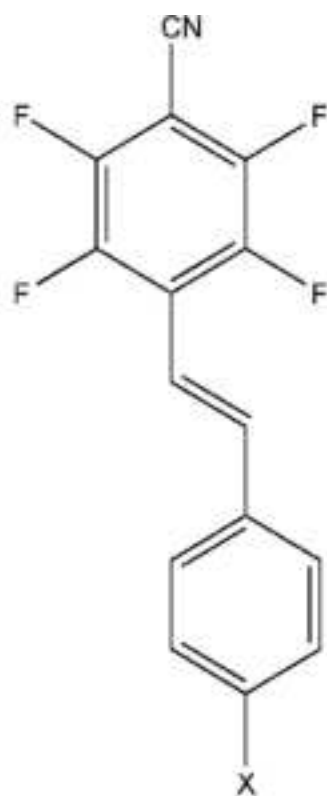




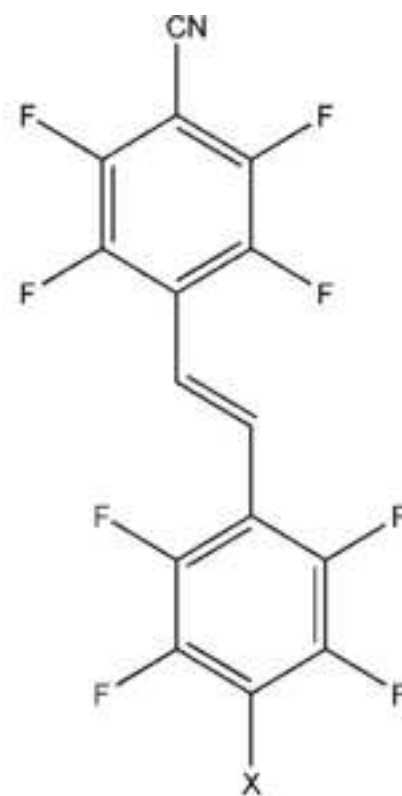
**16,17,18**



**19,20,21**

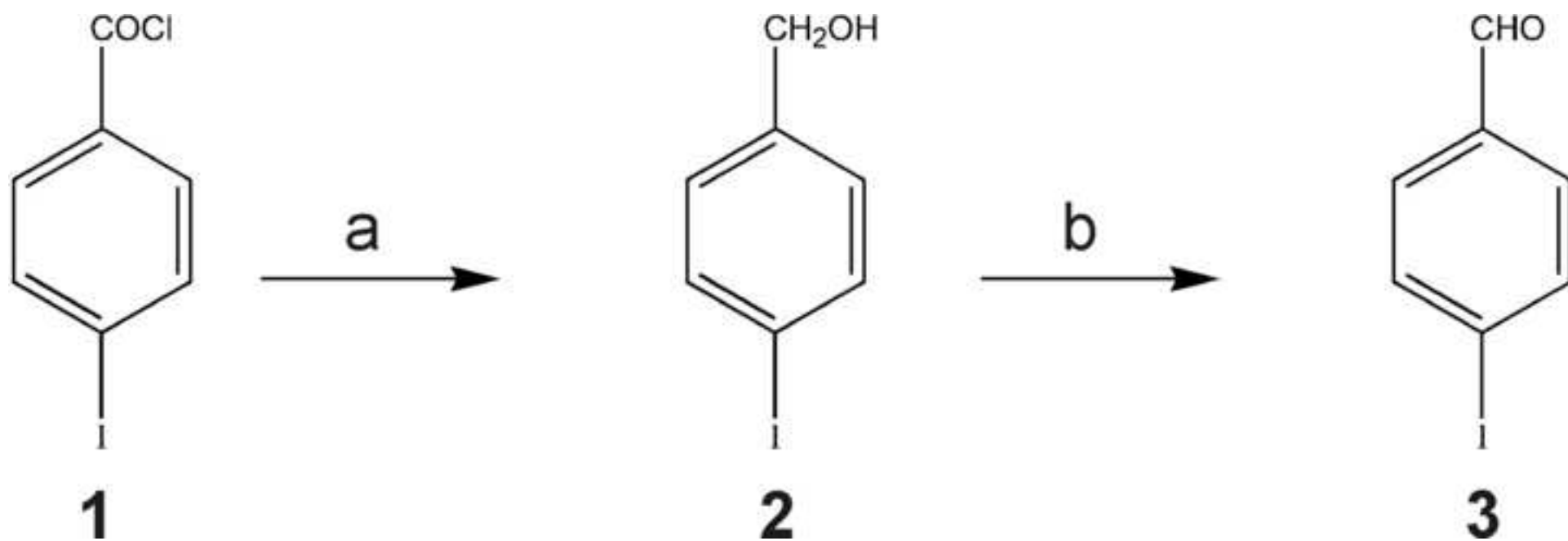


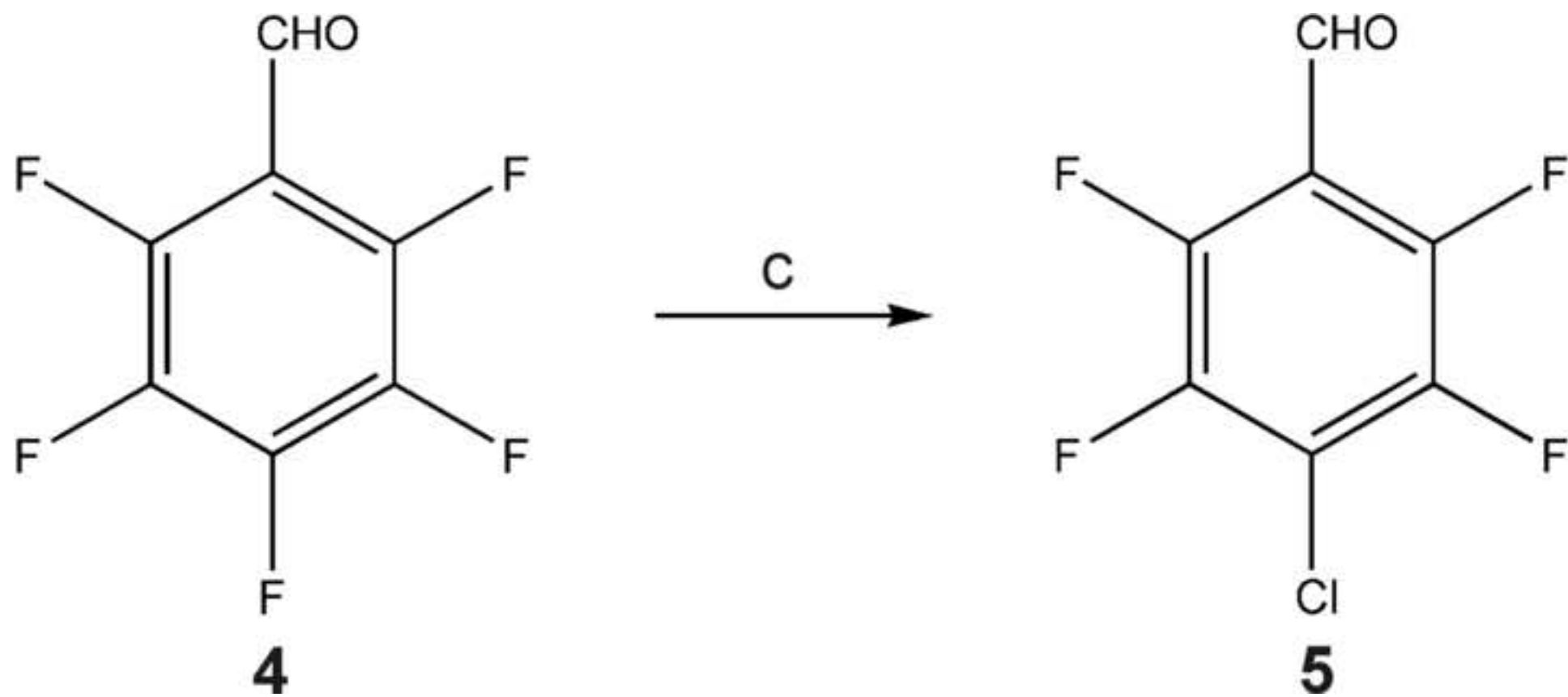
**22,23,24**

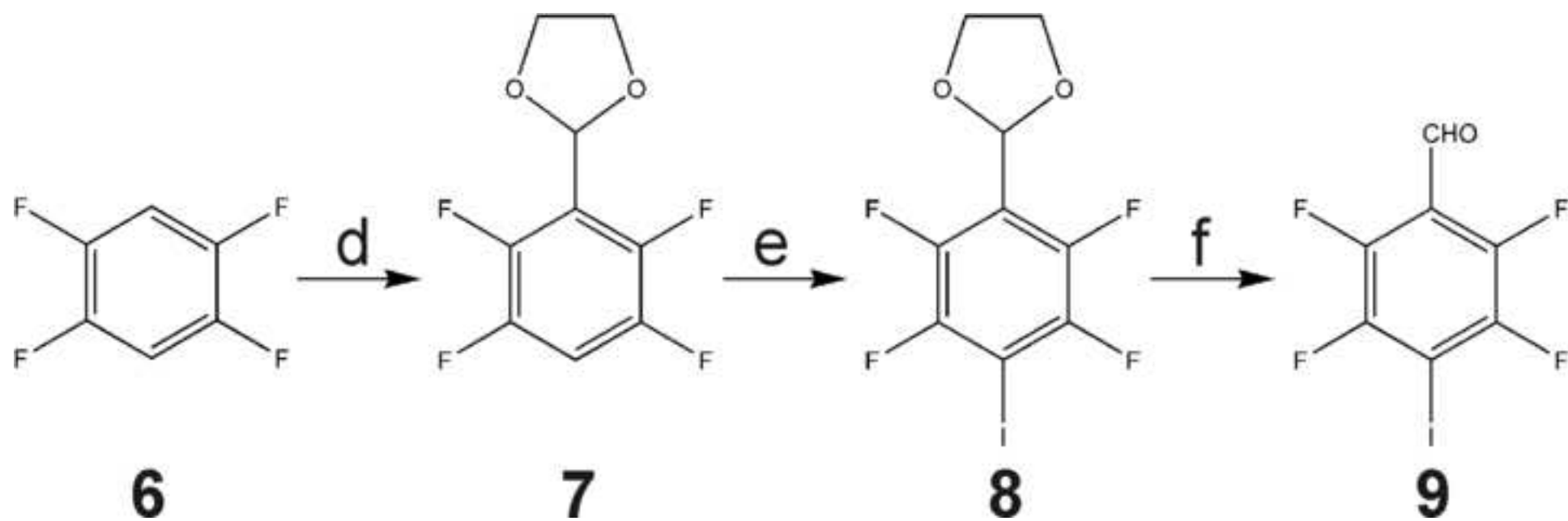


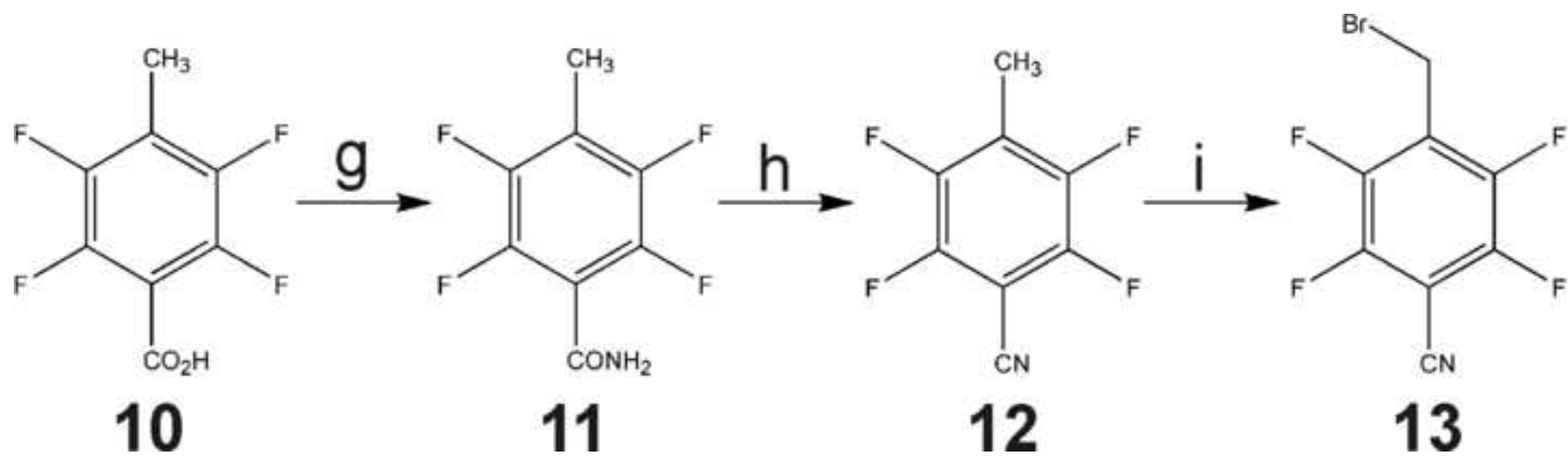
**25,26,27**

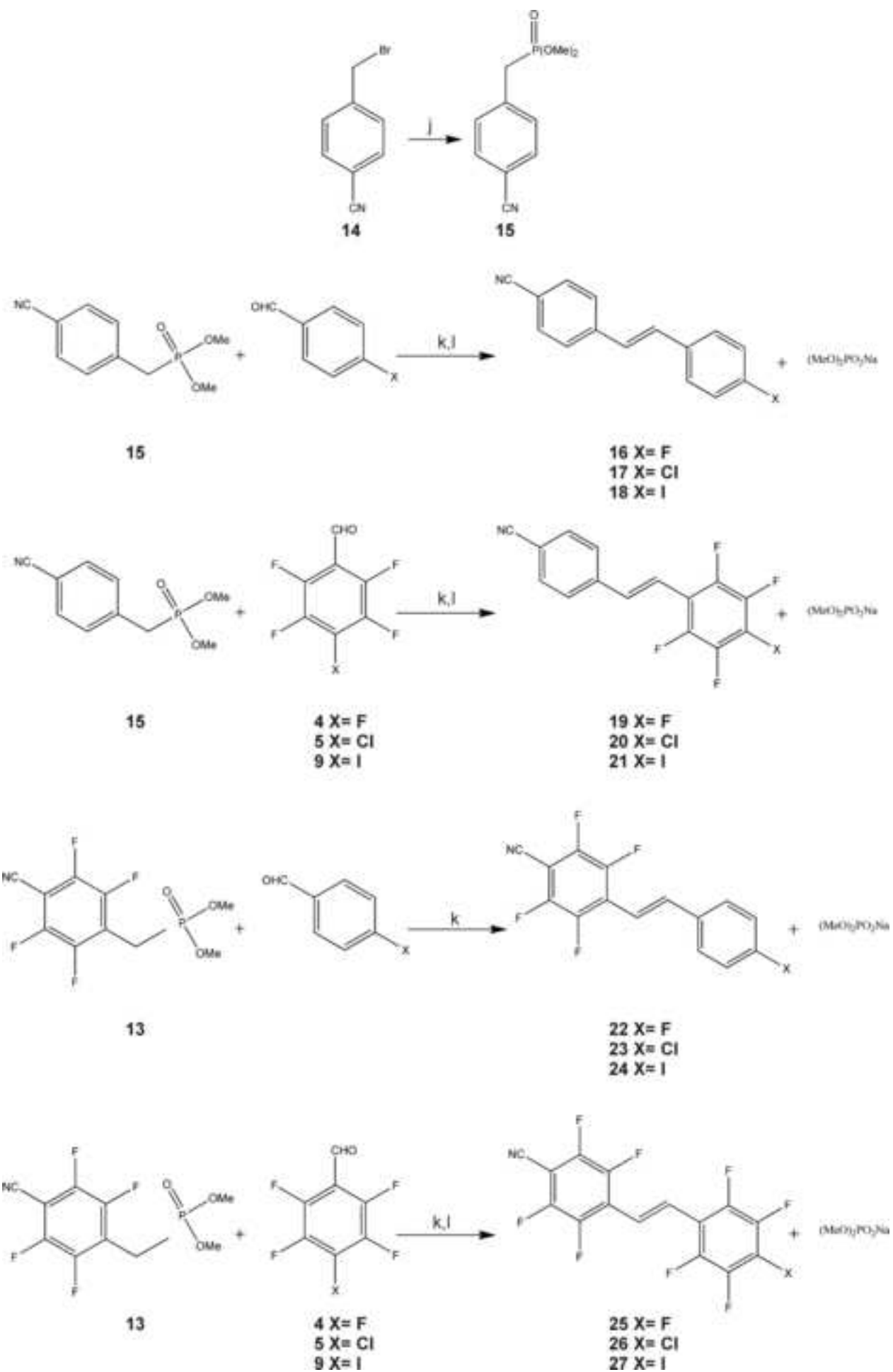
X= F, Cl, I

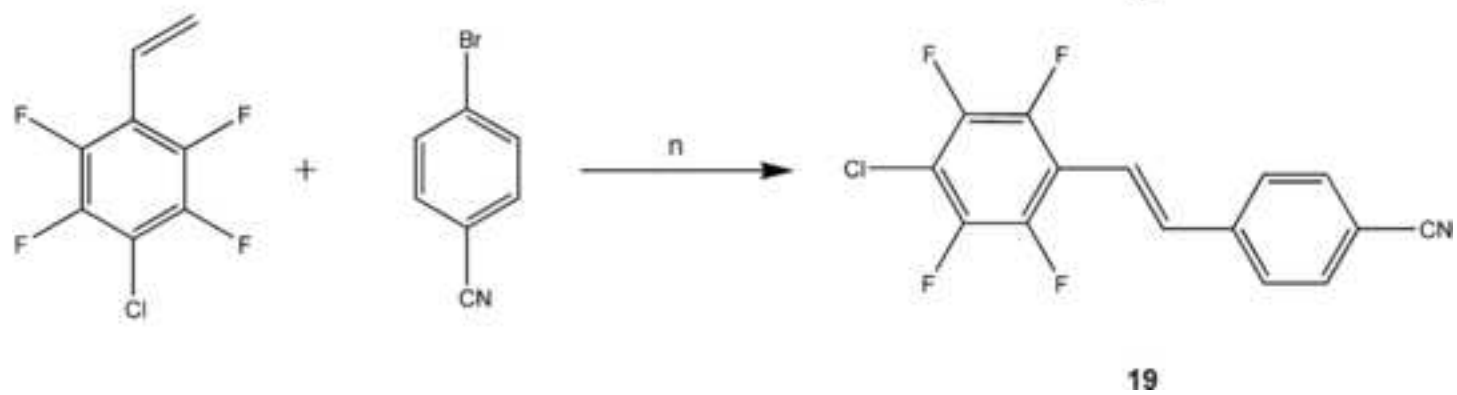
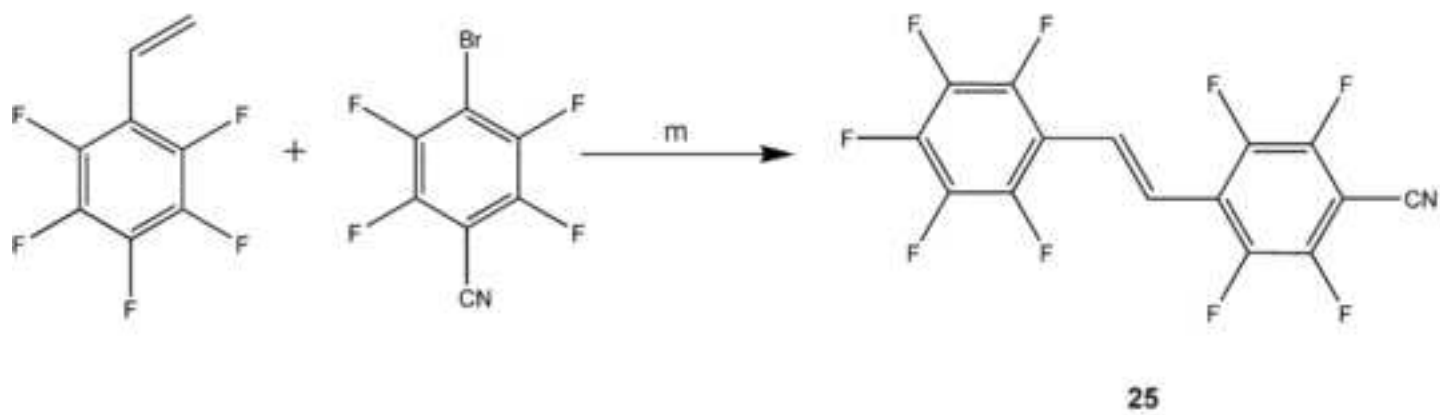
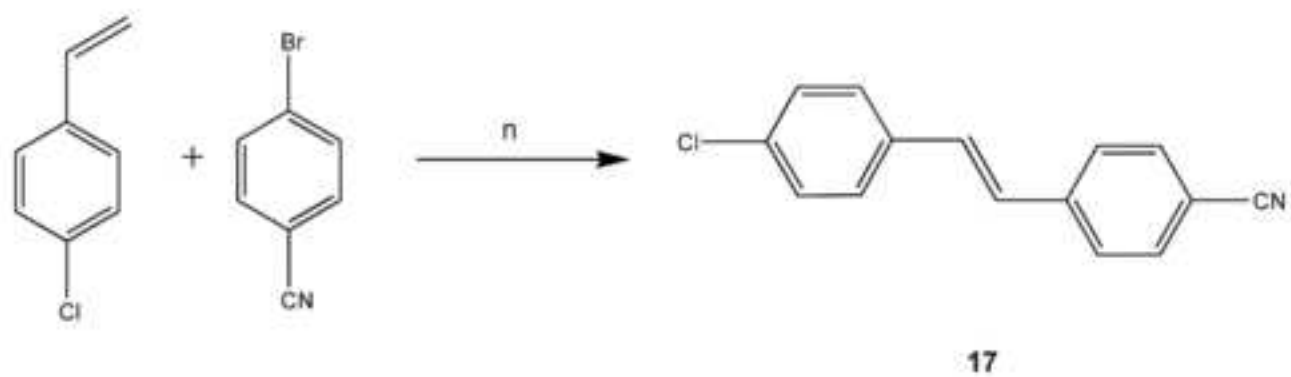
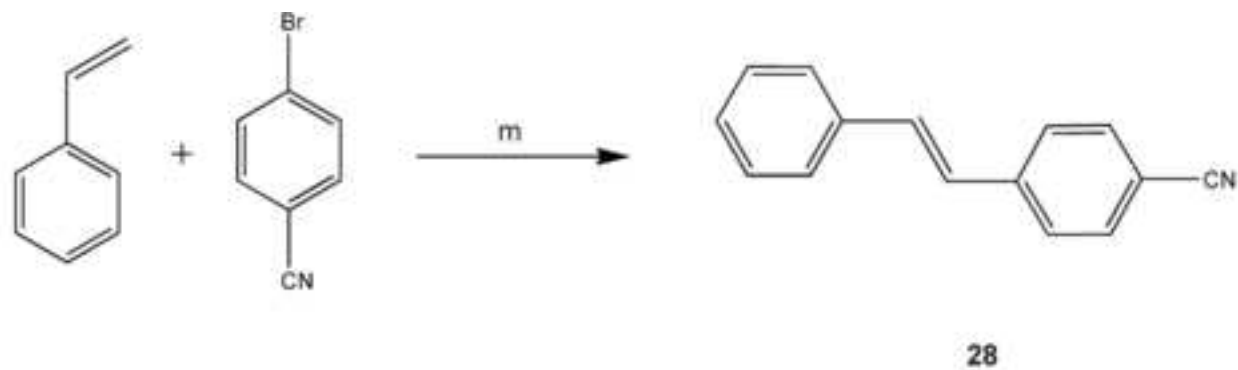


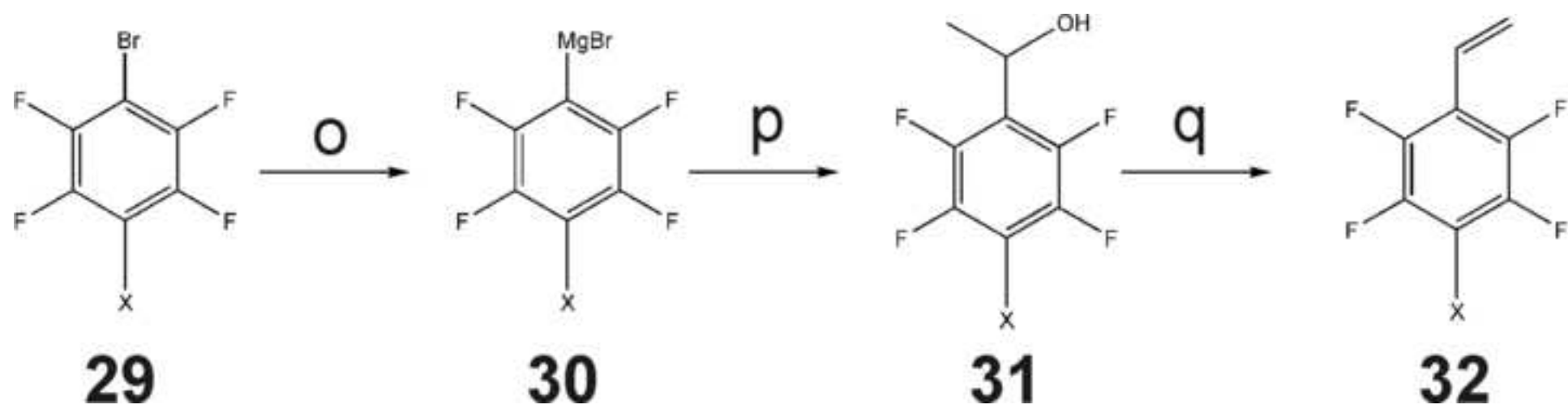


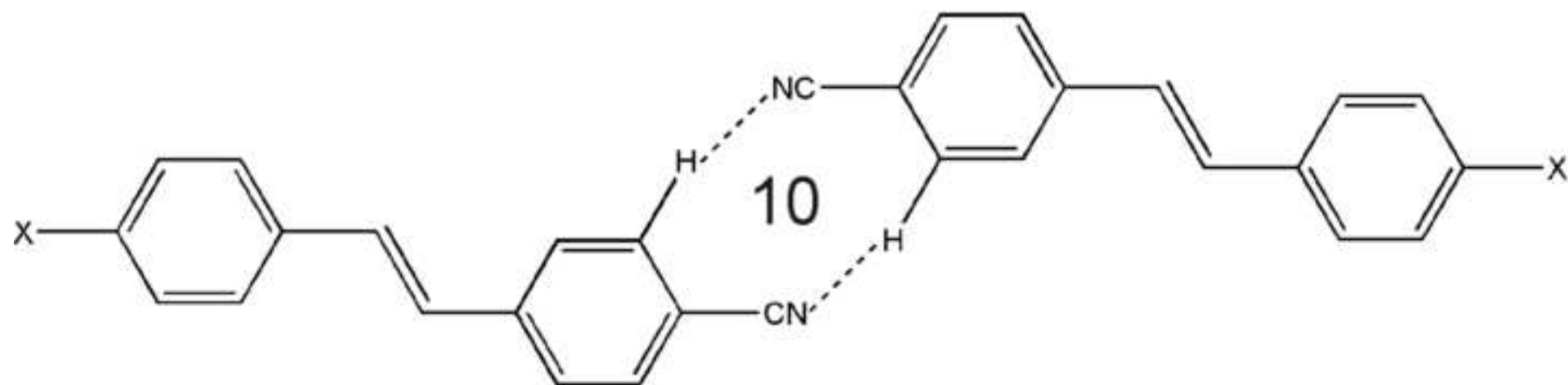






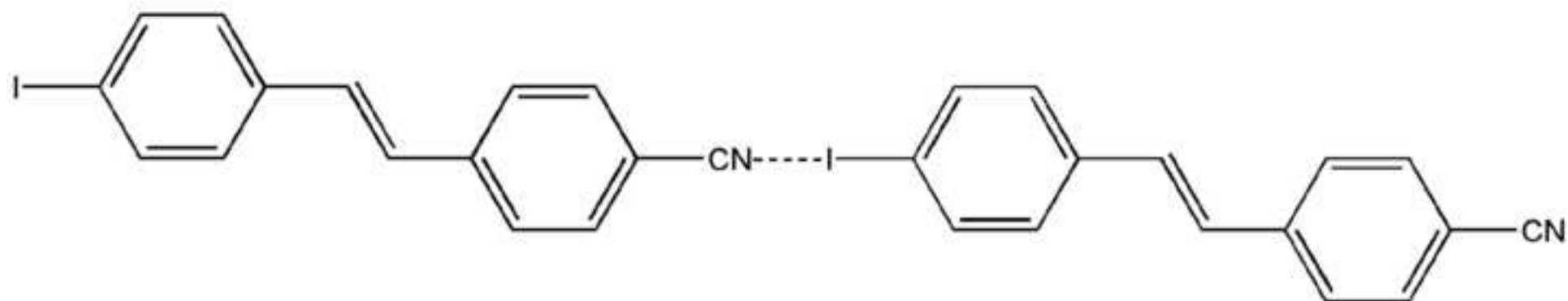


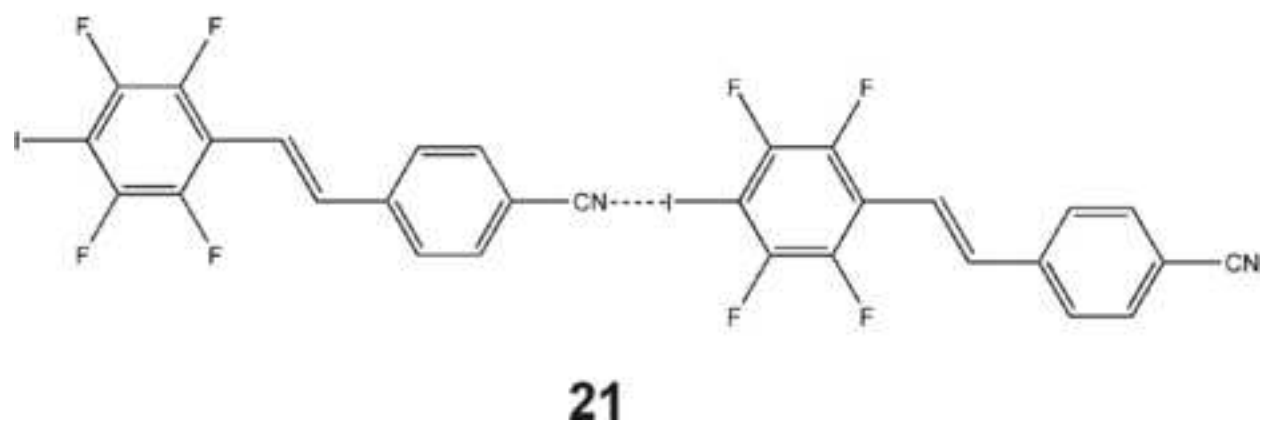
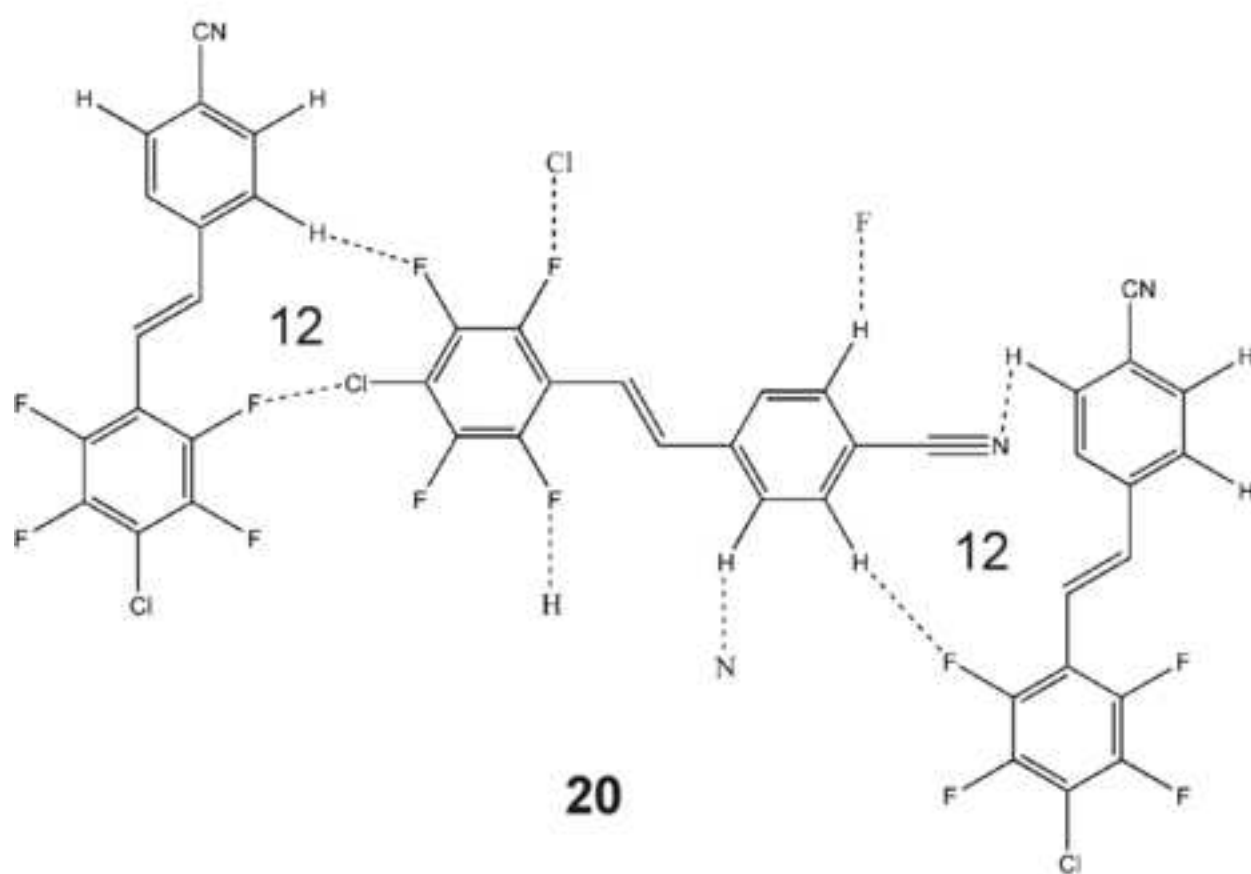
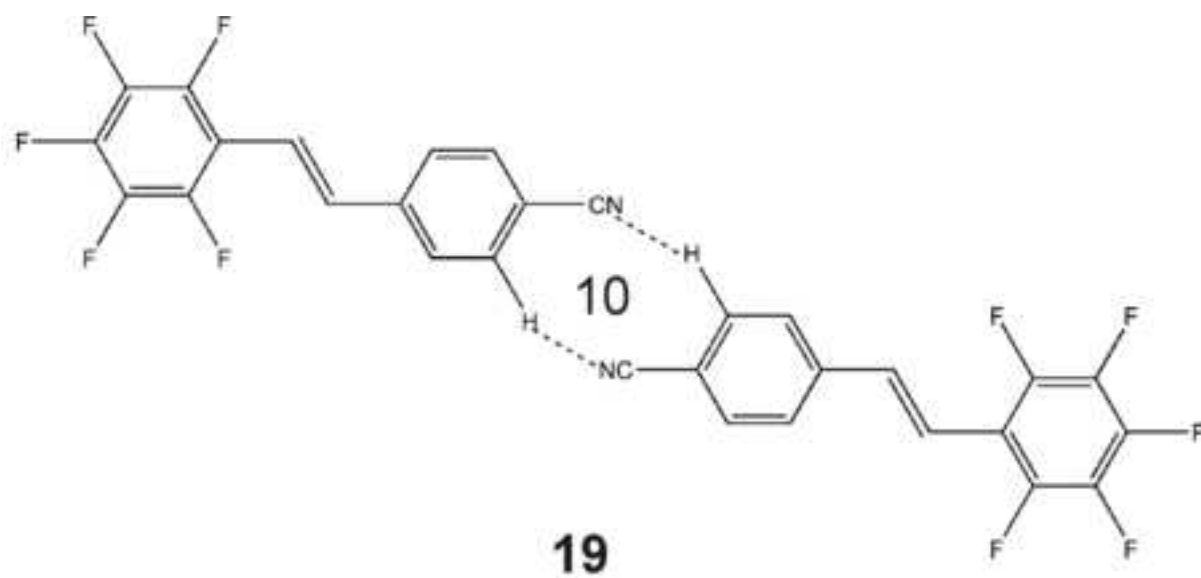


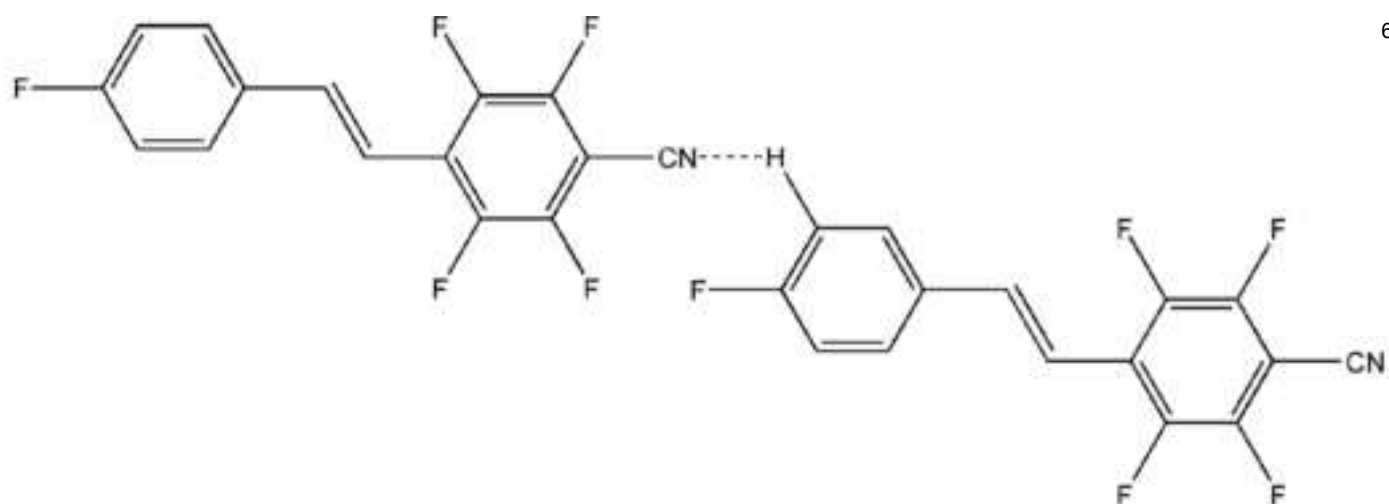
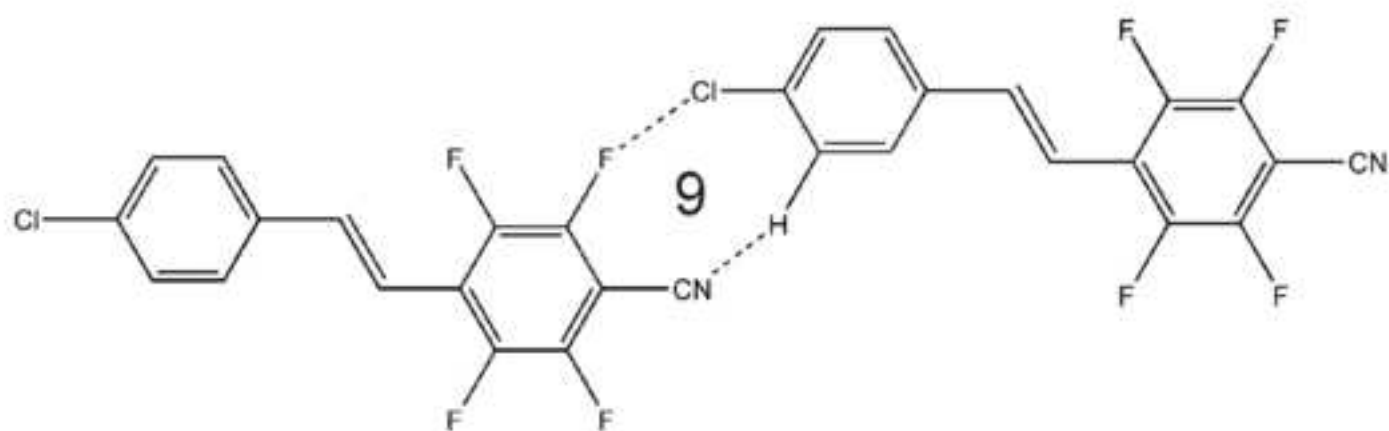
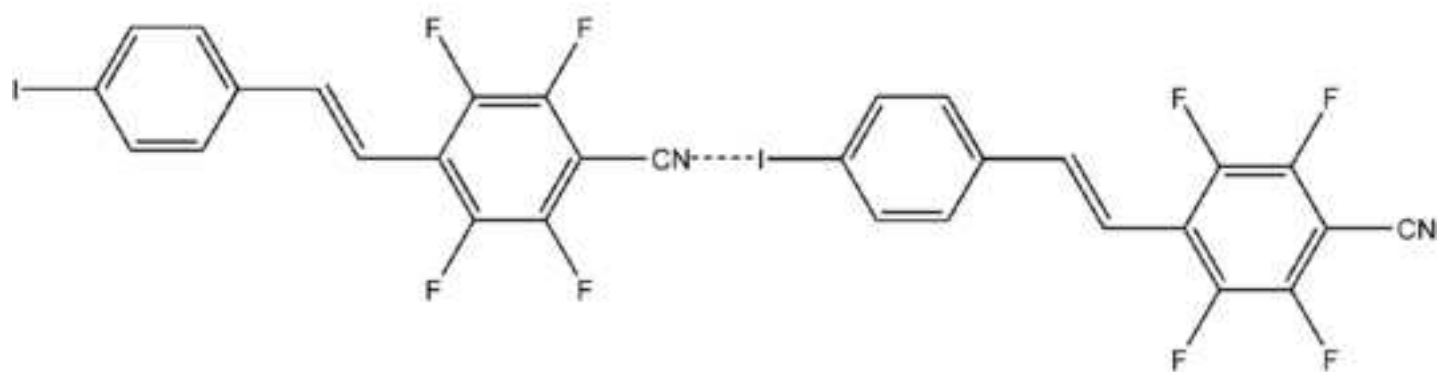


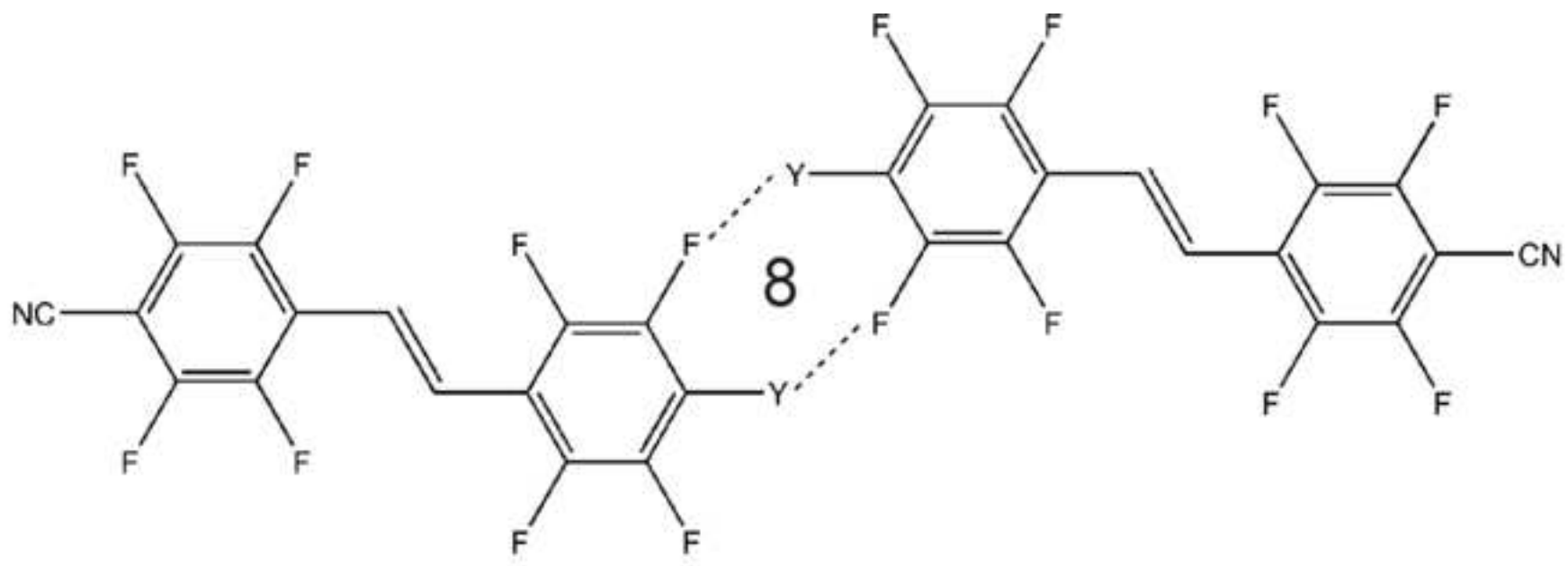
**16 X= F**

**17 X= Cl**

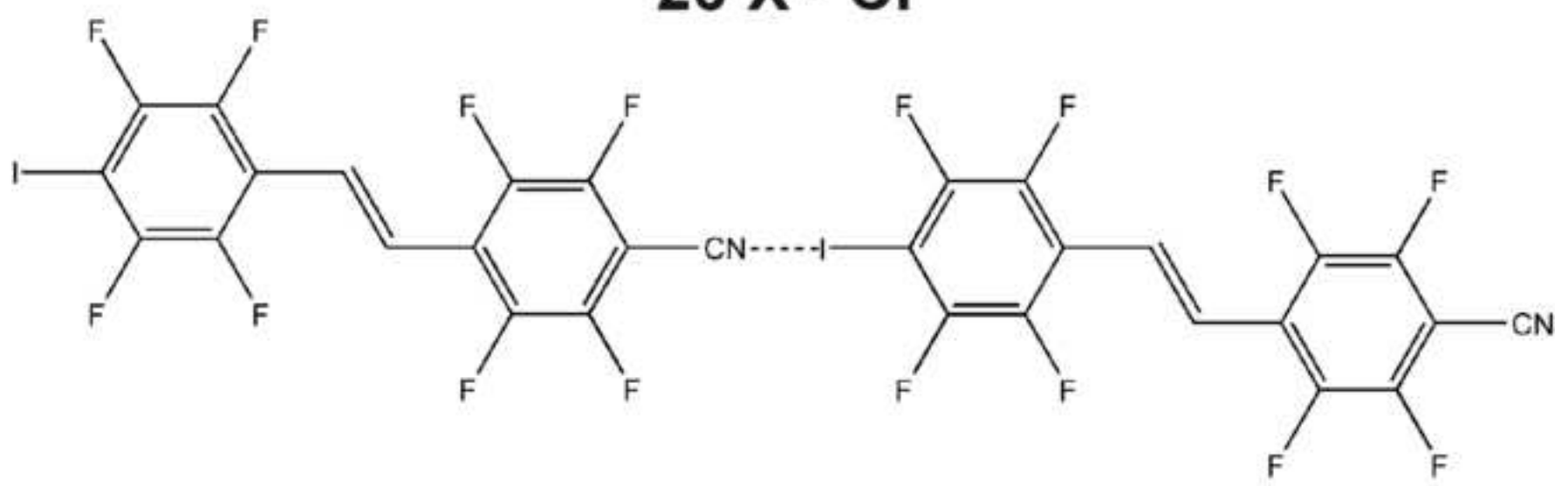




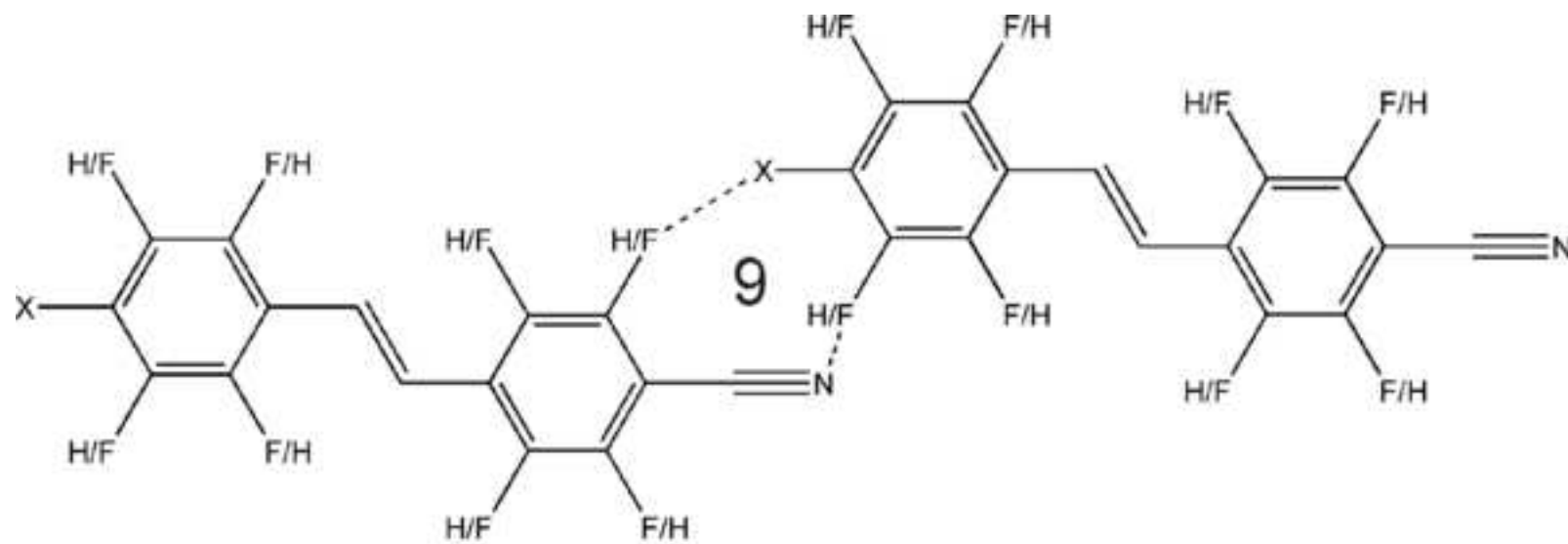
**22****23****24**



**25 X= F**  
**26 X= Cl**

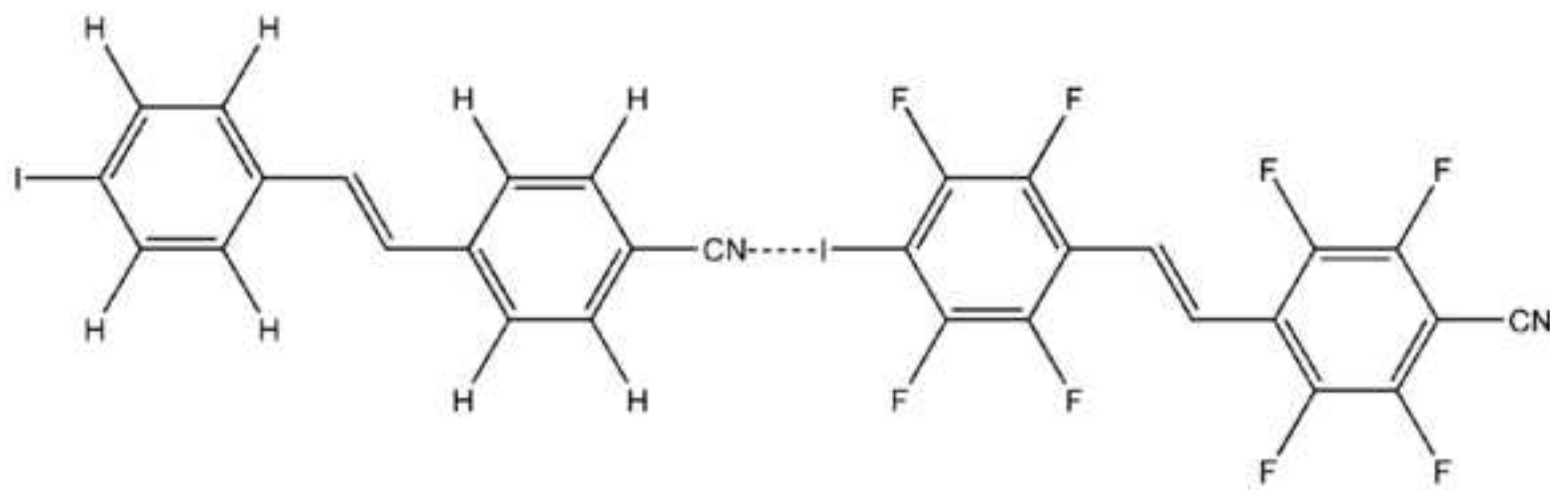


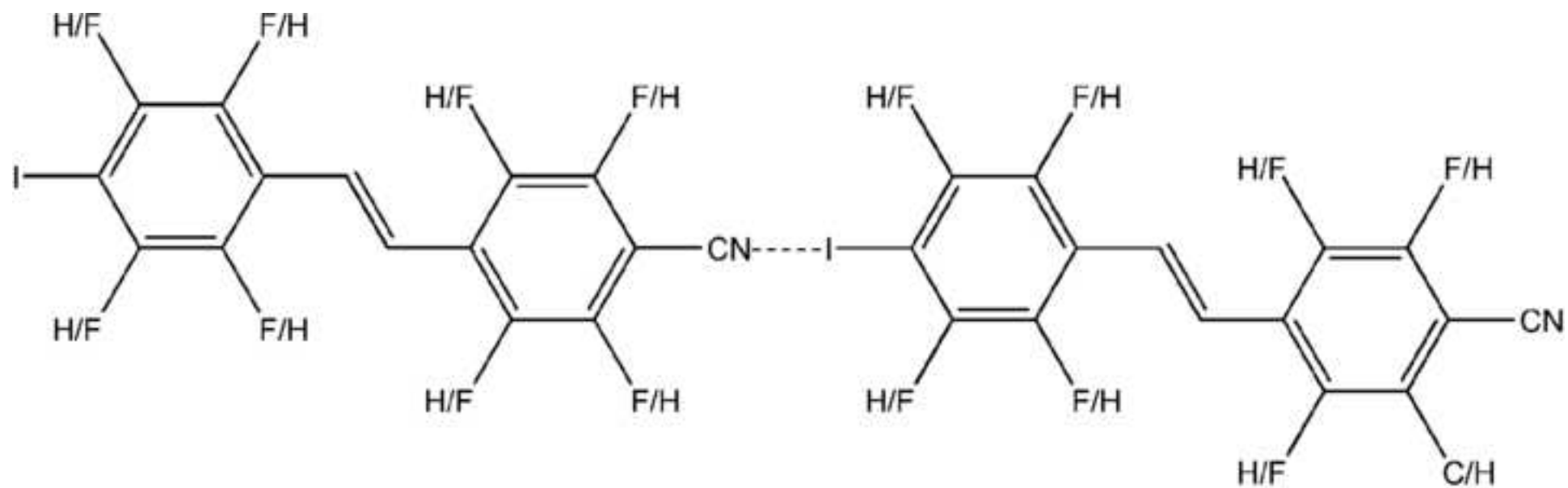
**27**



**[16-25] X= F**

**[17-26] X= Cl**





**[21 • 24]**

**Table 1.** Yield, melting point, packing modes, SHG and UV spectra of trans-stilbenes.

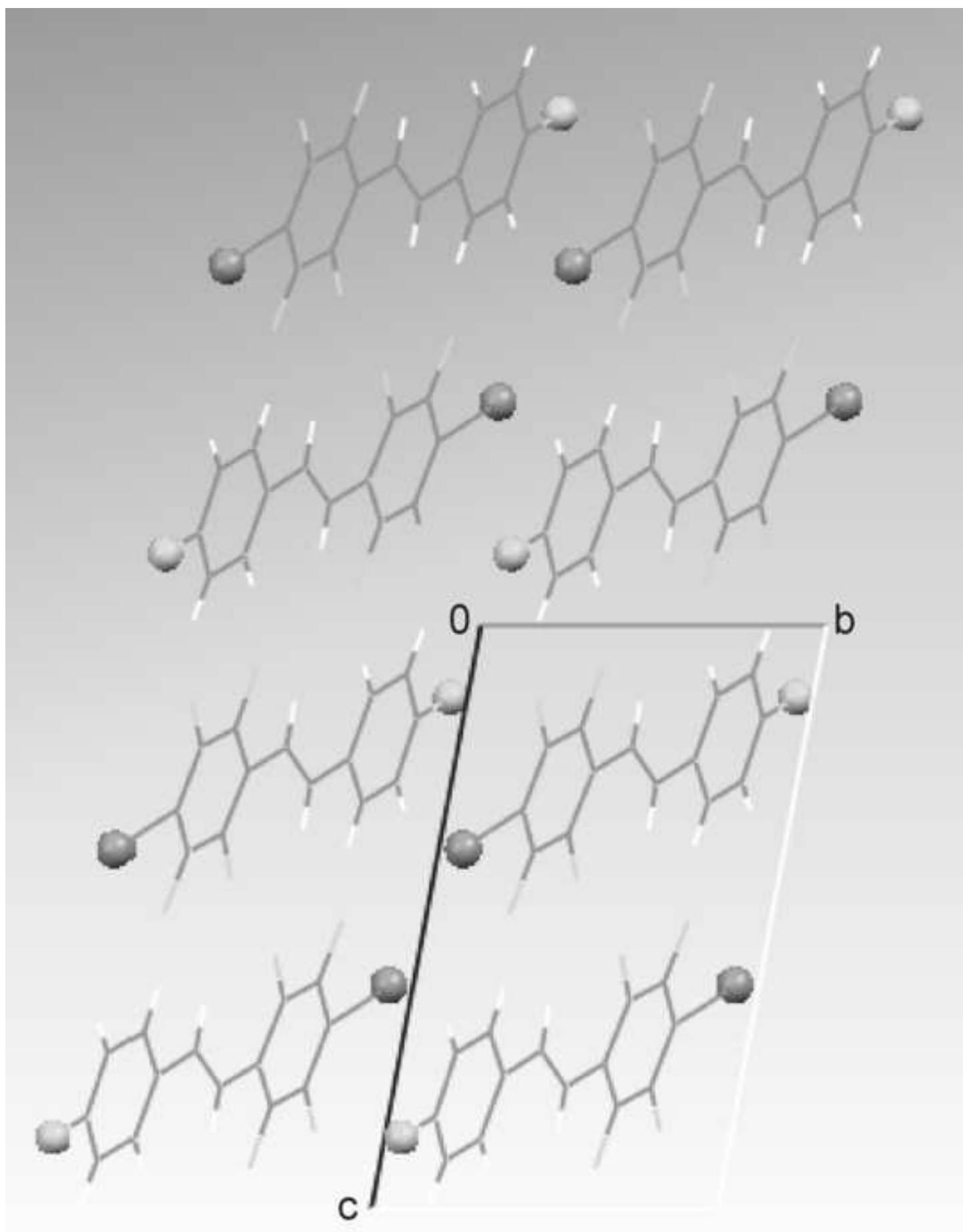
Molecule	packing	SHG	Mp (°C)	$\lambda_{\max}$	$\epsilon_{\max}$	Yield (%)
16 F-C <sub>6</sub> H <sub>4</sub> -CH=CH-C <sub>6</sub> H <sub>4</sub> CN	herringbone 1-D chain-like + 3-D network	+	183 -185	322	25000	42
17 Cl-C <sub>6</sub> H <sub>4</sub> -CH=CH-C <sub>6</sub> H <sub>4</sub> CN	herringbone 1-D chain-like + 3-D network	+	174 -177	329	48000	56
18 I-C <sub>6</sub> H <sub>4</sub> -CH=CH-C <sub>6</sub> H <sub>4</sub> CN	- 1-D chain-like + 2-D network	-	189 -195	329	67500	70
19 F-C <sub>6</sub> F <sub>4</sub> -CH=CH-C <sub>6</sub> H <sub>4</sub> -CN	herringbone 1-D chain-like + 3-D network	+	150 - 153	312	52400	16
20 Cl-C <sub>6</sub> F <sub>4</sub> -CH=CH-C <sub>6</sub> H <sub>4</sub> -CN	herringbone 3-D network	-	185 - 187	318	62000	57
21 I-C <sub>6</sub> F <sub>4</sub> -CH=CH-C <sub>6</sub> H <sub>4</sub> -CN	- 1-D chain-like + 2-D network	+	>240	334	25000	50
22 F-C <sub>6</sub> H <sub>4</sub> -CH=CH-C <sub>6</sub> F <sub>4</sub> -CN	- 1-D chain-like + 3-D network	-	145 - 147	328	26100	54
23 Cl-C <sub>6</sub> H <sub>4</sub> -CH=CH-C <sub>6</sub> F <sub>4</sub> -CN	herringbone 1-D chain-like + 3-D network	-	212 - 214	332	33100	66
24 I-C <sub>6</sub> H <sub>4</sub> -CH=CH-C <sub>6</sub> F <sub>4</sub> -CN	herringbone 1-D chain-like + 3-D network	+	211 - 213	339	66300	56
25 F-C <sub>6</sub> F <sub>4</sub> -CH=CH-C <sub>6</sub> F <sub>4</sub> -CN	herringbone 3-D network	-	84 - 87	312	54000	51
26 Cl-C <sub>6</sub> F <sub>4</sub> -CH=CH-C <sub>6</sub> F <sub>4</sub> -CN	herringbone 3-D network	-	136 - 138	318	65000	31
27 I-C <sub>6</sub> F <sub>4</sub> -CH=CH-C <sub>6</sub> F <sub>4</sub> -CN	- 1-D chain-like + 3-D network	+	211	326	72000	42
Br-C <sub>6</sub> H <sub>4</sub> CH=CH-C <sub>6</sub> H <sub>4</sub> CN <sup>a</sup>	herringbone 3-D network	-	195			
Br-C <sub>6</sub> F <sub>4</sub> CH=CH-C <sub>6</sub> H <sub>4</sub> CN <sup>a</sup>	- 1-D chain-like + 3-D network	-	150			
Br-C <sub>6</sub> H <sub>4</sub> CH=CH-C <sub>6</sub> F <sub>4</sub> CN <sup>a</sup>	herringbone 1-D chain-like + 3-D network	-	196			
Br-C <sub>6</sub> F <sub>4</sub> CH=CH-C <sub>6</sub> F <sub>4</sub> CN <sup>a</sup>	- 3-D network	-	149			

a: Syntheses and crystal structures described elsewhere [3].

**Table 2.** Summary of X-ray diffraction crystal structures.

Sample	16	17	18	19	20	21	22	23	24	25	26	27	[16•25]	[17•26]	[18•27]	[21•24]
Space group	$P2_1$	$P2_1/c$	$P2_1/n$	$P2_1/c$	$P2_1/c$	$P-1$	$P-1$	$P2_1/c$	$Cc$	$C2/c$	$C2/c$	$P-1$	$P2_1/c$	$P2_1/c$	$P-1$	$P1$
a (Å)	4.7403(9)	4.7445(3)	6.2058(5)	14.8605(13)	7.7730(7)	7.9947(16)	7.1424(16)	9.3335(12)	20.9120(12)	7.5372(8)	7.6169(15)	7.4365(6)	4.7078(11)	4.7677(10)	7.7885(15)	8.0489(16)
b (Å)	9.970(2)	10.2736(10)	7.5004(8)	10.0540(5)	13.7839(13)	8.401(2)	7.2901(17)	10.7836(10)	17.2400(8)	9.3970(7)	9.3431(19)	8.1145(7)	10.229(3)	10.518(2)	13.683(3)	8.6192(17)
c (Å)	12.063(2)	12.1462(9)	27.182(2)	17.1887(16)	12.0296(13)	10.348(3)	12.239(3)	12.5299(17)	13.9210(8)	35.668(4)	37.386(7)	13.7580(11)	12.998(3)	12.914(3)	13.946(3)	10.368(2)
$\alpha$ (°)	90	90	90	90	90	91.56(3)	98.886(19)	90	90	90	90	80.017(7)	90	90	66.616(14)	92.09(3)
$\beta$ (°)	99.29(3)	99.557(6)	94.462(9)	109.350(7)	92.662(8)	94.99(3)	96.147(19)	97.490(10)	127.109(4)	92.797(9)	94.87(3)	77.778(7)	99.199(18)	99.09(3)	84.745(15)	94.78(3)
$\gamma$ (°)	90	90	90	90	90	107.76(3)	103.197(18)	90	90	90	90	61.853(6)	90	90	74.775(15)	106.89(3)
V (a (Å <sup>3</sup> ))	562.63(18)	583.83(8)	1261.37(19)	2423.1(3)	1287.5(2)	658.3(3)	606.2(3)	1250.4(3)	4002.5(4)	2523.2(4)	2651.0(9)	712.83(10)	617.9(3)	639.4(2)	1316.1(4)	684.5(2)
$\rho$ (g.cm <sup>-3</sup> )	1.318	1.363	1.744	1.618	1.608	2.034	1.617	1.656	2.007	1.933	1.922	2.213	1.56	1.601	2.034	1.966
Measurement Temperature	173(2)	153(2)	173(2)	153(2)	173(2)	173(2)	173(2)	173(2)	173(2)	153(2)	173(2)	173(2)	173(2)	173(2)	173(2)	173(2)
SOF	0.553(11)	n.a.	n.a.	n.a.	n.a.	n.a.	n.a.	n.a.	n.a.	n.a.	n.a.	n.a.	0.534(14)	0.524(10)	n.a.	0.845(3)
Flack parameter	0(4)	n.a.	n.a.	n.a.	n.a.	n.a.	n.a.	n.a.	0.50(3)	n.a.	n.a.	n.a.	n.a.	n.a.	n.a.	0.51(6)
reflections collected	3918	8346	8573	25790	18012	5131	8677	15529	38546	10272	2325	13910	4383	4060	22729	5182
unique reflections	1941	1617	2443	6419	3474	2380	3273	3382	10532	2263	2325	3827	1091	1106	7144	4290
unique reflections ( $I > 2\sigma(I)$ )	1636	1558	1791	4990	2615	1238	1884	2934	8720	1767	1731	3375	588	780	4804	3667
R <sub>int</sub>	0.165	0.049	0.052	0.062	0.045	0.134	0.048	0.033	0.076	0.119	0	0.049	0.084	0.076	0.1	0.069
R <sub>sigma</sub>	0.108	0.026	0.05	0.038	0.026	0.214	0.045	0.02	0.05	0.072	0.029	0.034	0.061	0.048	0.077	0.047
R1 ( $I > 2\sigma(I)$ )	0.1	0.076	0.03	0.052	0.054	0.11	0.048	0.031	0.047	0.062	0.108	0.028	0.141	0.1	0.053	0.06
R1 (all reflections)	0.108	0.078	0.049	0.07	0.072	0.165	0.092	0.037	0.057	0.079	0.123	0.033	0.19	0.124	0.09	0.068
wR2	0.294	0.16	0.074	0.142	0.139	0.336	0.14	0.091	0.126	0.187	0.309	0.082	0.45	0.297	0.157	0.152
goof	1.149	1.3	0.986	1.095	1.119	1.076	0.991	1.032	1.075	1.059	1.138	0.666	1.594	1.097	1.069	1.011
$\Delta\rho^+$ (eÅ <sup>-3</sup> )	0.22	0.26	0.82	0.38	0.27	2.71	0.21	0.29	2.33	0.37	0.59	0.6	0.96	0.53	1.17	1.04
$\Delta\rho^-$ (eÅ <sup>-3</sup> )	-0.2	-0.24	-0.58	-0.23	-0.33	-2.14	-0.24	-0.27	-1.81	-0.42	-0.51	-1.11	-0.48	-0.34	-1.99	-1.49
Nos CCDC	693729	693730	693731	693732	693733	693734	693735	693736	693737	693738	693739	693740	693741	693742	693743	693744

Figure 13



	C(7)=C(8)···Ph	3.541		F(1)···Ph	3.749
<b>24</b>	C(1)-I(1)···N(1)	3.26	171.75	F(1)···Ph	3.85
	C(21)-I(2)···N(2)	3.188	163.71	F(2)···Ph	3.864
	C(41)-I(3)···N(3)	3.17	163.62	F(2)···Ph	3.919
	C(2)-H(2)···F(22)	2.615	126.92	F(3)···Ph	3.452
	C(3)-H(3)···F(22)	2.701	122.57	F(3)···Ph	3.54
	C(22)-H(22)···F(2)	2.745	122.59	F(4)···Ph	3.754
	C(47)-H(47)···F(23)	2.446	172.27	F(4)···Ph	3.673
	C(10)-F(1)···F(21)	2.821	142.03	F(21)···Ph	4.064
	C(13)-F(3)···F(23)	2.881	90.57	F(22)···Ph	3.772
<b>25</b>	C(2)-F(1)···F(4)	2.88	161.77	F(23)···Ph	3.488
	C(3)-F(2)···F(3)	2.849	138.9	F(24)···Ph	3.738
	C(10)-F(5)···F(9)	2.864	167.44	F(51)···Ph	3.367
	C(11)-F(6)···F(8)	2.903	135.66	F(52)···Ph	3.956
	C(12)-F(7)···F(8)	2.894	165.2	F(53)···Ph	3.816
	C(15)-N(1)···Ph	3.086		F(54)···Ph	4.026
<b>26</b>	C(2)-F(1)···Cl(1)	3.203	142.09		
	C(6)-F(4)···Cl(1)	3.178	148.47		
	C(2)-F(1)···F(4)	2.922	155.59		
	C(3)-F(2)···F(3)	2.888	147.08		
	C(13)-F(12)···F(13)	2.886	146.74		
	C(12)-F(11)···F(14)	2.919	155.77		
	C(8)-N(1)···Ph	3.11			
<b>27</b>	C(1)-I(1)···N(1)	3.042	172.46		
	C(2)-F(1)···F(7)	2.925	144.47		
	C(2)-F(2)···F(6)	2.927	81.38		
	C(5)-F(3)···F(5)	2.745	126.28		
	C(5)-F(3)···F(6)	2.906	166.94		
	C(6)-F(4)···F(5)	2.93	119		
	F(6)···Ph	3.656			
	I(1)···Ph	3.732			
<b>[16.25]</b>	C(6)-H(2)···N(1)	2.625	168.73		
	C(6)-H(2)···F(5)	2.625	168.73		
	C(6)-F(4)···N(1)	2.247	161.03		
	C(2)-F(1)···N(1)	2.638	151.76		
	C(3)-F(2)···N(1)	2.781	169.76		
	C(2)-F(1)···F(3)	2.468	137.17		
	C(2)-F(1)···F(4)	2.706	132.47		
	C(6)-F(4)···F(4)	2.843	88.91		
	C(7)-N(1)···Ph	3.497			
	F(5)···Ph	3.477			
	C(8)=C(8)···Ph	3.475			